Title
Hydrophobic polyelectrolytes as osmotic agents for a mechanochemical insulin pump

Author
Cornejo-Bravo, Jose Manuel

Publication Date
1992

Peer reviewed|Thesis/dissertation

Hydrophobic Polyelectrolytes as Osmotic Agents for a Mechanochemical Insulin Pump

by

Jose Manuel Cornejo-Bravo

B.S. Autonomous University of Baja California, 1984
M.S. Autonomous University of Baja California, 1986

DISSERTATION

Submitted in partial satisfaction of the requirements for the degree of

DOCTOR OF PHILOSOPHY

in

Pharmaceutical Chemistry

in the

GRADUATE DIVISION

of the

UNIVERSITY OF CALIFORNIA

San Francisco

Date University Librarian

Degree Conferred: 9/6/92

To

Mom and Dad,

Juliana, Miguel, Carmen, Luz and Alejandro,

for their love and support

To my wife Lourdes and my son Manuel Alejandro for all the

happiness that they have brought to my life

Acknowledgments

I would like to acknowledge all the people that in one way or another made it possible for me to obtain my Ph. D. degree in Pharmaceutical Chemistry.

To my research advisor Dr. Ronald A. Siegel for his guidance, encouragement and motivation. Thank you for showing me what a scientist should be.

I wish to express my gratitude to Dr. Frances C. Szoka and Dr. Richard Guy for their valuable guidance, both as my academic advisors and as members of my thesis committee.

My orals committee of Drs. Tom Tozer (chairman), Roger Cooke, Richard Shafer, and Dick Stigter for their comments on my research and for allowing me to advance to candidacy on the first try.

To Pam de Moor, Seaung Oh, and Bruce Firestone for their friendship, for being such good peers and for their great introduction to Polymer Chemistry. Thanks to Jim Uchizono and Dr. Chris Cullander for helping me to set the data logger. Without their help the kinetics experiments would not have been possible.

My gratitude to the Department of Pharmaceutical Chemistry at UCSF for giving me the opportunity to fulfill my dream of a Ph. D. degree. To the Graduate Division for awarding me the Non Resident Fellowship during the five years of my studies.

I want to express my appreciation to all my colleagues in the Faculty of Chemical Sciences, UABC for their support and encouragement. A Especial thanks to Mrs. Evangelina Herrán de Cruz for her written support. To Hector Salgado, Dr. Carlos Ramón García and Ricardo Guerra for all their help and motivation. To the Department of Academic Affairs of the Autonomous University of Baja California for all their help and support.

José M. Cornejo-Bravo

Hydrophobic Polyelectrolytes as Osmotic Agents for a Mechanochemical Insulin Pump

by

Jose Manuel Cornejo-Bravo

Departments of Pharmacy and Pharmaceutical Chemistry
University of California, San Francisco

Abstract

This thesis deals with the synthesis and characterization of a series of hydrophobic polyelectrolytes containing the monomer N,N-diethylaminoethyl methacrylate (DEA). These polymers are potential osmotic agents for a novel mechanochemical insulin pump.

The hydrochloride form of the homopolymer of DEA [p(DEA•HCl)] is water soluble, but it becomes hydrophobic and insoluble when neutralized with sodium hydroxide. During titration, at a certain degree of neutralization, a precipitate phase appears. Beyond this point, the system behaves as an excellent buffer with a "buffering" pH around 7.6 when the ionic strength (set by NaCl) is 0.1 M. The "buffering pH" can be increased or decreased by incorporating hydrophilic or hydrophobic unionizable comonomers respectively.

The colloid osmotic pressures produced by p(DEA•HCl) and copolymers of DEA•HCl and methyl methacrylate were studied as a function of polyelectrolyte concentration and composition, degree of neutralization, and ionic strength of the reference solution. The "Cell Model" for polyelectrolyte solution is successful in predicting the colloid osmotic pressure produced by p(DEA•HCl), but the model is successful only at low concentrations for the copolymers.

The kinetics of colloid osmotic pressure development are shown to be too slow for the precipitating system to be used in the

proposed mechanochemical insulin pump.

Precipitation of the polyelectrolytes was inhibited by the incorporation of a small fraction of permanent charge which was accomplished by partial quaternization of the DEA groups. The resulting polyelectrolytes show fast kinetics of colloid osmotic pressure development, but poorer buffering quality.

Thesis Chairman: 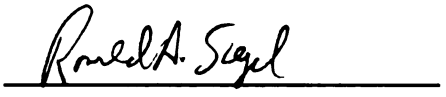 Ronald A. Siegel Sc. D

Table of Contents

List of Tables

List of Figures

Chapter 1

Chapter 2.

Chapter 3.

Chapter 4.

Chapter 5.

Chapter 1

Introduction

1.1 The Problem: Diabetes Mellitus

Inadequate production of insulin results in lack of utilization of blood glucose. This condition elevates the blood glucose concentration and leads to the disease called diabetes mellitus. If insulin therapy is not administrated, the patient suffers ketoacidosis and coma, which lead to death.

The usual treatment procedure for insulin-dependent diabetes is a regimen of subcutaneous insulin injections. The rate of absorption of insulin is not determined by the blood glucose levels (closed-loop control) as occurs in the nondiabetic pancreas (1). While the treatment prevents the acute manifestation of the disease, it does not provide good control of blood glucose concentrations and the patient is usually hyperglycemic. The long term effects of diabetes are blindness, neuropathy, nephropathy and arteriosclerosis. These complications are believed to be caused by the high levels of blood glucose in the diabetic patient (2).

It is obvious that the development of better methods for insulin administration are required. Such methods must mimic the closed loop response of the normal pancreas. Several self-regulated (closed-loop) delivery systems have been proposed. In the next section these systems will be reviewed briefly.

1.2 Self-Regulated Insulin Delivery Systems

The "artificial beta cell" has been developed by Albisser et al. (3,4). The patient's blood is continuously sampled by a catheter and analyzed for glucose. The glucose level is fed into a computer which then determines the insulin delivery rate. Insulin is infused into the patient through a second catheter. The insulin delivery is actuated by a peristaltic pump which is controlled by the computer. While this

system has produced good blood glucose control, it is much too large to be used by ambulatory patients. Moreover, the use of catheters to sample blood and administer insulin causes patient discomfort and carries the risks of infections and catheter clogging.

Closed-loop systems that use biochemical and chemical means have been considered. Beta cells have been encapsulated as microspheres or surrounded by macroporous, hydrophilic membranes (5,6). These systems mimic the pancreas, except for a short time delay which results from the diffusion of insulin and glucose through the artificial membranes. At present, problems remain in maintaining cell viability and avoiding tissue encapsulation over long periods of time.

Another system utilizes the concept of competitive binding affinity of glucose and glycosylated insulin (G-insulin) to the plant lectin Concanavalin A (ConA) (7-9). G-insulin is bound to ConA, and its displacement and release is proportional to the glucose concentration. A solution of ConA-glycosylated insulin is surrounded by a macroporous, hydrophilic membrane that allows passage of glucose and insulin, but blocks plasma proteins.

A third approach consists of a polymer matrix system containing a modified basic insulin with an iso-electric point of 7.4 (trilysine-insulin) along with the enzymes glucose oxidase and catalase. Glucose is converted to gluconic acid by the following reaction:

$$\text{Glucose} + H_2O + O_2 \xrightarrow{\text{GluOx}} \text{Gluconate}^- + H^+ + H_2O_2$$

The result is a decrease in the pH in the microenvironment inside the matrix. The drop in pH increases the solubility of the modified insulin so that more insulin is released as the concentration of glucose increases (10).

Other approaches using the enzyme glucose oxidase as a sensor

have been pursued. In one example, a saturated insulin solution is surrounded by a porous membrane, the pores of which are grafted with poly(acrylic acid) (11). At physiological pH, poly(acrylic acid) chains are in the ionized, extended form, blocking the pores. When the pH decreases below 5, poly(acrylic acid) becomes unionized and the chains collapse onto the pore walls. The pores open and insulin diffuses out. This approach has the difficulty that a pH as low as 5 is difficult to produce by the glucose oxidase reaction.

Other methods use an insulin reservoir surrounded by a crosslinked hydrogel membrane the permeability of which to insulin is pH dependent. These membranes contain the ionizable tertiary amine N,N-dimethylaminoethyl methacrylate and some comonomers. The gel membranes are moderately hydrophilic at normal pH and become more hydrophilic as the pH is lowered and the tertiary amine groups are protonated. The increase in hydrophilicity and the osmotic forces generated by the ionization of the amine groups increase the degree of swelling of the membranes. This swelling stretches the mesh of the polymer network, enabling the insulin macromolecule to permeate. The permeability to insulin is rendered glucose dependent by trapping glucose oxidase and catalase into the membrane (12-14), or in an adjacent hydrophilic membrane (15,16). The major disadvantage of these systems is that insulin can clog the the membrane, or it may denature or aggregate (17). Finally, pH-sensitive bioerodible polymers have been developed for the release of insulin (18). Here again, the glucose reaction is used to generate the stimulus.

1.3 The Mechanochemical Insulin Pump

The basic problem of the reservoir type, self-regulated insulin delivery system is that insulin is required to diffuse from the aqueous reservoir through a polymeric mesh. As mentioned previously, insulin tends to form aggregates. The use of additives to maintain the peptide in solution is inconvenient because they will leak out of the device before insulin has been released. Clogging of the size-selective gel can be expected.

In order to solve the mentioned problems, a self-regulated "mechanochemical" insulin pump has been proposed (19). The term "mechanochemical" is used because the pump function by converting chemical energy into mechanical energy. The mechanochemical pumps is similar in some ways to osmotic pumps which have been used for controlled drug release. It will be useful to briefly review osmotic pumps.

Several osmotic pumps have been designed for the controlled release of drugs. The first design proposed is the Rose-Nelson pump (20). The pump consists of three chambers: a drug chamber, a low molecular salt chamber containing excess solid salt, and a water chamber. The salt and the water chambers are separated by a semipermeable membrane (permeable to water but not to salt). The difference in osmotic pressure across the membrane moves water from the water chamber into the salt chamber. The water flux increases the volume of the salt chamber, distending the latex diaphragm separating the salt and drug chambers, thereby pumping drug out of the device. As long as there is enough solid salt to maintain a saturated solution, the drug is released at a constant rate.

Several variations of the Rose-Nelson pump have been proposed. The "ALZET" pump (21) has no water chamber; it is activated by water imbibed from the surrounding physiological environment. The semipermeable membrane forms the outer rigid case (Figure 1.1). The device is loaded with the desired agent immediately prior to use. When the device is placed in an aqueous environment (e.g. subcutaneously implanted), release of the agents follows the time course set by the salt used in the salt chamber and the permeability of the outer membrane casing.

The mechanochemical insulin pump also releases insulin using an osmotic force. The difference is that the osmotic agent in the mechanochemical insulin pump produces an osmotic pressure when only the blood glucose level increases above a certain concentration above the basal level. At basal blood glucose concentration the

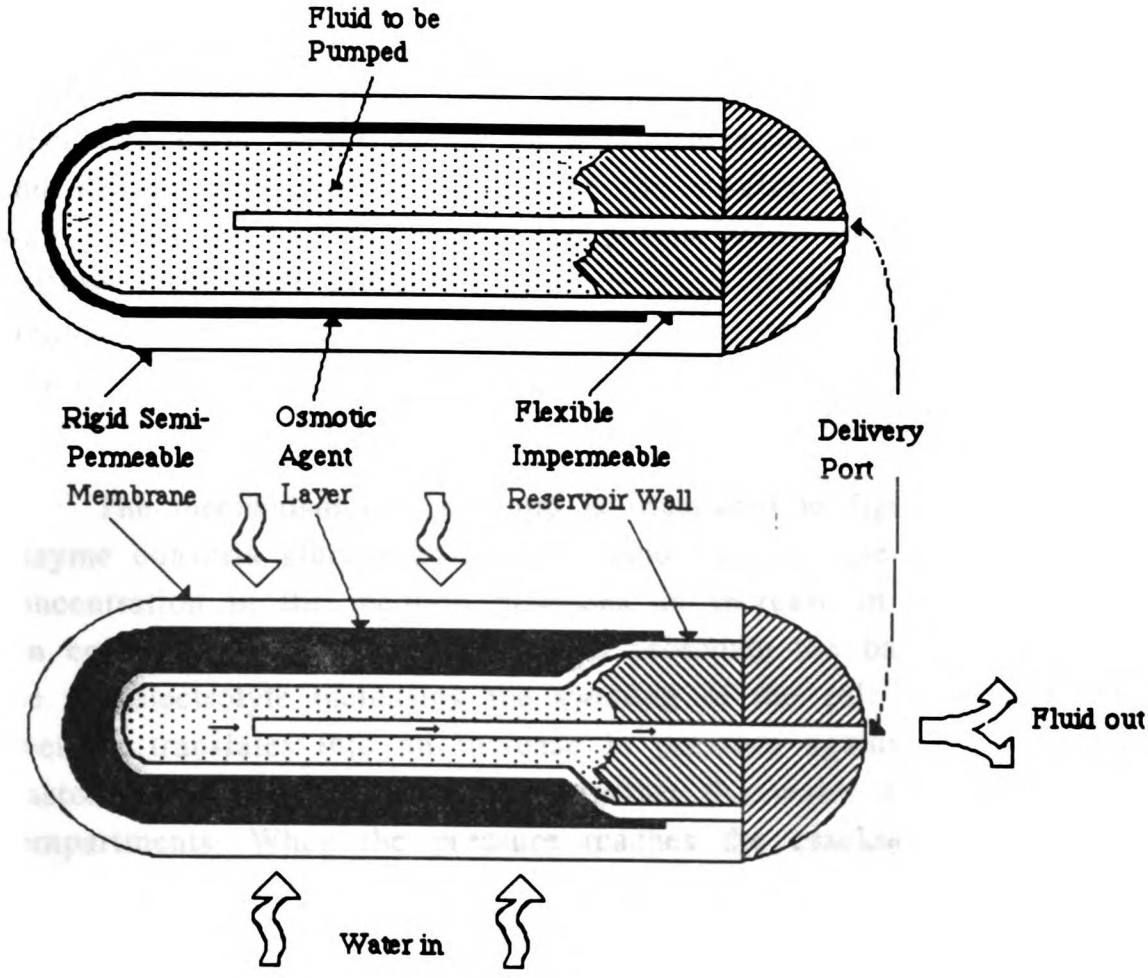

Figure 1.1. The ALZET osmotic pump.

osmotic agent is inactivated. The mechanochemical insulin pump is the first proposed example of reversible osmotic pump.

The mechanochemical insulin pump is illustrated in figure 1.2. The enzyme glucose oxidase is trapped in a hydrophilic gel (e.g. an acrylamide gel). The trapped enzyme is coupled to a polybasic gel confined between a rigid screen and an elastomeric diaphragm. The other two parts of the pump are a compartment containing water and another compartment containing the insulin formulation. One-way valves are included which can permit water inflow and insulin outflow from their respective compartments. Since the insulin compartment is separated from the polyelectrolyte compartment, insulin can be formulated in different ways to prevent aggregation or denaturalization, without affecting the polyelectrolyte.

The mechanism of the pump is illustrated in figure 1.3. The enzyme converts glucose to gluconic acid. An increase in glucose concentration in the medium produces an increase in the hydrogen ion concentration. The hydrogen ions protonate the basic groups of the polyelectrolyte increasing the swelling of the gel. This increase in swelling translates into an increase in pressure against the elastomeric diaphragm and hence against the water and insulin compartments. When the pressure reaches the cracking pressure of the one-way valve leading from the drug reservoir, the valve opens releasing a dose of insulin. After release of insulin, the blood glucose level returns to normal, the hydrogen ion concentration decreases due to diffusion and the gel contracts, lowering the pressure in the pump. When the pressure difference between the inside of the pump and the external medium is reduced below the (negative) cracking pressure of a the one-way valve leading to the water chamber, water will flow into the chamber in a volume equal to the insulin formulation expelled from the pump.

1.4 Linear Polyelectrolytes as Osmotic Agents for the Mechanochemical Insulin Pump

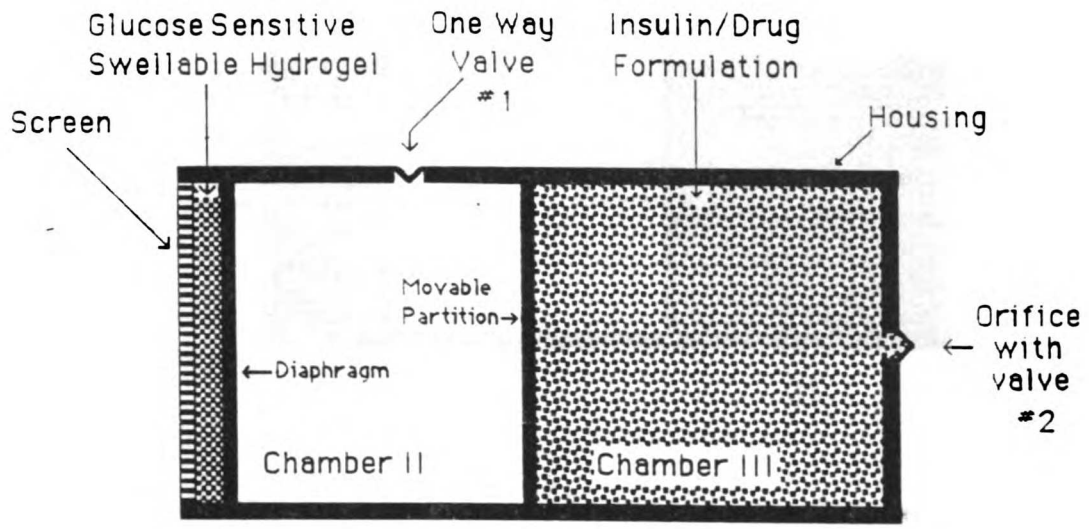

Chamber I - Polymer System, Glucose oxidase membrane (sensor)

Chamber II - Aqueous Fluid Compartment

Chamber III - Drug Compartment

Figure 1.2. Schematic diagram of the proposed mechanochemical insulin pump.

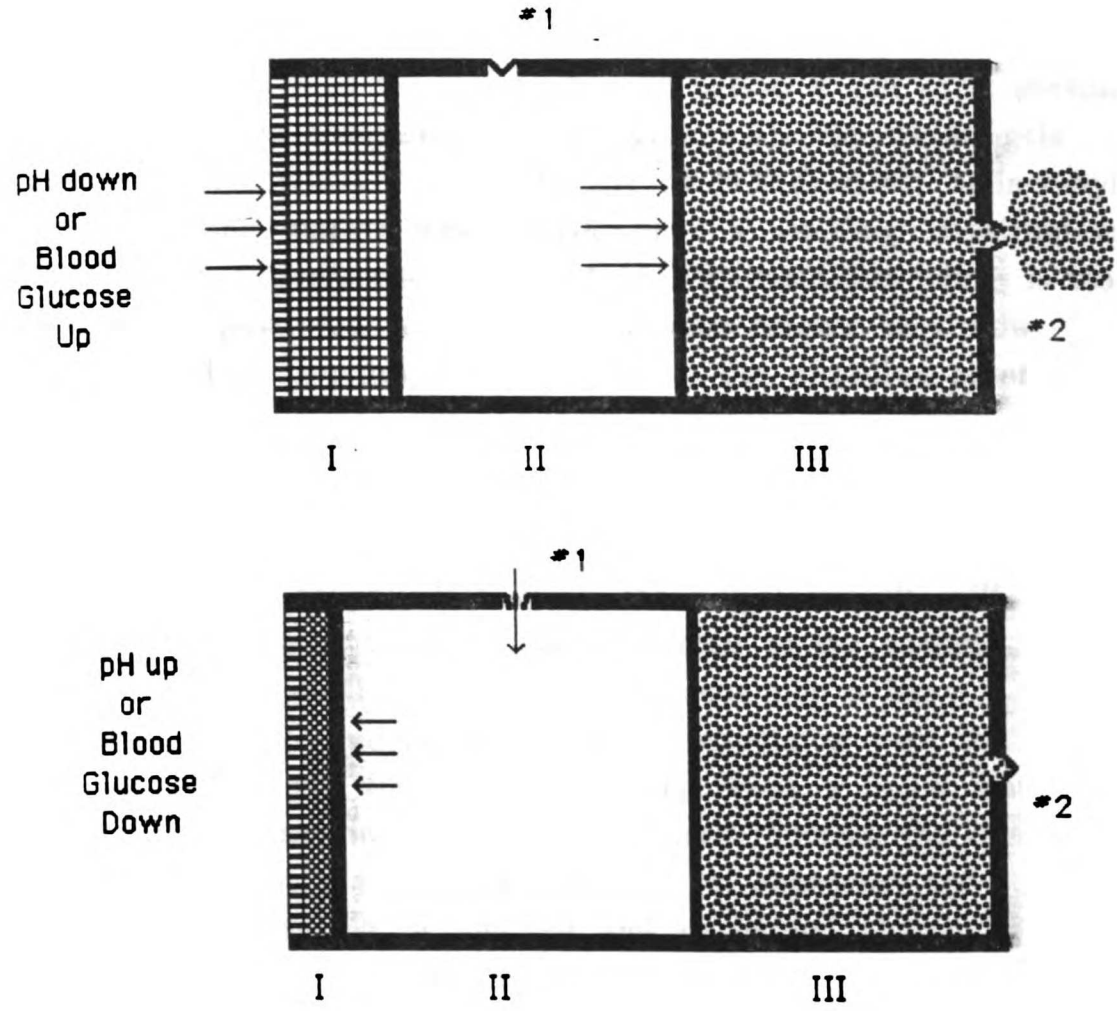

Figure 1.3. Mechanism of action of the proposed mechanochemical insulin pump.

The use of a crosslinked gel as the "engine" for the proposed "mechanochemical" pump presents several problems. Difficulties are observed when trying to load a gel into a small compartment. If the gel is too large, excess pressure develops in the pump. If the gel is too small, then it must fill the void space before it can exert pressure on the formulation compartment (see figure 1.4). The model gels studied for this application, copolymers of N,N-dimethyl aminoethyl methacrylate and methyl methacrylate have a swelling transition at a pH of 6.6 at an ionic strength of 0.1 M. This transition point is too far below the physiological pH. The gels also present very slow swelling kinetics, especially at pHs close to the transition point (22,23).

If a linear (uncrosslinked) polyelectrolyte is confined in a finite volume by a semipermeable membrane (permeable to water and microions but not to polyelectrolyte), the polyelectrolyte will develop Donnan osmotic forces upon ionization, similar to the osmotic forces that cause gels to swell. A liquid system containing a linear polyelectrolyte could reduce the problems associated with the use of gels as osmotic agents for the insulin pump. First, a liquid system always fills the space in which it is contained. Second, the crosslinks in a gel produce an elastic force opposing gel expansion and preventing interdiffusion of charged and uncharged chains, thus slowing down the osmotic expansion. Therefore, liquid polyelectrolyte systems without crosslinks may be more efficient mechanochemical energy converters than gels.

On the other hand, it must be recognized that a liquid system will require an extra component: the semipermeable membrane. In addition to making the system somewhat more complex, this membrane will add an extra barrier to the transport process that must occur for osmotic pressure to occur.

1.5 Other Applications of Polyelectrolytes

Polyelectrolytes (24) are polymers having repeating ionizable

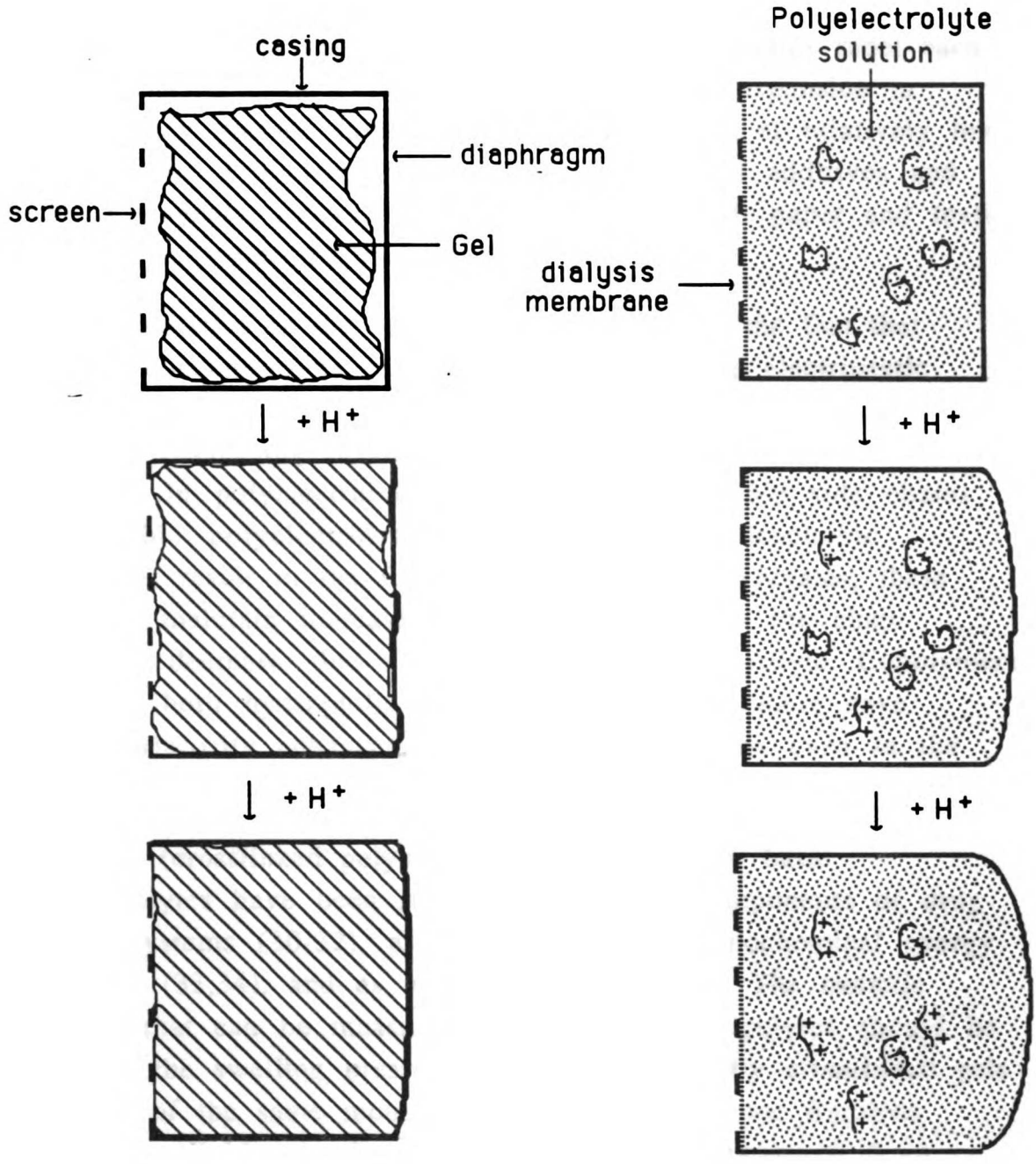

Figure 1.4. Pressure produced by pH-sensitive crosslinked gels and linear polyelectrolytes.

groups. The ionized groups in the polyelectrolyte chains repel each other, producing chain expansion. Because of this expansion in solution, they provide large viscosity enhancement at relatively low concentrations. Polyelectrolytes are widely used as additives and thickening agents, especially in the pharmaceutical, paper and textile industries, in water treatment and oil recovery.

A limitation in the use of polyelectrolytes is the fact that moderate concentrations of electrolytes screen the electrostatic repulsions between the charges and decrease the degree of polyion expansion, decreasing in this way the viscosity enhancement properties. In polyelectrolytes containing hydrophobic side chains (hydrophobic polyelectrolytes), intermolecular hydrophobic associations result in the formation of polymer aggregates; these aggregates maintain increased viscosity, even when the chain dimensions decrease, due to the screening by electrolyte. Copolymers containing both hydrophilic and hydrophobic monomers have provided viscosity enhancement at low concentration even in the presence of electrolytes (25-29).

Gels (crosslinked polymers) of weak acidic or basic polyelectrolytes have been studied as possible components of drug delivery systems (30-32), as mediators of mechanochemical energy conversion (33,34), and as ion-exchangers (35,36). The osmotic pressures that can be measured in linear polyelectrolytes should be similar to the swelling pressures occurring in lightly crosslinked gels consisting of the same monomers at the same volume fractions. Therefore, colloid osmotic (or Donnan) pressure measured from liquid polyelectrolyte systems can explain the swelling behavior of polyelectrolyte gels in response to changes in pH and ionic strength (22, 23, 31-33, 37-40).

1.6 Scope of Thesis

An appropriate polyelectrolyte to be used in the "mechanochemical" insulin pump has to be osmotically inactive at

normal blood glucose concentrations. When the concentration of blood glucose increases above basal levels, the polyelectrolyte has to "turn on" and become osmotically active in order to release insulin. These requirements can be achieved by a polyelectrolyte that is unionized at physiological pH, but becomes protonated when the local pH drops below 7.4 (after enzymatic conversion of glucose). In order to have a margin of safety, in case of a naturally occurring drop in pH (i.e. metabolic acidosis), protonation at pH 7.2 would be appropriate.

Shatkay and Michaeli (41) studied the titration behavior of poly(N,N-diethylaminoethyl methacrylate) [p(DEA)]. The hydrochloride form of the homopolymer is water-soluble, whereas the basic form is hydrophobic and water-insoluble. The titration curve of p(DEA) shows that this system has an excellent buffer capacity when the precipitate is present. The precipitate appears at pH $\cong$ 7.6, at an ionic strength of 0.1 M set by NaCl. The titration curve indicates that above pH 7.6 the polyelectrolyte is unionized and consequently osmotically inactive. When acid is added to the medium the polyelectrolyte ionizes and should become osmotically active, with very little change in the pH of the solution. This last observation indicates that the ionization is a very efficient process.

Our goal is to modify p(DEA) in ways that fulfill the properties required for the "mechanochemical" pump. We changed the hydrophobicity of the polyelectrolyte by intercalating hydrophobic or hydrophilic unionizable comonomers into the polyelectrolyte chains. The comonomers used are the hydrophilic 2-hydroxyethyl methacrylate (HEMA) and the hydrophobic methyl methacrylate (MMA) and n-butyl methacrylate (BMA). The structures of these comonomers are shown in figure 1.4.

Chapter 2 describes of the methods and apparatus required to synthesize and purify the polyelectrolytes. In chapter 3, the polyelectrolytes are characterized. The reactivity ratios of DEA and MMA are determined, and the hydrophobicity of their copolymers are evaluated by water absorption measurements. The density of the

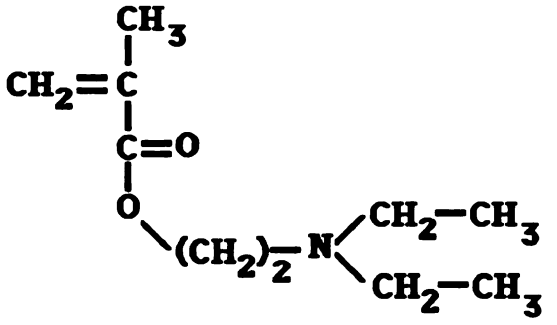

N,N-diethylaminoethyl methacrylate (DEA)

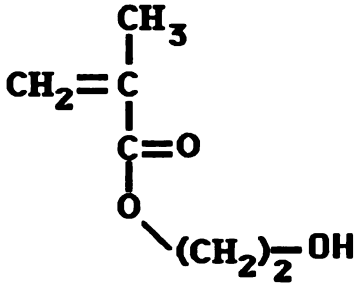

2-hydroxyethyl methacrylate (HEMA)

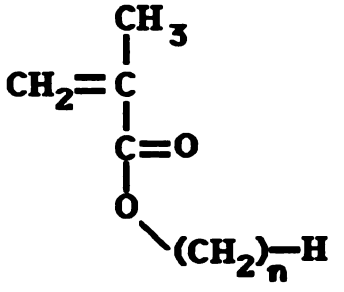

n=1 methyl methacrylate (MMA)

n=4 n-butyl methacrylate (BMA)

Figure 1.5. Structures of the monomers used to prepare the polyelectrolytes in this work.

polyelectrolytes is obtained and used to calculate the χ parameter of the copolymers of DEA and MMA using the Flory-Huggins theory. The density of the polyelectrolytes is also used in the modelling of colloid osmotic pressure in chapter 5.

The titration curves of the polyelectrolytes are presented and discussed in chapter 4. Emphasis is placed on understanding the processes of precipitation and buffering. In chapter 5, the colloid osmotic pressure produced by the polyelectrolytes is studied. Several factors are analyzed, such as copolymer composition, effect of ionic strength and degree of neutralization. Predictions of colloid osmotic pressure are obtained using models available in the literature.

The effects of introducing quaternary amine comonomers into

the p(DEA•HCl) chains, and of partially quaternizing the DEA/MMA copolymers, on the titration curves and colloid osmotic pressure are reported in chapter 6. Chapter 7 deals with the kinetics of colloid osmotic pressure development for the hydrophobic polyelectrolytes (quaternized and non-quaternized). Finally, conclusions and suggestions for future work appear in chapter 8.

References

1. O.P. Ganda, J. L. Day, J. S. Soelder, J.J. Connon, and R.E. Gleason, *Diabetes*, **27**, 525 (1978).

2. G.F. Cahill, D.D. Etzwiler, and N. Freinkel, *Diabetes*, **25**, 237 (1976).

3. A.M. Albisser, *Proc. IEEE*, **67**, 1308 (1979).

4. B. Zinman, E.F. Stokes, A.M. Albisser, A.K. Hanna, H.L. Minuk, A.N. Stein, B.S. Liebel, and E.B. Marliss, *Metabolism*, **28**, 511 (1979).

5. F. Lim and A.M. Sun, *Science*, **20**, 908 (1980).

6. M.V. Sefton, R.L. Broughton, M.E. Sugamori and C.L. Mallabone, *J. Controlled Release*, **6**, 177 (1987).

7. S.Y. Jeong, S.W. Kim., M.J.D. Eenik, and J. Feijen, *J. Controlled Release*, **1**, 57 (1984).

8. S. Sato, S.Y. Jeong, J.C. McRea, and S.W. Kim, *J. Controlled Release*, **1**, 67 (1980).

9. S.Y. Jeong, S.W. Kim, D.L. Holmberg, and J.C. McRea, *J. Controlled Release*, **2**, 143 (1985).

10. F. Fischel-Ghodsian, L. Brown, E. Mathiowitz, D. Brandenburg and R. Langer, *Proc. Natl. Acad. Sci.*,**85**, 2403 (1988).

11. H. Iwata and T. Matsuda, *J. Membr. Sci.*, **38**, 185 (1988).

12. J. Kost, T.A. Horbett, B.D. Ratner, and M. Singh, *J. Biomed. Mater. Res.*, **19**,1117 (1984).

13. G. Albin, T.A. Horbett, and B. Ratner, *J. Controlled Release*, **2**, 153 (1985).

14. G. Albin, T.A. Horbett, S.R. Miller, and N.L. Ricker, *J. Controlled Release*, **6**, 267 (1987).

15. K. Ishihara, M. Kobayashi, N. Ishimaru and I. Shinohara, *Polym. J.*, **16**, 625 (1984).

16. K. Ishihara and K. Matsui, *J. Polym. Sci., Polym. Lett. Ed.*, 24, 423

(1986).

17. W.D. Lougheed, H. Woulfe-Flanagan, J.R. Clement, and A.M. Albisser, *Diabetologia*, **19**, 1 (1980).

18. J. Heller, *J. Controlled Release*, **8**, 111 (1987).

19. R.A. Siegel and B.A. Firestone, *Journal of Controlled Release*, **11**, 181 (1990).

20 S. Rose and J.F. Nelson, *Australian J. Exp. Biol.*, **33**, 415 (1955).

21. F. Theeuwes and S.I. Yum, *Ann. Biomed. Eng.*, **4**, 343 (1976).

22. R.A. Siegel and B.A. Firestone, *Macromolecules*, **21**, 3254 (1988).

23. B.A. Firestone and R.A Siegel, *Polym. Commun.*, **29**, 204 (1988).

24. R.M. Fuoss, *Science*, **108**, 545 (1948).

25. D.N. Schultz, J.J. Kaladas, J.J. Maurer, J. Block, S.J. Pace, and W.W. Schulz, *Polymer*, **28**, 2110 (1987).

26. C.L. McCormick, T. Nonaka, and C.B. Johnson, *Polymer*, **29**, 731 (1988).

27. P.L. Valint and J. Bock, *Macromolecules*, **21**, 175 (1988).

28. K.T. Wang, I. Iliopoulos, and R. Audebert, *Polym. Bull.*, **20**, 577 (1988).

29. J.C. Middleton, D. Cummins, and C.L. McCormick, *Polymer Preprints*, 348 (1989).

30. R.A. Siegel, M. Falamarzian, B. Firestone, and B.C. Moxley, *J. Controlled Release*, **8**, 179 (1988).

31. M. Pradny and J. Kopecek, *Makromol. Chem.*, **191**, 1887 (1990).

32. L. Brannon-Peppas and N.A. Peppas, *Biomaterials*, **11**, 635 (1990).

33. W. Kuhn, B. Hargutay, A. Katchalsky, and H. Eisenberg, *Nature*, **165**, 515 (1950).

34. W. Kuhn, A. Ramel, D.H. Walters, G. Ebner, and H.J. Kuhn, *Fortschr.*

Hochpolym-Forsh., **1**, 540 (1960).

35. F. Helfferich, Ion Exchange, McGraw-Hill, New York, 1962.

36. J. Marinsky, Ion Exchange, Ed.; Marcel Dekker: New York, NY, 1966, Vol. 1.

37. I. Michaeli and A. Katchalsky, *J. Polym Sci.*, **23**, 638 (1957).

38. J. Hasa, M. Ilavsky, and K. Dusek, *J. Polym. Sci.*, **13**, 253 (1975).

39. J. Ricka and T. Tanaka, *Macromolecules*, **17**, 2916 (1984).

40. P.E. Grimshaw, J.H. Nussbaum, M.L. Yarmush and A.J. Grodzinsky, *J. Chem. Phys.*, **93**, 4462 (1990).

41. A. Shatkay and I. Michaeli, *J. Phys Chem.*, **70**, 3777 (1966).

Chapter 2

Polyelectrolyte Preparation

2.1 Introduction

In this chapter, the methods and apparatus used to prepare and purify linear poly(N,N-diethylaminoethyl methacrylate•HCl), poly(N,N-diethylaminoethyl methacrylate•HCl/n-alkyl methacrylate) linear copolymers, and the free base forms, are described. The chapter also includes the methods for monomer and initiator purification, a requirement for well-controlled polymerization (1).

2.2 Materials and Apparatus

The vinylic monomers methyl methacrylate (MMA), butyl methacrylate (BMA), 2-hydroxyethyl methacrylate (HEMA), N,N-diethylaminoehtyl methacrylate (DEA) and the free radical initiators 2,2'-azobisisobutyronitrile (AIBN) and ammonium persulfate were obtained from Polysciences, Inc. Water was double distilled and deionized using the Barnstead Nanopure System. Methanol (Fisher Scientific, A.C.S. grade), absolute ethanol (Gold Shield Chemical Company), the antioxidant Ethanox 330 (1,3,5-trimethyl-2,4,6-tris[3,5-di-tert-butyl-4-hydroxybenzyl] benzene) (Ethyl Corporation) and cuprous chloride (Aldrich Chemical Company, Inc.) were all used as received. Temperature in the polymerizations was controlled using a Lauda Model MS immersion Circulator (Fisher Scientific).

2.3 Monomer Storage and Purification

Commercially supplied monomers for addition polymerization contain polymerization inhibitors or stabilizers which prevent polymerization during shipment and storage. Esters of methacrylic acid usually contain the inhibitor hydroquinone (1,4-dihydroxybenzene, HQ) or hydroquinone methyl ether (MEHQ) at levels of 10-2000 ppm (2). HQ or MEHQ can be removed by distillation of the monomer, extraction with dilute NaOH solutions or

by passing the monomer through an anion exchange resin. Distillation of the monomers under reduced pressure was the most convenient method of monomer purification for our purposes. After the inhibitor is removed, the monomer is used immediately or stored under an inert atmosphere (nitrogen or argon) in a tightly sealed container at -20°C.

2.3.1 Monomer Distillation

All n-alkyl methacrylates used, N,N-diethylaminoethyl methacrylate and 2-hydroxyethyl methacrylate are liquid at room temperature. The apparatus used in the distillation procedure is shown in Figure 2.1. An antioxidant was added to the monomers to suppress heat-induced polymerization. Ethanox 330 was used in the distillation of n-alkyl methacrylates and DEA. In the case of 2-hydroxyethyl methacrylate (a more hydrophilic monomer), cuprous chloride was used as the antioxidant (3). The boiling points of the monomer are listed in table 2.1. All distilled monomers are colorless, transparent liquids. As a qualitative check for the presence of polymer, a few drops of distilled monomer can be added to methanol. Turbidity indicates the presence of polymer.

Table 2.1. Boiling Points of Monomers.

Monomer	Formula Weight	Boiling Point (°C)	Reference
methyl methacrylate	100.1	99-100 (760 mm Hg)	(2)
n-butyl methacrylate	142.2	163-164 (760 mm Hg)	(2)
2-hydroxyethyl methacrylate	130.14	80 (5 mm Hg)	(3)
N,N-diethylaminoethyl methacrylate	185.28	108-109 (25 mm Hg)	(4)

Procedure:

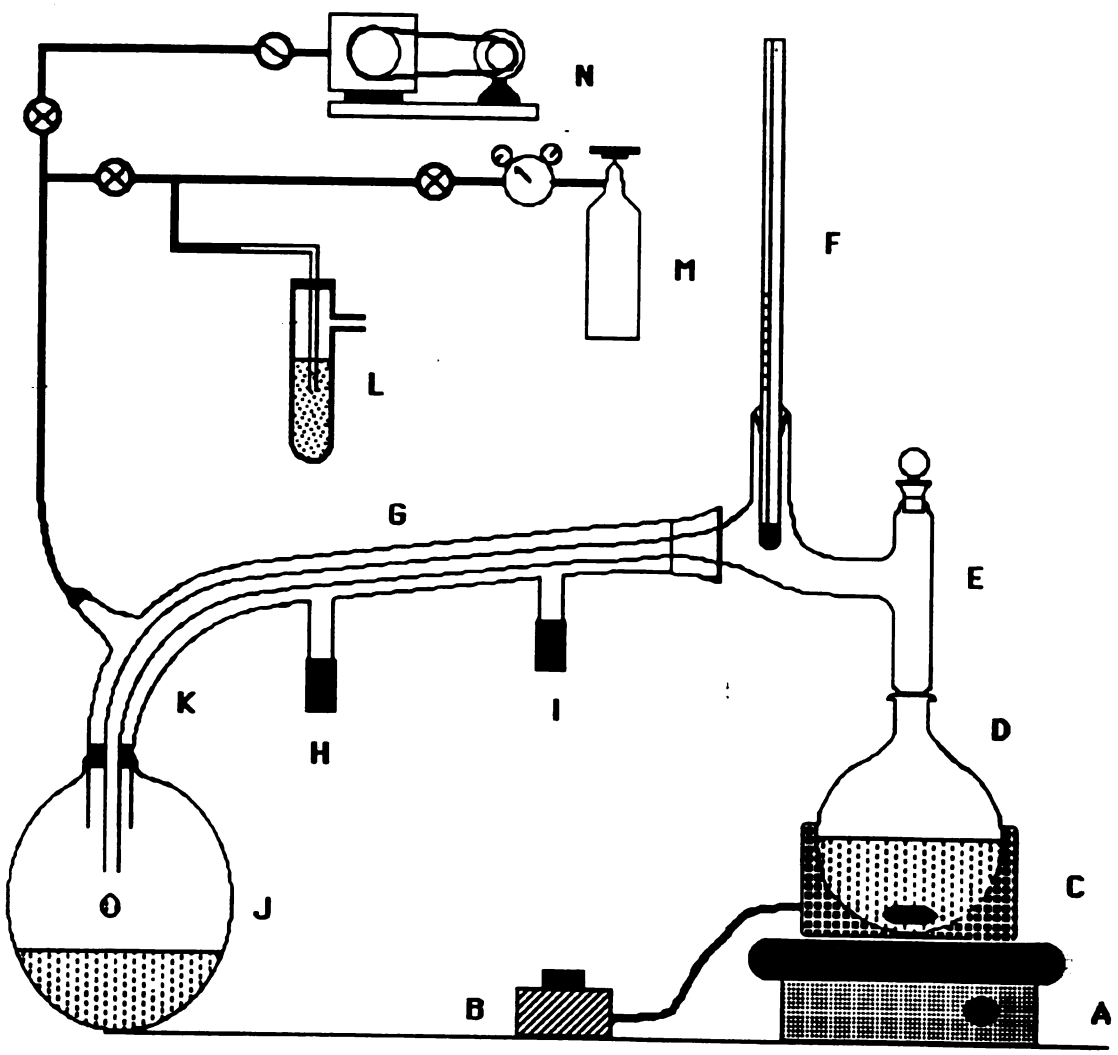

Figure 2.1 Apparatus for the vacuum distillation of monomers. A, magnetic stirrer; B, Variac voltage regulator; C, heating mantle; D, distillation flask; E, Claisen head; F, thermometer; G, condenser; H, water inlet; J, receiving flask; K, vacuum adapter; L, bubbler; M, argon tank; N, vacuum pump.

1) The distillation flask is filled with monomer to not more than 50% of the flask's capacity.

2) Approximately 100 mg/100 ml monomer with the proper antioxidant is added. The solution is vigorously stirred with a magnetic bar.

3) A vacuum pump equipped with a cold trap (dry ice/ethanol) is attached to the system. Vacuum is applied.

4) The distillation head is connected. The temperature is slowly increased.

5) The first distilled fraction is discarded (5-10 ml). The major fraction is collected.

6) Distillation is stopped by removing the heating mantle. The system is purged with argon. The distilled monomer is poured into a bottle (preferably amber) under argon. The bottle is tightly capped and Parafilm is wrapped around the cap to exclude moisture. The bottle is stored in the freezer at -20°C.

2.4 Purification of AIBN

Commercial grade AIBN from Polysciences is a white granular solid. It is purified by recrystallization from ethanol/water before use in copolymer synthesis.

Procedure:

1) A solution of crude AIBN in absolute ethanol (approximately 25 mg/ml) is prepared. Sonication is usually necessary for complete dissolution.

2) Solution is filtered.

3) Water is added to the filtrate with stirring until the solution becomes turbid (solution composition at this point is approximately 7/10 water/ethanol (v/v)).

4) Solution is filtered to isolate crystals.

6) Crystals are air dried in the dark at room temperature for several hours and then dried under vacuum at room temperature for 24 hours. Recrystallized AIBN is stored at 4°C in a tightly sealed bottle wrapped with Parafilm to exclude moisture.

A typical yield of AIBN after recrystallization is 70-80%.

2.5 Polyelectrolyte Preparation

2.5.1 Materials

The purification of the monomers methyl methacrylate (MMA), butyl methacrylate (BMA), 2-hydroxyethyl methacrylate (HEMA) and N-N-diethylaminoethyl methacrylate (DEA), and the radical initiator 2,2'-azobisisobutyronitrile (AIBN) are described above. Diethyl ether (Fisher Scientific), NaCl (Fisher Scientific), H_2SO_4 conc. (Mallinckrodt, Inc.), HCl conc. (Fisher Scientific), Na_2SO_4 (Fisher Scientific), and ammonium persulfate Polysciences Inc.) were analytical reagent grade and were used as received.

2.5.2 p(DEA•HCl) Synthesis

P(DEA•HCl) was synthesized as the hydrochloride by a free radical aqueous solution polymerization according to the method reported by Shatkay *et al.* (4).

Procedure:

1) A 100 ml sample of the monomer was added to 2000 ml of dry diethyl ether at room temperature. Dry gaseous HCl, generated by addition of H_2SO_4 conc. to NaCl, is passed

through the solution with cooling and stirring. DEA•HCl monomer precipitates as a white powder.

2) The precipitate is filtered with a glass filter and subsequently dissolved in an excess of HCl.

3) On addition of 2 liters of dry diethyl ether, the hydrochloride monomer salt precipitates. The precipitate is washed with dry ether and dried in vacuo at room temperature.

4) The polymerization is carried out in aqueous solution (approximately 400 g of monomer per liter) at 40°C with ammonium persulfate (0.55 g/l) as initiator.

5) After 5 hr, an equal volume of methanol is added. The resulting solution is divided into lots of 250 ml, and each lot is poured into 1 liter of acetone. Poly (DEA•HCl) precipitates.

6) The precipitate is filtered onto a glass filter and dried to a constant weight in vacuum at room temperature.

2.5.3 p(DEA•HCl/methacrylates) Synthesis.

To synthesize copolymers of DEA•HCl with different unionizable methacrylates, the method of p(DEA•HCl) synthesis has to be modified because of the insolubility of the methacrylates in water. The approach used is to synthesize the copolymers in the neutral form by a free radical polymerization (using AIBN as initiator) in a suitable solvent, followed by the conversion to the hydrochloride salt of the amine groups of DEA. The reaction is carried to less than 10% conversion in order to maintain a relatively constant concentration of monomers in the feed, and hence to prevent composition drift. The time required to obtain 10% conversion varies with the proportion of monomers, decreasing as the proportion of MMA in the feeding solution increases. For a initial composition of

DEA/MMA 50/50 w/w%, the time required for less of 10% conversion is 20 min.

Procedure:

1) A solution containing a methacrylate monomer and DEA at the desired composition is prepared in a round bottom flask at room temperature. AIBN and methanol are added to the mixture.

2) The flask is fitted with a manifold and degassed for 5 minutes by applying a light vacuum with stirring.

3) The flask is sealed with a rubber septum and the solution is bubbled with argon.

4) The solution is reacted for 20 minutes at 70 °C in a water bath.

5) The reaction is stopped by cooling the reaction flask with running water. Then the reaction mixture is poured slowly with stirring into distilled water. A white precipitate appears.

6) The precipitate is filtered and dissolved in the minimum amount of ethanol. The resulting solution is filtered onto a glass filter, poured into dry ethyl ether, and dried with Na_2SO_4.

7) Dry gaseous HCl, generated by adding concentrated H_2SO_4 to NaCl, is passed through the solution with cooling and stirring. Poly (DEA•HCl/alkyl methacrylate) precipitates as a white powder.

8) The precipitate is filtered onto a glass filter and subsequently dissolved in excess HCl.

9) The resulting solution is poured into acetone. Poly (DEA•HCl/alkyl methacrylate) precipitates.

10) The precipitate is filtered onto a glass filter and dried to constant weight under vacuum at room temperature.

2.5.4 p(DEA/methacrylates) Synthesis.

The synthesis of the free base of the copolymer follows the first 5 steps of the hydrochloride synthesis given in the previous subsection; the remaining steps deal with the purification of the free base copolymers.

6) The copolymer is dissolved in methanol (40 ml methanol/g polymer).

7) The resulting solution is poured slowly with stirring into distilled water. The copolymer precipitates.

8) The polymer is filtered and dried in vacuo at room temperature.

9) The polymer is dissolved in methylene chloride. Sodium sulfate is added to the solution as a dessicant. The solution is filtered and the solvent is eliminated by evaporation under vacuum.

2.5.5 p(DEA) Synthesis

The solvents used for the copolymers of DEA with the methacrylates (i.e. methanol, methylene chloride, etc.) seem to act as plasticizers for the homopolymer of DEA. In other words, it is very difficult to obtain a homopolymer free of organic solvent. For this reason we decided to obtain a pure sample of p(DEA) by emulsion polymerization. With this polymerization method, no organic solvent is required for synthesis and purification of the homopolymer. The polymerization mixture was (5):

DEA	9.2 g
distilled water	18 ml

lauryl sulfate	0.2477 g
Ammonium persulfate	0.0323 g.

The mixture was polymerized at 40°C with stirring. After 12 hrs of reaction the polymerization mixture was poured into a beaker containing distilled water. The polymer precipitated. It was separated by filtration, washed with distilled water and dried under vacuum at room temperature for several days.

References

1. E.A. Collins, J. Bares, and F. W. Billmayer, Jr., Experiments in Polymer Science, Chapter 3 & 4, John Wiley & Sons, New York 1973.

2. Chemical and Supply Catalog, Polysciences, Inc., 1990-91.

3. G.R. Davidson III and N.A. Peppas, *Journal of Controlled Release*, **3**, 243 (1986).

4. A. Shatkay and I. Michaeli, *J. Phys. Chem.*, **70**, 3777 (1966).

5. P.J. Flory, Principles of Polymer Chemistry, Chapter V, Cornell University Press 1953.

Chapter 3

Polyelectrolyte Characterization

3.1 Introduction

In this chapter, the copolymers of DEA and MMA are characterized. The composition of the polymers is determined by elemental analysis. The monomer reactivity ratios are then calculated to find the most probable sequential distribution of the monomers in the polymer chains. The density of the polyelectrolytes is determined by sedimentation of the free base form of the polymers in a density gradient solution. The χ parameter (from the Flory-Huggins theory), which measures the copolymer's hydrophobicity, is determined from the amount of water adsorbed by the polymer at various vapor pressures.

3.2 Copolymer Compositions

Purified polymer samples were sent to the Microanalytical Laboratory in the Department of Chemistry, University of California, Berkeley for carbon and nitrogen elemental analysis. For the hydrochloride salts, the content of chloride was also obtained.

The exact composition of the copolymer with respect to the molar proportion of the monomers incorporated into the chains can be determined from the percent of carbon and nitrogen found in the elemental analysis. The contribution from the initiator is ignored in the calculations since the initiator constitutes a very small percentage of the product. The equations used to determinate the mole percent of the copolymers incorporated into the chains are listed below:

$$\%DEA = 100-\%copolymer \tag{3.2.1}$$

$$\%copolymer = 100L/(L + 1) \tag{3.2.2}$$

where

$$L = [(1.166\ \%C/\%N) - 10]/D \qquad (3.2.3)$$

In the latter equation D is the number of carbon atoms in the comonomer.

The fraction of salt conversion for the hydrochlorides is determined from the equation:

$$\text{Ionization (salt conversion)} = 0.394(\%Cl/\%N) \qquad (3.2.4)$$

The numerical constants in the above equations serve to convert reported weight percentages (%C, %N, %Cl) to mole percentages.

3.3 Determination of Monomer Reactivity Ratios

It was found that the composition of the copolymers differs from the composition of the comonomer feed in the copolymerization mixture. This is due to the fact that the different monomers have different relative rates of polymerization (1). This difference in "reactivity" also determines the statistical arrangement of units along the copolymer chain (2). Hence, the reactivity of the comonomers is determined to reveal the most probable sequential distribution of the monomers in the copolymer chains.

3.3.1 Kinetics of chain propagation in copolymerization

In copolymers synthesized by addition polymerization from a reaction mixture of two monomers, M_1 and M_2, two types of propagating radicals are considered, one with M_1 at the propagating end and the other with M_2 (3). We represent these by $-M_1^{\bullet}$ and $-M_2^{\bullet}$, where $-M_1^{\bullet}$ represents a growing chain with an $M_1^{\bullet}$ radical at its end, and $-M_2^{\bullet}$ is defined analogously. If we assume that the reactivity of a particular radical depends only on the monomer unit at the end of the growing chain, four propagation reactions are then possible

Reaction			Rate	
$-M_1^{\bullet} + M_1$	$\longrightarrow$	$M_1^{\bullet}$	$k_{11}[-M_1^{\bullet}][M_1]$	(3.3.1)
$-M_1^{\bullet} + M_2$	$\longrightarrow$	$M_2^{\bullet}$	$k_{12}[-M_1^{\bullet}][M_2]$	(3.3.2)
$-M_2^{\bullet} + M_1$	$\longrightarrow$	$M_1^{\bullet}$	$k_{21}[-M_2^{\bullet}][M_1]$	(3.3.4)
$-M_2^{\bullet} + M_2$	$\longrightarrow$	$M_2^{\bullet}$	$k_{22}[-M_2^{\bullet}][M_2]$	(3.3.4)

The rates of monomer incorporation into the copolymer are equal to the rates of monomer depletion from the feed, and are given by

$$-d[M_1]/dt = k_{11}[-M_1\bullet][M_1] + k_{21}[-M_2^{\bullet}][M_1] \quad (3.3.5)$$

$$-d[M_2]/dt = k_{12}[-M_1\bullet][M_2] + k_{22}[-M_2^{\bullet}][M_2] \quad (3.3.6)$$

Due to their high reactivity, free radicals undergo mutual termination very rapidly and are removed from the reaction system. If the initiation reaction is slow, steady state is attained where the rate of formation of radicals is balanced by their rate of disappearance. Under these conditions, a steady state concentration of free radicals is achieved. As long as the initiator concentration is essentially unchanged, the equilibrium concentrations of the propagating free radicals can be assumed to be constant. This is the steady-state assumption (4). Applying this assumption to each of the radicals gives

$$k_{21}[M_2^{\bullet}][M_1] = k_{12}[M_1^{\bullet}][M_2] \quad (3.3.7)$$

By defining $r_1=k_{11}/k_{12}$ and $r_2=k_{22}/k_{21}$ and combining eqns. 3.3.5, 3.3.6, and 3.3.7 it can be shown that the composition of copolymer being formed at any instant is given by

$$\frac{d[M_1]}{d[M_2]} = \frac{[M_1]}{[M_2]} \frac{r_1[M_1] + [M_2]}{[M_1] + r_2[M_2]} \quad (3.3.8)$$

Equation 3.3.8 is known as the *copolymer ratio equation.*

The monomer reactivity ratios r_1 and r_2 are the ratios of the rate constants for a given radical adding its own monomer to the rate constant for its adding the other monomer. Thus $r_1 > 1$ means that the radical $M_1^\bullet$ prefers to add M_1; $r_1 < 1$ means that it prefers to add $M_2^\bullet$; and correspondingly for r_2.

3.3.2 Types of Copolymerization

Random. A copolymer system is said to be random when the two radicals show the same preference for either monomer: $r_1 = 1/r_2$. In this case, the end group on the growing chain has no influence on the rate of addition, and the two types of units are arranged at random along the chain in relative amount determined by the composition feed and the relative reactivities of the two monomers.

Alternating. Each radical prefers to react exclusively with the other monomer: $r_1, r_2 \ll 1$. The monomer alternates regularly along the chain, regardless of the composition of the monomer feed.

Block. If both r_1 and r_2 are greater than unity, each radical prefers to react with the same monomer producing blocks of the same monomer.

3.3.3 Experimental Evaluation of Monomer Reactivity Ratios

The reactivity ratios can be determined graphically using, for example, the Fineman-Ross (5) and the Kelen-Tüdos (6) methods.

In the Fineman-Ross method, the copolymer composition eqn. 3.3.8 is rewritten as

$$f = F(r_1F + 1)/(r_2 + F) \qquad (3.3.9)$$

where $f = d[M_1]/d[M_2]$ and $F = [M_1]/[M_2]$. Rearranging, one obtains:

$$F(f-1)/f = r_1F^2/f - r_2 \qquad (3.3.10)$$

If $F(f-1)/f$ is plotted versus F^2/f a straight line is obtained with slope $= r_1$ and intercept $= r_2$. Eqn. 3.3.9 can also be arranged to:

$$(f-1)/F = -r_2 f/F^2 + r_1 \qquad (3.3.11)$$

In this case, the slope of a plot of (f-1)/F vs f/F^2 is $-r_2$ and the intercept is r_1.

The f values are obtained from measuring the composition of the synthesized copolymers; F is determined from the proportion of monomers in the corresponding reaction mixture which remain approximately constant provided the polymerization is stopped before 10% completion.

A disadvantage of the Fineman-Ross method is that the experimental data are unequally weighted and the data obtained under extreme experimental conditions (very high and very low M_1) have the greatest influence on the slope of the line. More uniform weights of the experimental data can be achieved with the Kelen-Tüdos method. Here eqn. 3.3.8 is rewritten as

$$G/(\alpha + H) = (r_1 + r_2/\alpha)H/(\alpha + H) - r^2/\alpha \qquad (3.3.12)$$

where α denotes an arbitrary constant ($\alpha > 0$),

$$G = F(f-1)/f \qquad (3.3.13)$$

and

$$H = F^2/f \qquad (3.3.14)$$

$H/(\alpha+H)$ can take only those values in the interval (0,1). By plotting $G/(\alpha+H)$ as a function of $H/(\alpha+H)$, r_1 and r_2 values can be obtained.

Uniform distribution of the experimental data in the interval (0,1) can be attained by proper choice of the α value. Kelen & Tüdos suggest $\alpha = 1$ when the reactivity ratios are nearly identical. In the case of markedly different reactivity ratios, or if the choice of $\alpha = 1$ produces rather asymmetrical data distribution along the interval (0,1), then

$$\alpha = (H_M H_m)^{1/2} \qquad (3.3.15)$$

(where H_M stands for the highest of the calculated H values and H_m for the lowest value) is suggested.

3.3.4 Experiments and Results

Copolymers from five different comonomer ratio feeds were prepared by the procedure described in Chapter 2. Polymerization was stopped before 10% conversion. The total concentration of monomers was held constant at 400 g/l of methanol. The initiator concentration used was 2 g/l of methanol. Polymerization results are given in Table 3.1. The composition of the copolymers was determined by elemental analysis and the results are summarized in Table 3.2.

Table 3.1. Polymerization time and conversion for feeds of different comonomer proportions.

DEA mole fraction in feed	Polymerization time (min)	Conversion (%)
0.70	7	8.03
0.65	7	5.97
0.60	7	5.14
0.52	7	8.25
0.40	7	7.14

Table 3.2. Results of copolymerization of N,N-Diethylaminoethyl methacrylate (DEA) and methyl methacrylate (MMA)

DEA mole fraction in feed	Nitrogen % (wt%)	DEA mole % in copolymer
0.70	5.91	68.16
0.65	5.64	60.25
0.60	5.45	57.51
0.52	4.82	49.51
0.40	3.76	33.78

The reactivity ratios were calculated by both the Fineman-Ross and the Kelen-Tüdos methods. The results are given in Table 3.3 and in figures 3.1, 3.2, and 3.3. The results by the Fineman-Ross method in table 3.3 is the mean of results from the two different fits (figs. 3.1 and 3.2). The two methods yield nearly identical results. The product r_1r_2 is not far from 1, indicating that the copolymerization is essentially random.

Table 3.3. Reactivity ratios determined by Fineman-Ross and Kelen-Tüdos methods for the copolymerization of MMA (r_1) and DEA (r_2).

	Fineman-Ross	Kelen-Tüdos (α=0.687)
r_1	1.42	1.38
r_2	1.03	1.00
r_1r_2	1.46	1.38

3.4 Density of p(DEA) and DEA/MMA copolymers

3.4.1 Introduction

The densities of the free base form of p(DEA), and of some of the copolymers of DEA and MMA, were determined by the position where they equilibrate in a density gradient solution. The density gradient solution was produced by high speed centrifugation of Percoll® in 0.25 M sucrose. The density at different points of the solution in the centrifugation tube was determined by using density marker beads of known buoyant density (7). Refractive index has a linear correlation with the density of a Percoll solution and the calibration curve in figure 3.4 was used to measure density at the points where the polymers band.

3.4.1 Experimental

3.4.1.1 Materials

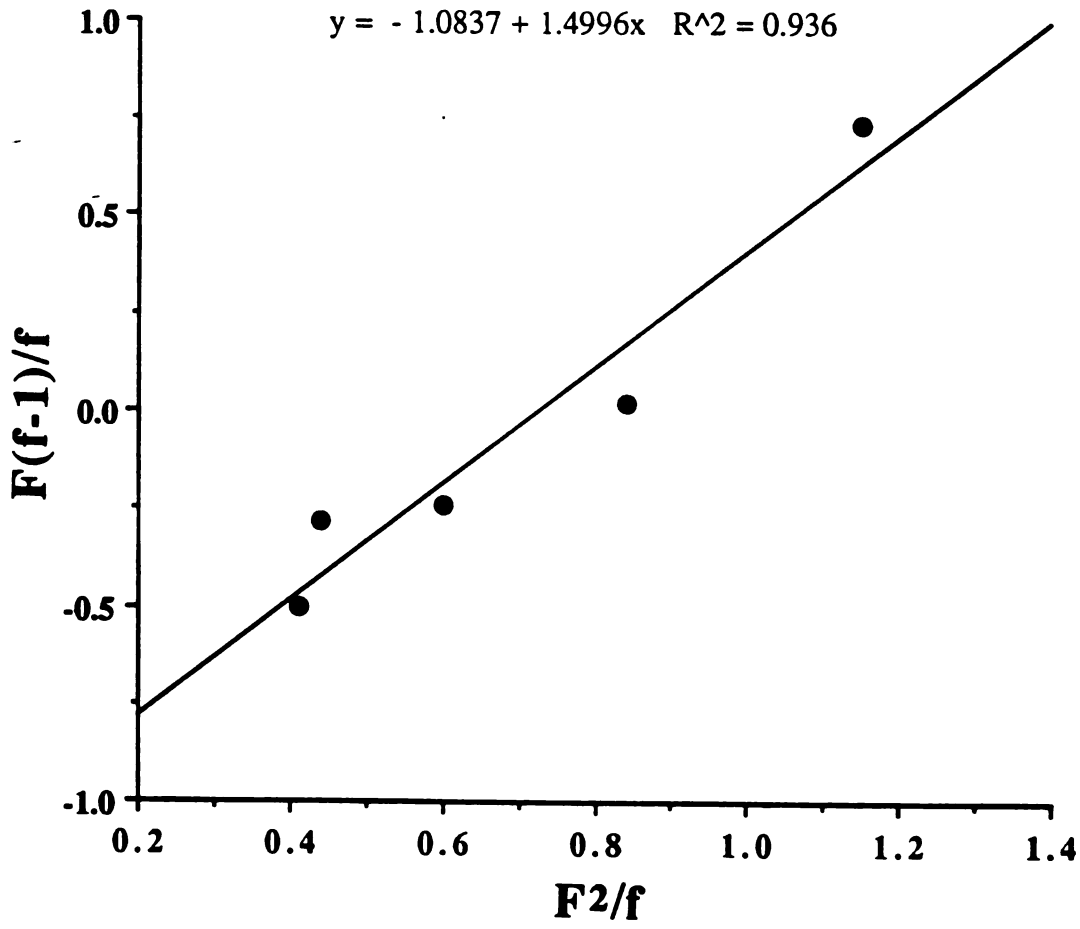

Figure 3.1. Fineman-Ross plot for the determination of monomer reactivity ratios using eqn. 3.3.10.

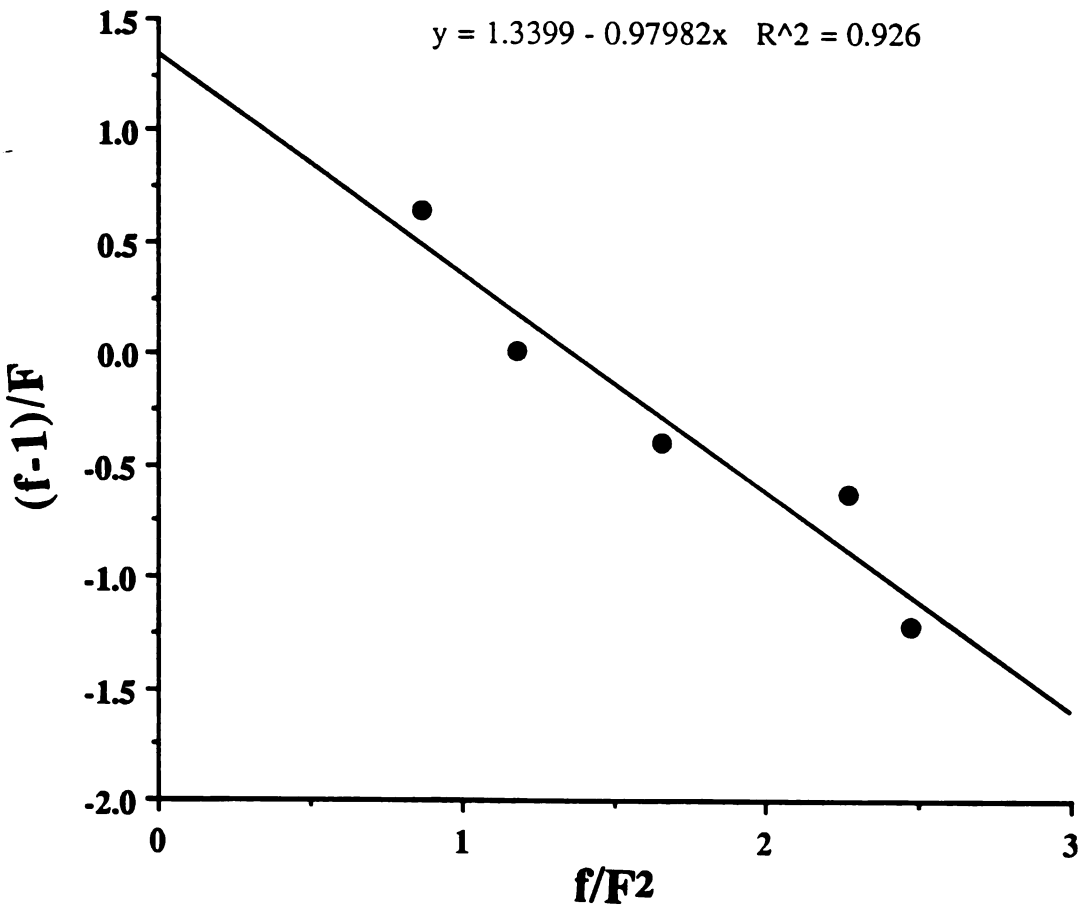

Figure 3.2. Fineman-Ross plot for the determination of monomer reactivity ratios using eqn. 3.3.11.

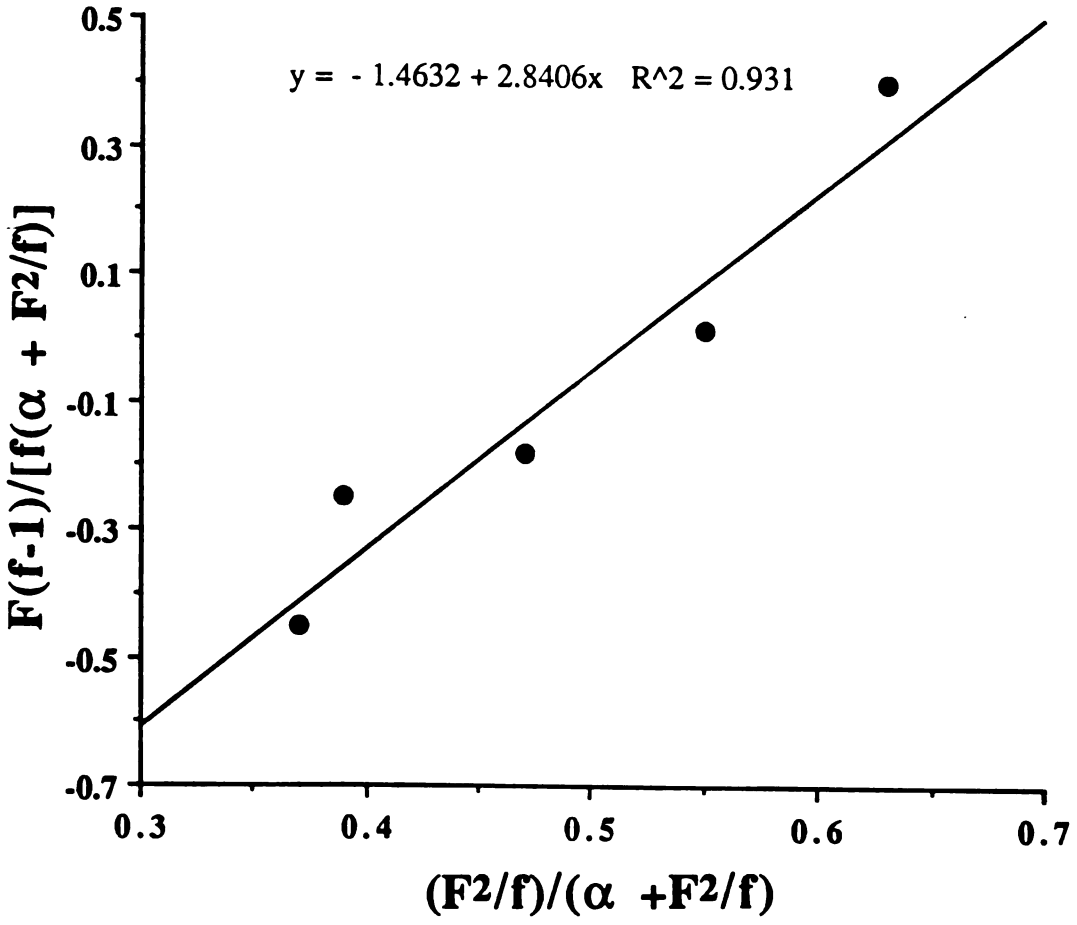

Figure 3.3. Kelen-Tüdos plot for the determination of monomer reactivity ratios (α=0.687, calculated from eqn. 3.3.15).

Sucrose (Sigma) and Percoll gradient (Pharmacia) were used as received. Density marker beads (Pharmacia) were soaked in distilled water prior to use. Water was double distilled and deionized.

3.4.1.2 Procedure

1. The gradient solution is prepared by diluting 9 parts (v/v) Percoll with 1 part (v/v) 2.5 M sucrose solution.

2. Two high speed centrifuge tubes are filled with the gradient solution. The marker beads are added to one of the tubes which acts as the external standard.

3. The tubes are spun at 20,000 rpm for one hour at a constant temperature in an ultracentrifuge. If the marker beads are not separated, the centrifugation time is prolonged.

4. The polymer sample is added to the second centrifugation tube being careful not to break the gradient.

5. The tubes are centrifuged for 30 min at 20,000 rpm.

6. After centrifugation, the positions of the density marker beads and of the polymer bands were recorded. A sample of solution is extracted from the position of the polymer band. The sample is filtered and the refractive index is measured. The density of the polymer is determined using the standard curve (Fig. 3.4). The result is compared with the expected density based upon the distance of the band from the meniscus.

3.4.3 Results

The densities of the polyelectrolytes analyzed are listed in table 3.4. A very small change in density is seen over the range of copolymer composition tested.

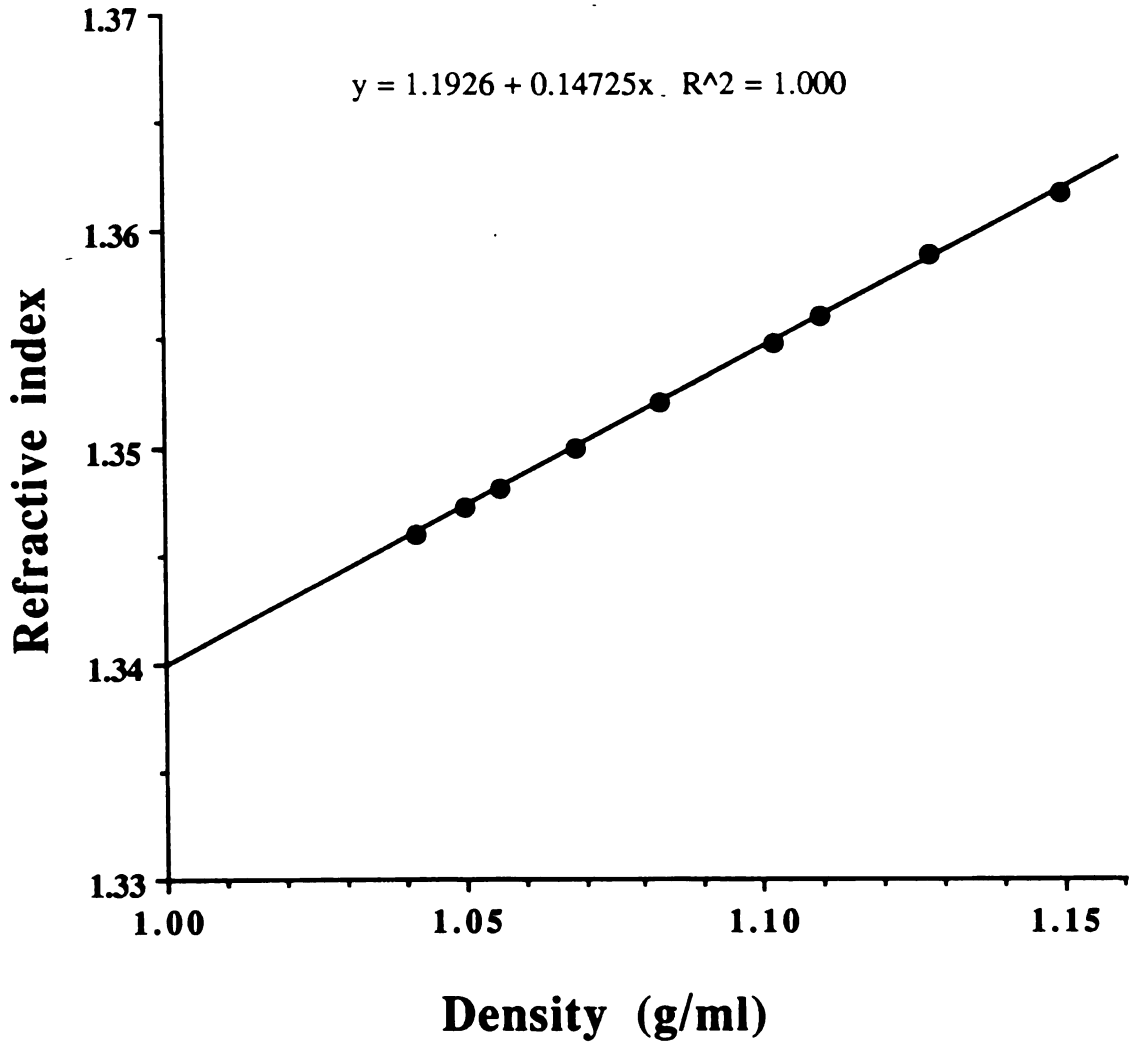

Figure 3.4. Density vs refractive index for percoll gradient solutions.

Table 3.4. Density of p(DEA) and DEA/MMA copolymers.

Polymer	Density (g/ml)
p(DEA)	1.10
p(DEA/MMA) 70/30	1.11
p(DEA/MMA) 60/40	1.11
p(DEA/MMA) 52/48	1.13

3.5 Water Sorption Experiments for p(DEA) and DEA/MMA Copolymers

3.5.1 Experimental

3.5.1.A Materials

KCl analytical grade (Fisher Scientific) was used as received. Water was distilled and deionized. Polymers, synthesized as in chapter 2, were dried for at least 24 hrs at 70°C at an applied vacuum of 25 in. Hg. P(DEA) was freeze dried before use.

3.5.1.B Water Sorption Setup

The weight of water adsorbed by a unit weight of polymer was determined using the isopiestic method (8). The chamber used was an inverted water bath sealed with plastic adhesive (figure 3.5). KCl solutions of known vapor pressure (9) were placed in a small container. Weighing bottles containing known amounts of dry polymer were placed in the chamber, beside the KCl solution. The temperature was held constant at 25 ± 0.2°C using a temperature controlled water circulator (Lauda model MS, Fisher Scientific). An empty weighing bottle was used in each chamber as a control. The polymer samples were weighed several times until they reached constant weight.

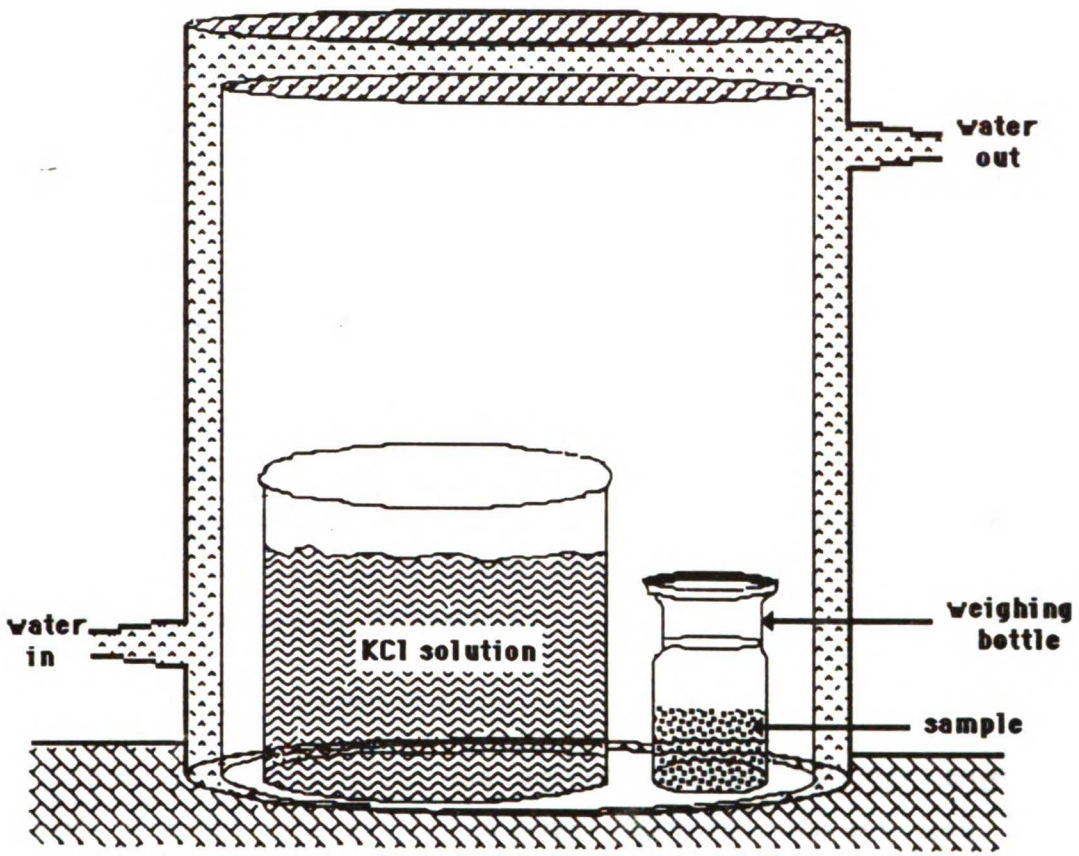

Figure 3.5. Setup for the isopiestic determination of water uptake by polymers.

3.5.2 Determination of the χ Parameter

We hypothesize that the "buffering pH" at which the copolymers precipitate (see chapter 4) can be modified by changing the hydrophobicity of the chains. The latter can be characterized by determining the degree of interaction between the polymer segments and water.

According to the Flory-Huggins theory (10,11), the change in the chemical potential of the solvent associated with the mixing of polymer and solvent is given by

$$\ln a_1 = \frac{\mu_1-\mu_1^o}{RT} = \ln v_1 + (1 - 1/x)v_2 + \chi v_2^2 \qquad (3.5.1)$$

where v_1 and v_2 are respectively, the volume fraction of solvent and polymer, x is the number of segments per polymer chain, R and T are the gas constant and the absolute (Kelvin) temperature, respectively and χ is a parameter characteristic of a given polymer-solvent pair, at a fixed temperature, defined by

$$\chi = 1/k_BT[\varepsilon_{12}-1/2(\varepsilon_{11} + \varepsilon_{22})] \qquad (3.5.2)$$

where $\varepsilon_{11}, \varepsilon_{22}, \varepsilon_{12}$, are the solvent-solvent, polymer segment-polymer segment and solvent-polymer segment contact free energies, respectively, and k_B is the Boltzmann constant. The smaller the value of χ, the greater the degree of polymer/solvent mixing. If the solvent in the system is water, then a small or negative value of χ indicates that the polymer is hydrophilic; a large value of χ indicates that the polymer is hydrophobic. The χ parameter for p(DEA) and several copolymers of DEA with MMA were determined at several water activities at 25°C.

To a first approximation, a_1 may be set equal to the relative vapor pressure P/P_0 of the diluent, P_0 being the vapor pressure when $v_1=1$ (12). χ can be determined by rearranging eqn. 3.5.1

$$\chi = [\ln(a_1/v_1)-v_2]/v_2 \qquad (3.5.3)$$

where the term 1/x in eqn. 3.5.1 is neglected because $1/x<<1$ for the system under study.

The volume fraction was readily determined from known densities of the pure components (section 3.4), assuming no volume change on mixing, i.e.

$$v_1 = 1 - v_2 \qquad (3.5.4)$$

$$v_2 = 1/[(\delta_1/\delta_2)c + 1] \qquad (3.5.5)$$

where c is the weight of penetrant sorbed per unit weight of polymer and δ_1 and δ_2 are the densities of solvent and polymer, respectively.

3.5.3 Results

Table 3.4 shows the amount of water adsorbed per gram of polyelectrolyte at several vapor pressures. The table also presents the calculated value for the χ parameter for each copolymer. χ decreases with a_1. For a given a_1, χ increases as the proportion of MMA increases indicating an increase in hydrophobicity

3.6 Discussion

The monomers reactivity ratios indicate that MMA is a more reactive monomer than DEA. This result was deduced before the calculations since the proportion of DEA incorporated into the polymers is always less than that in the polymerization mixture feed. Fortunately, the product of the reactivity ratios, r_1r_2, is very close to unity, and we can therefore conclude that the monomers are randomly distributed in the polyelectrolyte chains. This result is important. One of the purposes of the copolymerization is to increase the separation between the ionizable groups. A random polymerization ensures that, as the proportion of the unionizable comonomer is increased, the average distance between ionizable groups increases proportionally. The somewhat higher reactivity of

Table 3.4. Results of the water adsorption measurements for p(DEA) and DEA/MMA copolymers at 25°C.

Polymer	[KCl] (molal)	water activity	c (g water/g polymer)	χ
p(DEA)	0.0	1.0000	1.077	0.779
	0.5	0.9839	0.643	0.867
	1.0	0.9679	0.292	1.150
	2.0	0.9363	0.186	1.337
p(DEA/MMA)	0.0	1.0000	0.560	0.899
70/30	0.5	0.9839	0.376	1.006
	1.0	0.9679	0.207	1.250
	2.0	0.9363	0.148	1.409
p(DEA/MMA)	0.0	1.0000	0.346	1.087
60/40	0.5	0.9839	0.163	1.360
	1.0	0.9679	0.128	1.480
	2.0	0.9363	0.092	1.644
p(DEA/MMA)	0.0	1.0000	0.072	1.941
52/48	0.5	0.9839	0.042	2.329
	1.0	0.9679	0.035	2.460
	2.0	0.9363	0.023	2.789

MMA will produce slight deviations from ideality, however. For alternating copolymers, there is always an unionizable group between two ionizable groups. In this case, changing the proportion of the unionizable copolymer will increase neither the distance between ionizable groups, nor the hydrophobicity of the chains. Block copolymers, in the other hand, will contain long runs of undiluted ionizable DEA units, interspersed with long runs of neutral hydrophobic units.

For extreme block copolymers, the polymerization may yield two populations of chains; one containing unionizable monomers, the other containing monomers which can be ionized. This latter seems to

occur when DEA is copolymerized with BMA. After conversion of the copolymer to the hydrochloride form, it is very clear that the precipitate consists of two populations; one powder-like, indicating high proportion of p(DEA•HCl), the other rubbery, indicative of a high content of BMA. Even though we did not gather data to calculate the monomer reactivity ratios for BMA and DEA, it appears that block copolymers are produced. For this reason, most of our studies were carried out using copolymers of DEA and MMA.

The densities of p(DEA), and of the DEA/MMA copolymers analyzed, are very similar. There is not a significative increase in the density when the proportion of MMA is increased.

The χ parameter is dimensionless, constant at a given temperature, and independent of concentration (10,11). The χ parameters for p(DEA) and the DEA/MMA copolymers decrease as the amount of water adsorbed by the polymer increases (v_2 decreases). Similar results have been observed in other systems where either the polymer unit or the solvent possesses a dipole (12,13). χ appears to vary throughout the concentration range and eqn. 3.5.2 can be used only as a semi-quantitative approximation only.

It is important to mention that the χ for a copolymer is actually an "effective" χ due to the combination of three different χ parameters resulting from the interaction among the two different monomers and the solvent and the interaction between the two monomers (14).

For a given water activity, it can be observed that the value of χ decreases as the proportion of MMA in the polymer decreases. As the χ parameter is measuring the interaction between polymer segments in water, it can be concluded that the hydrophobicity of the chains increases as MMA is incorporated into the copolymer.

3.7 Conclusions

DEA and MMA form copolymers with a random distribution of monomers. The hydrophobicity of the comonomers increases as the proportion of MMA increases. The polymers have the same density that is virtually independent of the proportion of the comonomers.

References

1. P.J. Flory, Principles of Polymer Chemistry, Cornell University Press, Ithaca, N.Y. 1953.

2. T. Alfrey, Jr. and G. Goldfinger, *J. Chem. Phys.*, **12**, 205 (1944).

3. H.R. Allcock and F.W. Lampe, Contemporary Polymer Chemistry, Prentice-Hall 1981.

4. A. M. North, The Kinetics of Free Radical Polymerization, Pergamon Press, N.Y. 1966.

5. M. Fineman and S.D. Ross, *J. Polym. Sci.*, **55**, 123 (1961).

6. T. Telen and F. Tüdos, J. *Macromol. Sci.-Chem.*, **A9(1)**, 1 (1975).

7. Pharmacia LKB Biotechnology Products Catalog. Percoll Manual.

8. A. Martin, S. Swarbrick, and A. Cammarata, Physical Pharmacy, Lea & Febinger, Philadelphia 1983.

9. R.A. Robinson and D.A Sinclair, *J. Am. Chem. Soc*, **56**,1838 (1934).

10. P.J. Flory, *J. Chem. Phys.*, **10**, 51 (1942).

11. M. L. Huggins, *J. Chem. Phys.*, **9**, 440 (1941).

12. M.J. Newing, *Trans. Faraday Soc.*, **46**, 613 (1950).

13. C.E.H. Bawn, R.F.J. Freeman, and A.R. Kamaliddin, *Trans. Faraday Soc.*, **46**, 677 (1950).

14. K.A. Dill, *Biochemistry*, **24**, 1501 (1985).

Chapter 4

Titration Behavior of Copolymers of DEA•HCl and Unionizable Methacrylate Esters

4.1 Introduction

The titration curves of hydrophilic weak acidic or weak basic polyelectrolytes, which are soluble at any pH, are steeper than the titration curves of the corresponding monomeric acids or bases (1-3) (see figure 4.1). As the polymer chains are charged, it costs progressively more free energy to ionize the weak basic or weak acid groups (4). This phenomenon is observed as a change in the apparent pK of the polymer with degree of ionization.

In the case of hydrophilic polyacids, the titration curves can be described by using an empirical modification of the Henderson-Hasselbach equation (5)

$$pH = pK - n \log \frac{1-\alpha}{\alpha} \qquad (4.1)$$

where α is the degree of neutralization (ionization for polyacids), and pK and n are constants that depend on the ionic strength of the solution. As the ionic strength of the solution increases, the electrostatic forces are screened and the polyelectrolyte resembles more closely the monomeric form in its titration behavior. In this case, n=1 and $pK=pK_o$ ("intrinsic" dissociation constant, characteristic of the ionizable group of the polymer and independent of the ionic strength).

A theoretical analysis leads to the general potentiometric equation for polymeric acids (6,7):

$$pH = pK_o - \log \frac{1-\alpha}{\alpha} + \frac{0.4343}{kT}\left(\frac{\delta F_e}{\delta v}\right)_\kappa \qquad (4.2)$$

where k is the Boltzmann constant, T is the absolute temperature, F_e

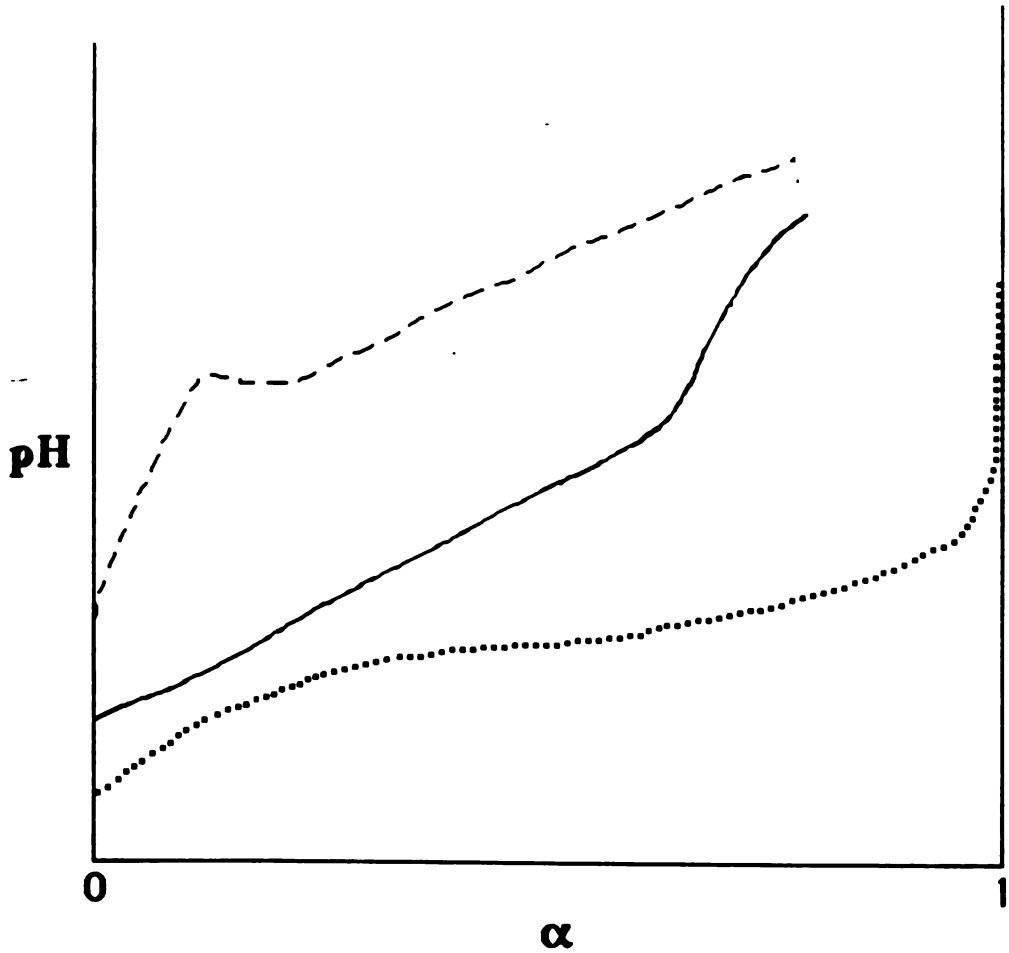

Figure 4.1. Differences between the titration curves of polyacids and a monomeric acid; (----) hydrophobic soluble polyacid (e.g. p(methacrylic acid)), (——) hydrophilic soluble polyacid (e.g p(acrylic acid)),(·····) monomeric acid (e.g. acrylic acid). α=moles of NaOH/moles acid groups (degree of neutralization).

is the free energy required to ionize the polyelectrolyte molecule up to ν negative charged groups, and κ is the inverse Debye radius determined by the concentration of small ions in solution:

$$\kappa = \left(\frac{F^2}{\varepsilon RT} \Sigma c_i^0 z_i^2 \right)^{1/2} \qquad (4.3)$$

Here F is the Faraday constant, ε is the dielectric permitivity of the medium, c_i^0 is the molar concentration of the i'th species in the bulk, z_i is the valence of the i'th species. The determination pK_o and $(\delta F_e/\delta \nu)$ requires electrophoretic measurements and/or potentiometric titration of the polyelectrolytes (8).

The titration curve of poly(methacrylic acid) shows a peculiar shape with three phases (8-10). The titration curve correlates with the curve of viscosity vs α. In the first region pK increases sharply, while viscosity increases very slowly. The region of large viscosity increase coincides with an almost constant pK. In the third region, both viscosity and pK increase moderately.

These phenomena have been related to conformational changes of the polyelectrolyte chains due to the repulsion between identically charged groups. The unionized form of poly(methacrylic acid) is a highly coiled molecule. In the first phase, the repulsive electrostatic forces are counteracted by attractive forces such as conformational free enthalpy of the chain and hydrophobic forces (attributed to the α-methyl group). As a result, the chain dimensions, and the viscosity of the solution, change very little, whereas there is a sharp increase in charge density (and consequently a sharp change in pK). When the chains reach a certain degree of ionization, the short-range hydrophobic forces are overwhelmed by the repulsion forces. The result is a large expansion of the chain in the second phase of the titration curve which can be observed as a steeper increase in viscosity and essentially no change in charge density. In the third region, the chains are in a highly extended form and charge density starts to rise again. The same three-phase titration curve has been

observed for alternating copolymers of maleic anhydride and alkyl vinyl esters (11) and for partially quaternized poly[thio-1-(N,N-diethylaminoethyl ethylene] (12). In the latter case, it is assumed that at the point where the titration curve flattens out, the polymer changes from a extended form to a globular structure (note that in the last example the polymer is a base, so that ionization increases with the lowering of the pH).

There are only a few studies involving precipitating hydrophobic polyelectrolyte systems (12-14). The titration curves for these systems differ from those of the non-precipitating polyelectrolytes. Two-phase systems have, as a rule, a high buffering capacity. Only when the precipitating polymer is almost completely neutralized is there a pronounced decrease in buffering capacity; thus an end point can be readily determined.

The homopolymer poly(N,N-diethylaminoethyl methacrylate) (p(DEA•HCl)) presents a "buffering pH" at around 7.6 at an ionic strength of 0.1 M (14). It was of interest to modify the buffering pH of p(DEA•HCl) to utilize the polyelectrolyte in a drug delivery system such as the mechanochemical insulin pump described in chapter 1. Our approach was to modify the hydrophobicity of the p(DEA•HCl) chains by insertion of unionizable comonomers.

In this chapter the titration curves of copolymers of DEA•HCl with unionizable methacrylate esters are presented. Also reviewed is the effect of ionic strength and counterion type on the titration behavior of p(DEA•HCl).

4.2 Experimental

4.2.1 Materials

Sodium chloride, sodium bromide, and sodium iodide (all from Fisher Scientific, A.C.S. grade) were used as received. Water used in all experiments was distilled and deionized using the Barnstead Nanopure System.

4.2.2 Polyelectrolyte Preparation

The homopolymer p(DEA•HCl), and the copolymers of DEA•HCl with 2-hydroxyethyl methacrylate (HEMA), methyl methacrylate (MMA), and butyl methacrylate (BMA) were prepared as described in Chapter 2.

4.2.3. Titration Studies

Precise aliquots of differing volumes 0.1 M NaOH solution were added to 20 ml vials containing an amount of polymer equivalent to 0.165 mmoles of DEA•HCl in 15 ml of salt solution at a specified ionic strength. In studying the effect of ionic strength on the titration curve of p(DEA•HCl), the salt used was NaCl. The pH in each vial was recorded using a standard pH meter. The points where a precipitate phase appeared were also recorded.

4.3 Results

4.3.1 Titration Curves for DEA•HCl Copolymers

In the titration of polybases, neutralization (α) corresponds to removal of ionizing protons from the polymer. Thus the degree of ionization is given by ($1-\alpha$), in contradiction to polyacids.

The titration curves for p(DEA•HCl) and unionizable copolymers, at an ionic strength of 0.1 M, are displayed in figures 4.2 and 4.3. As the proportion of the hydrophobic copolymers (BMA, MMA) is increased, the "buffering pH" is shifted to lower pH values. On the other hand, the copolymer with a hydrophilic monomer (HEMA) has a "buffering pH" higher than p(DEA•HCl). It is also observed that the point, at which the precipitate is initially observed (α_{ppt}), occurs at lower values of degree of neutralization (α) as the chain hydrophobicity increases.

4.3.2 Effect of Ionic Strength on the Titration Curve of p(DEA•HCl)

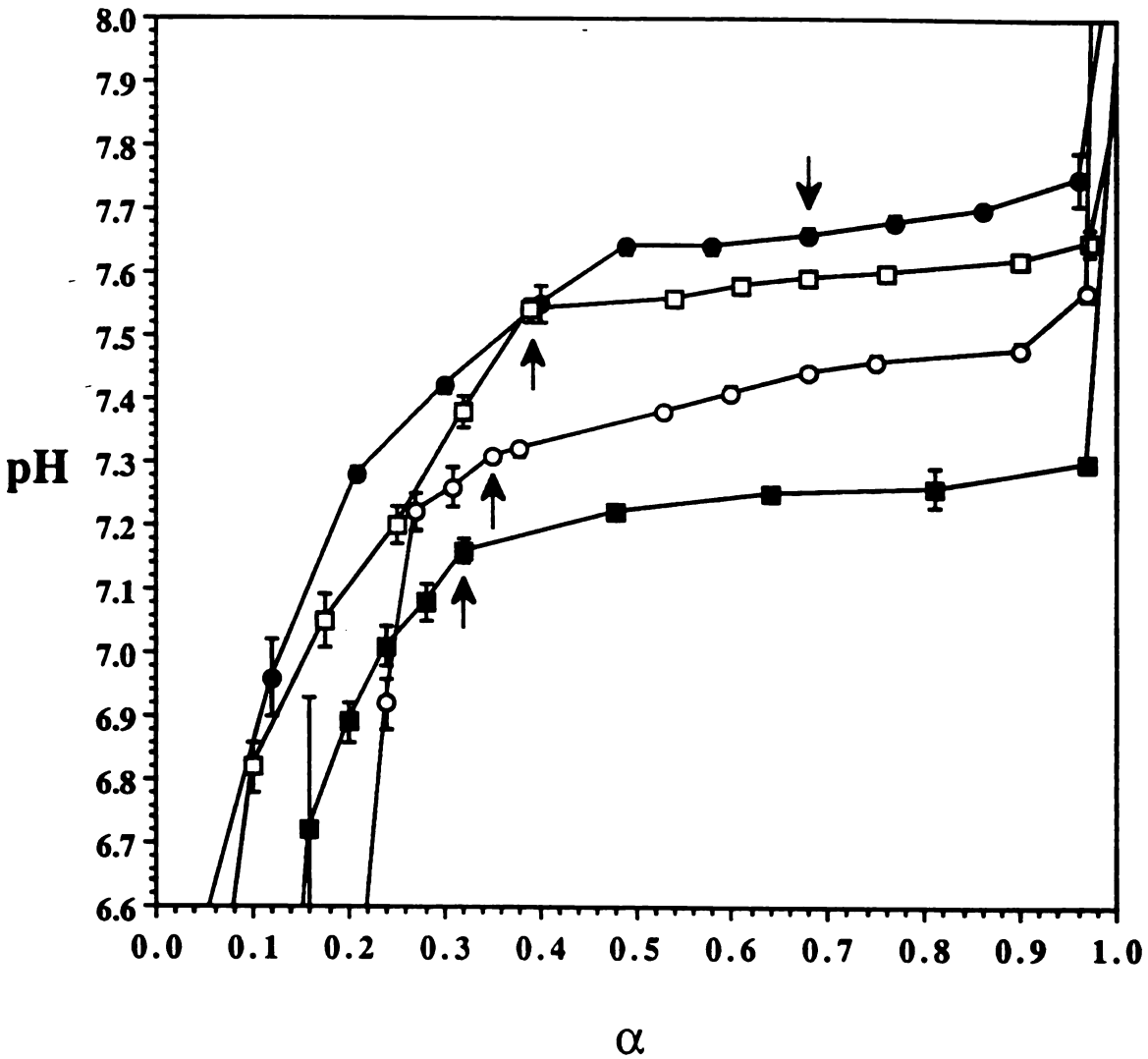

Figure 4.2. Titrations curves for p(DEA•HCl), DEA•HCl/HEMA copolymer, and DEA•HCl/BMA copolymers in 0.1 M NaCl solutions. Arrows indicate the point at which precipitate is first observed. (❑) p(DEA•HCl), (○) p(DEA•HCl/BMA) 92/8, (■) p(DEA•HCl/BMA) 80/20, (●) p(DEA•HCl/HEMA) 56/44.

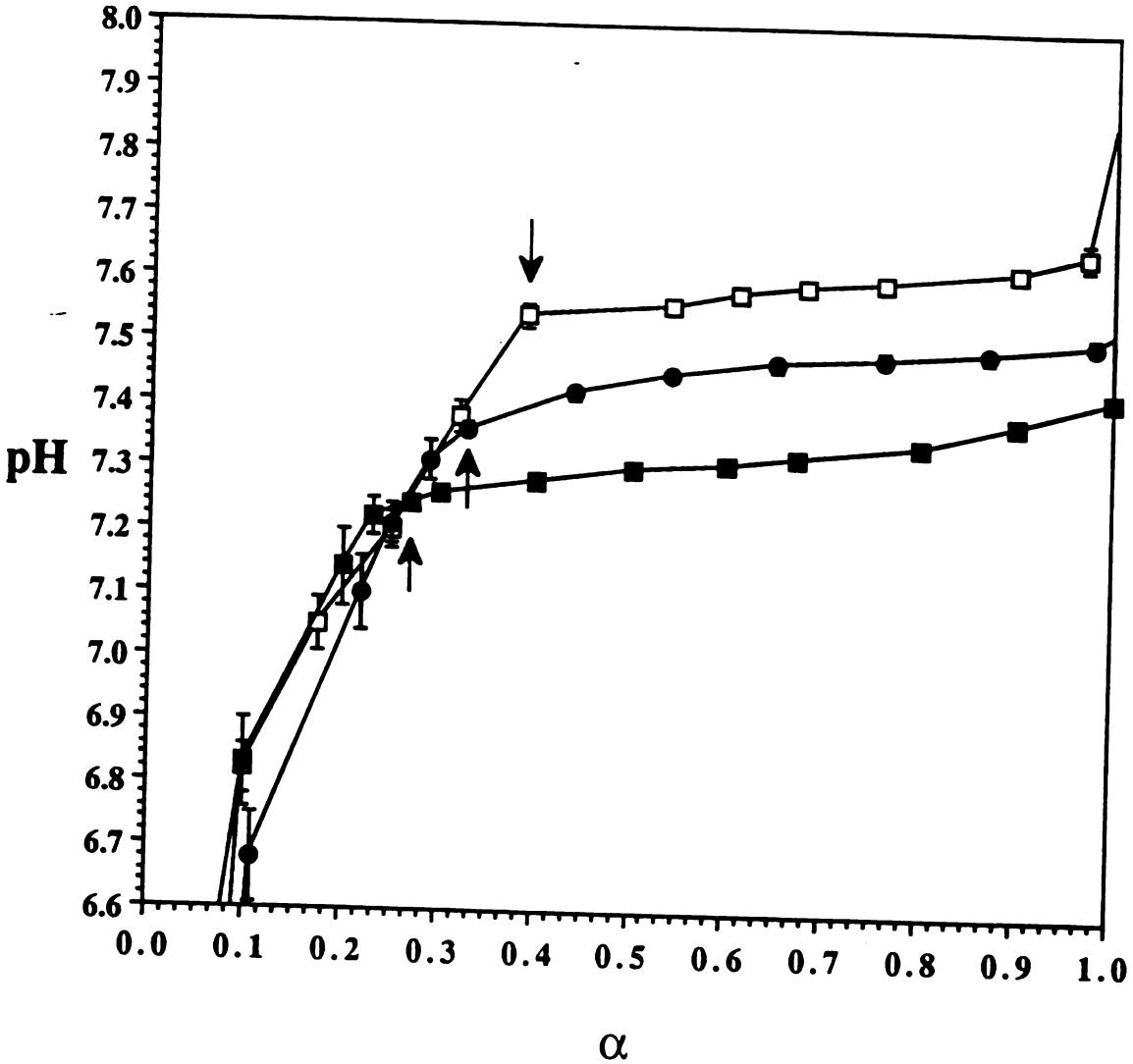

Figure 4.3. Titration curves for DEA•HCl/MMA copolymers in 0.1 M NaCl solutions. Arrows indicate point at which precipitate is first observed. (❑) p(DEA•HCl), (●) p(DEA•HCl/MMA) 81/19, (■) p(DEA•HCl/MMA) 56/44.

Figure 4.4 shows the effect of ionic strength on the titration curve of p(DEA•HCl). As the ionic strength increases, the "buffering pH" increases. However, the point at which the precipitate phase appears is shifted to lower values of α.

4.3.3 Effect of Counterion on the Titration Curve of p(DEA•HCl)

The effect of counterions (Cl^-, Br^-, and I^-) on the titration curve of p(DEA•HCl) was studied at an ionic strength of 0.2 M. The results are in figure 4.5. As the hydrated size of the counterion decreases (higher molecular weight), the "buffering pH" is increased, while the point at which the precipitate appears is practically unchanged. When the ionic strength is set using NaI, the titration curve is not flat after the precipitate phase appears, indicating poor buffering.

4.4 Discussion

The homopolymer of DEA is hydrophobic and insoluble in water in the unionized state; when ionized, however, it is completely soluble. In the present study, the polymer is synthesized in the fully ionized, hydrochloride form. The polymer is dissolved in a salt solution and titrated with NaOH. Initially, a steep dependence of pH upon α is observed. At $\alpha \cong 0.39$, a precipitate phase appears. After this point the titration curve flattens out, and the system behaves as an excellent buffer.

As for soluble polyelectrolytes, these observations can be explained in terms of repulsive and attractive (hydrophobic) forces. When the polyelectrolyte is fully ionized, the repulsive forces overwhelm the attractive forces, and the polyelectrolyte chains prefer to be in solution. At a certain critical degree of neutralization, α_{ppt}, the hydrophobic forces are large enough to compensate the repulsive forces and the chains are driven out of the solution into a precipitate phase. The precipitating chains lose their bound protons and precipitate totally unionized. This has been proved experimentally (14). The release of bound protons during

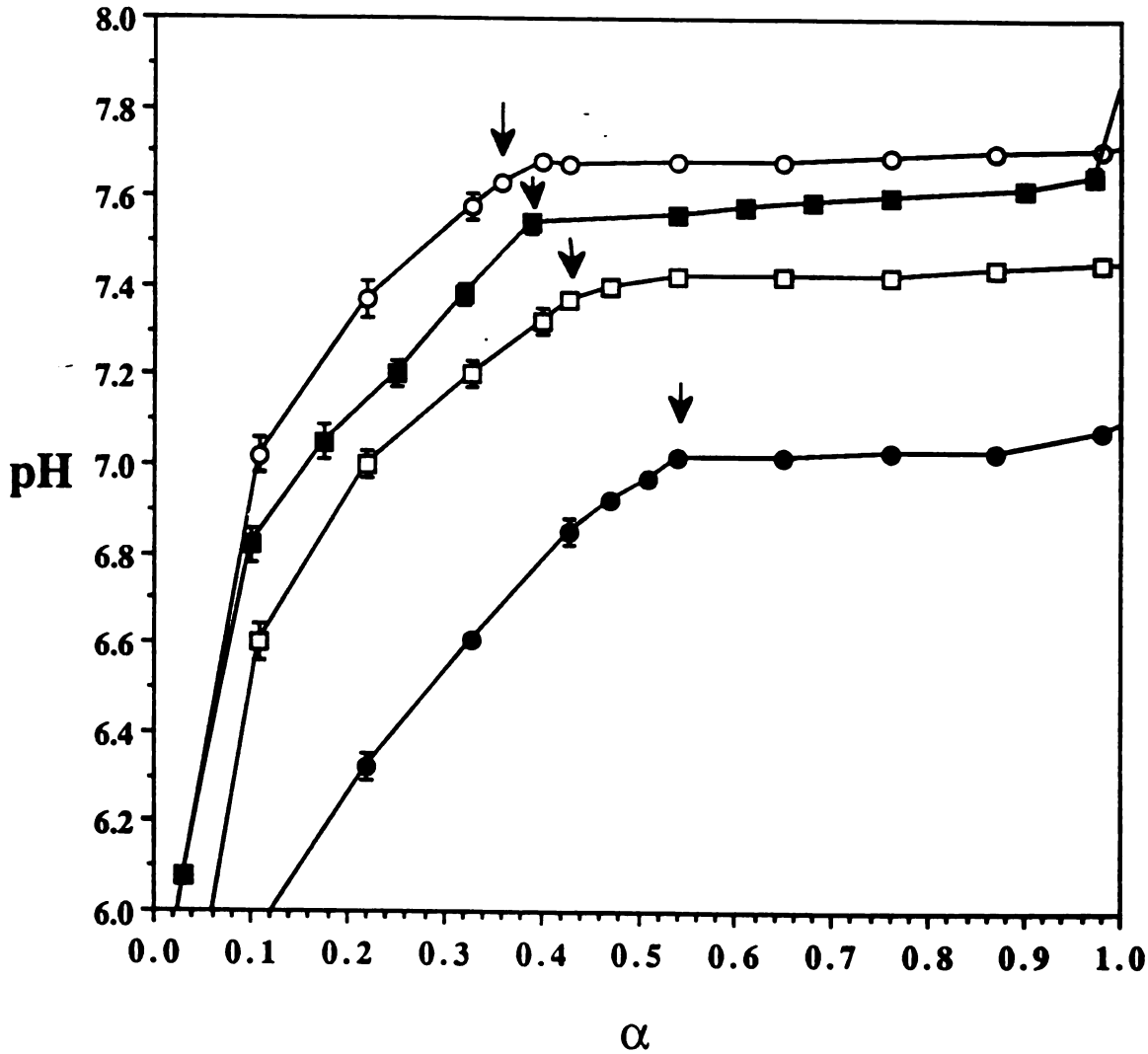

Figure 4.4. Effect of ionic strength on the titration curve of p(DEA•HCl). Ionic strength set with NaCl. Arrows indicate the point at which precipitate is first observed. (○) no added salt, (■) I=0.05 M, (●) I=0.1 M, (❑) I=0.2 M.

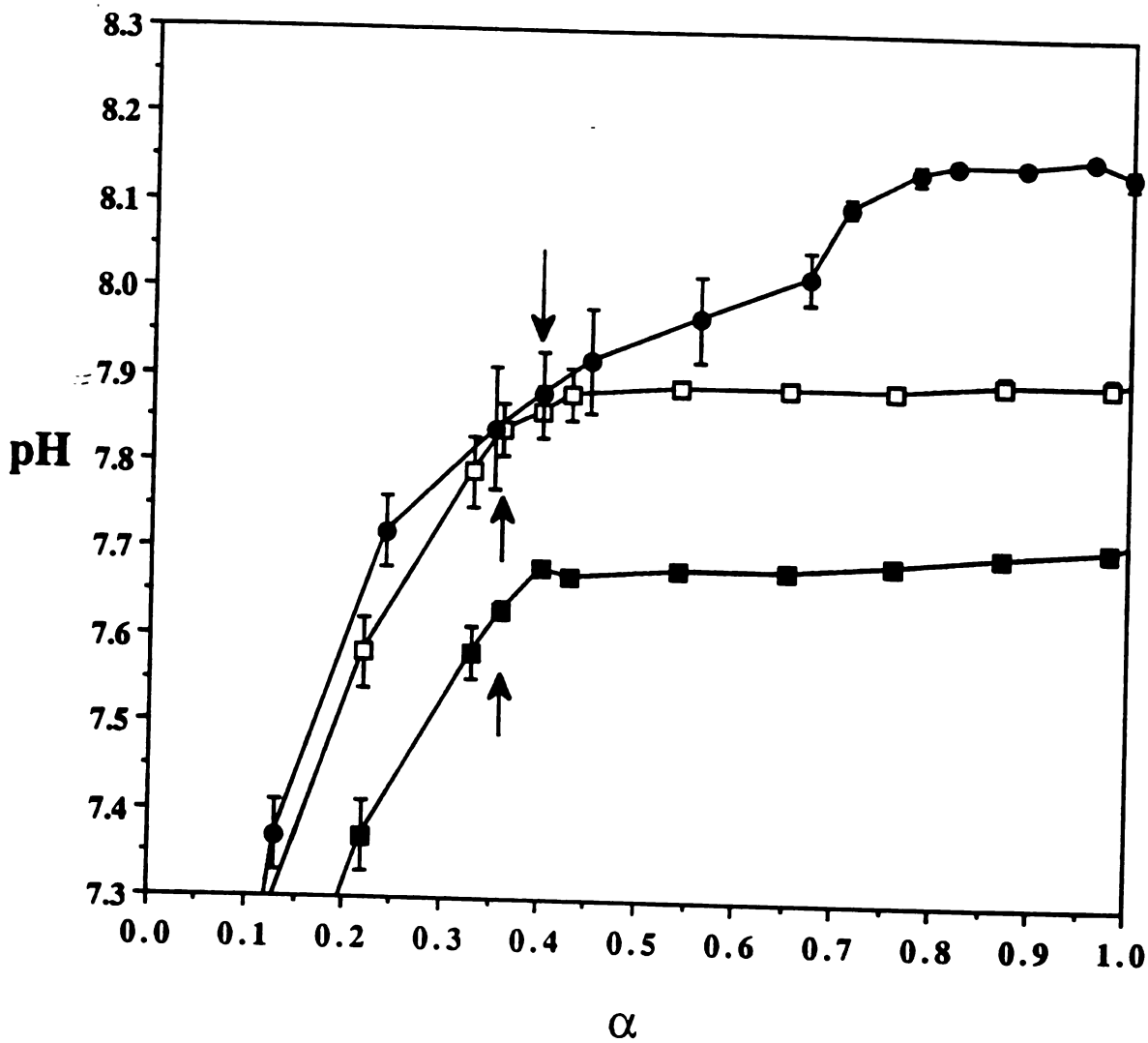

Figure 4.5. Effect of counterion on the titration curve of p(DEA•HCl). I=0.2 M. (■) NaCl, (❑) NaBr, (●) NaI. Arrows indicate the point at which precipitate is first observed.

neutralization provides a sink for the titrant which is being added to the solution; hence, the pH remains almost constant upon further addition of NaOH.

According to these arguments, increasing the hydrophobicity of the chains will facilitate the precipitation process. A lower hydroxide activity would be required to precipitate the polyelectrolyte (or a higher proton activity would be required to ionize the polyelectrolyte). In other words, if the hydrophobicity of the chains increases, the polyelectrolyte will precipitate at a lower pH (and vice versa). These predictions are confirmed in figures 4.2 and 4.3. As the hydrophobicity of the chains is increased by incorporating the hydrophobic monomers BMA or MMA, the "buffering pH" is shifted to lower pH values. However, the copolymer of DEA•HCl with the relatively hydrophilic monomer HEMA presents a "buffering pH" higher than that the presented by p(DEA•HCl).

Based on the same arguments, it is expected that, as the hydrophobicity increases, the precipitate phase will appear at lower degrees of neutralization (smaller α_{ppt}). This expectation is also confirmed by the data in figures 4.2 and 4.3.

Because the precipitate phase is considered a complicating factor, there are only a few thermodynamic analyses of hydrophobic precipitating polyelectrolyte systems (14-16). The most important contribution is the equation:

$$P(1-\overline{\alpha^*}) = \frac{d}{d\ pH}\left(-\log Cp + 0.4343\ \frac{\mu_0}{RT}\right) \qquad (4.4)$$

where P is the number of ionizable amine groups per chain, $1-\overline{\alpha^*}$ is the mean degree of ionization of the polymer chains in the solution phase, Cp is the molar concentration of polymer in solution, and μ_0 is the chemical potential of the polymer in the precipitate (note that $\overline{\alpha^*}$ and α are different quantities: the former refers to the soluble chains, while the latter refers to both the soluble and the precipitated chains. Shatkay and Michaeli measured Cp and $1-\overline{\alpha^*}$ for

each titration point of p(DEA•HCl) with NaOH. Eqn. 4.3 describes the data well, even if the term in μ_0 is disregarded. This is possible since the chemical composition of the precipitate does not change during the titration process (14). Eqn. 4.3 predicts that if μ_0 is kept constant when the precipitate is present, large changes in polymer concentration will occur with very small changes in pH, since the product $P(1-\alpha^*)$ is large.

The copolymers studied are expected to present some compositional heterogeneity. In this case, the more hydrophobic chains will precipitate first during the titration process, leaving the more hydrophilic chains in solution. This separation process will produce changes in μ_0 during the course of the titration. The $(1/RT)(d\mu_0/dpH)$ term could decrease the term $P(1-\alpha^*)$ in which case the buffering capacity will decrease. The titration curves of the copolymers show a slighly larger slope than the homopolymer curve. This experimental observation is then explained by eqn. (4.3).

The increase in "buffering pH" with increasing ionic strength for the polyelectrolytes (figure 4.3) can also be explained in terms of precipitate vs solution stability. With increasing ionic strength, the repulsive coulombic interactions between the ionized groups on the chains are screened. This lowers the ionization "force" ($\delta F_e/\delta v$ of eqn. 4.2) such that the attraction of the amine groups for the protons increases and the chains are more stable in solution. Thus, a higher hydroxide activity (or lower proton activity), is required to precipitate the polymer. Again, this translates into a higher "buffering pH" with increasing ionic strength.

One might also expect α_{ppt} to be shifted to higher values as the ionic strength increases. However, figure 4.3 shows that, as the ionic strength is increased, the α_{ppt} decreases. This observation indicates than the salt added to the polyelectrolyte solution produces an effect in addition to the shielding of charges which is as yet unexplained.

To better understand the effect of added microions on the titration behavior of this class of hydrophobic polyelectrolyte, the

effect of different counter ions on the titration curve of p(DEA•HCl) was studied. Figure 4.5 shows that, for a constant ionic strength (0.2 M), the buffering pH increases as the hydrated size of the counterion decreases ($Cl^- > Br^- > I^-$). However, α_{ppt} is practically identical for the three counterions. For I^-, the titration curve does not present the excellent buffering as shown for the other counterions. The observations seem to be the result of a lyotropic effect; the smaller the hydrated size of the microion (higher molecular weight), the smaller the distance of closest approach to the macroion. From this follows a more efficient the screening of the charges, and hence an increase in buffering pH. The interaction of iodide (as I_3^-) with polymers such as polyvinylacetate and starch is well known (17,18). The binding of the microion should make the polymer chains more hydrophilic. The interaction of iodide with p(DEA•HCl) would decrease the hydrophobicity of the polyelectrolyte and it would explain the poor buffering presented by the polyelectrolyte when the counterion present is iodide. We can speculate that such interaction should be smaller for more polar anions such as Br^- and Cl^-.

4.5 Conclusions

The "buffering pH" for polyelectrolytes containing the monomer DEA•HCl can be shifted to higher or lower pH values by introducing, respectively, hydrophilic and hydrophobic unionizable monomers into the polyelectrolyte chains.

The "buffering pH" depends on the ionic strength of the medium and the sodium salt used to set it. The "buffering pH" is increased by increasing the ionic strength and by using a higher molecular weight counterion at a determined concentration.

References

1. M. Mandel, *Eur. Polym. J.*, **6**, 807 (1970).

2. E. Katchalsky, I. Grossfeld, and M. Frankel, *J. Am. Chem. Soc.*, **70**, 2094 (1948).

3. D. D. Reynolds and W. O. Kenyon, *J. Am. Chem. Soc.*, **159**, 193 (1941).

4. J. Th. Overbeek, *Bull. Soc. Chim. Belges*, **57**, 252 (1948).

5. A. Katchalsky and P. Spitnik, *J. Polym. Sci.*, **2**, 432 (1947).

6. A. Katchalsky and J. Gillis, *Rec. Trav. Chim.*, **68**, 879 (1949).

7. A. Arnold and J. Th. Overbeek, *Rec. Trav. Chim.*, **69**, 192 (1950).

8. A. Katchalsky, N. Shavit, and H. Eisenberg, *J. Polym. Sci.*, **13**, 69 (1954).

9. J. C. Leyte and M. Mandel, *J. Polym. Sci.*, **13**, 69 (1964).

10. I. Noda, T. Tsuge, and M. Nagasawa, *J. Phys. Chem.*, **74**, 710 (1970).

11. P. Dubin and U. Strauss, *J. Phys. Chem.*, **74**, 2842 (1970).

12. O. Vallin, J. Huguet, and M. Vert, *Polym. J.*, **12**, 113 (1980).

13. A. Grönwall, *Compt. rend. trav. lab. Carlsberg, Sér. chim.*, **24**, 185 (1942).

14. A. Shatkay and I. Michaeli, *J. Phys. Chem.*, **70**, 377 (1966).

15 K. Linderström-Lang, *Arch. Biochem.*,**11**,191 (1946).

16. I. Michaeli. *J. Phys. Chem.*, **11**, vol 71 3384 (1967)

17. S. Hayashi, T. Hirai, and N. Hojo, *J. Polym. Sci.*, **20**, 839 (1982).

18. A. Cesáro, J. C. Benegas, and D. R. Ripoll, *J. Phys. Chem.*, **90**, 2787 (1986).

Chapter 5

Equilibrium Colloid Osmotic Pressure Studies for p(DEA•HCl) and Copolymers of DEA and MMA

5.1 Introduction

The hydrostatic pressure required to maintain equilibrium between a polyelectrolyte solution with an external salt solution through a membrane permeable to both salt and water, but not permeable to polyelectrolyte, is called the colloid (or Donnan) osmotic pressure. This pressure arises from the higher concentration of microions in the polyelectrolyte phase compared to the outer solution: this concentration difference arises from the bulk electroneutrality requirement in the two phases (1).

The mechanochemical insulin pump described in chapter 1 requires that, after blood glucose concentration increases and glucose is converted into gluconic acid, the osmotic agent (polyelectrolyte) exert pressure on the formulation compartment until this pressure reaches the cracking pressure of a one-way valve, which then opens and releases a bolus of insulin.

It is of great interest, therefore, to examine the colloid osmotic properties of the family of precipitating polyelectrolytes containing DEA•HCl and its copolymers with MMA. The effects of polyelectrolyte composition, concentration and degree of neutralization have been considered. We have also studied the effect of ionic strength on the colloid osmotic pressure produced by p(DEA•HCl) solutions. The experimental results are compared to theories available in the literature. These theories are discussed in section 5.2.

Most colloid osmotic pressure determinations involve low concentrations of polyelectrolytes (e.g. proteins), typically with the purpose of determining molecular weight. These measurements have been performed with standard water column osmometers since the colloid osmotic pressures produced are small (2). Moderate colloid

osmotic pressures (up to 0.08 atm) have been measured with osmometers in which the pressure is determined by a Hg manometer (3,4) or with "membrane" osmometers (5).

Vilker *et al.* (6) measured the colloid osmotic pressure of highly concentrated albumin solutions using a static membrane osmometer built to withstand the several atmospheres of pressure generated by these solutions (up to 5.9 atm). The osmotic cell consisted of two chambers, one for the standard solution and one for the polyelectrolyte. The chambers were separated by a semipermeable membrane. Each chamber had a volumetric capillary to measure volume displacement. The osmotic pressure generated was opposed by gas pressure applied against the capillary leading from the colloid chamber. The gas pressure required to equilibrate the liquid levels in the capillaries was taken as the colloid osmotic pressure of the solution.

One disadvantage of the osmometer cell designed by Vilker *et al.* is that it does not allow the kinetics of colloid osmotic pressure build-up to be followed. Also, it requires a trial an error estimation of the colloid osmotic pressure of the solution to be able to equilibrate the capillary columns. We therefore designed an osmometer cell using a membrane pressure transducer as the pressure sensor (figure 5.1). The device consists of two chambers: Chamber I contains the reference solution against which the colloid osmotic pressure is to be measured. Chamber II contains the polyelectrolyte solution to be analyzed. The chambers are formed by sandwiching a semipermeable membrane between two Plexiglass rings. The membrane is supported by metallic screens on either side. The unit is clamped together by 6 rods equally spaced around the chambers. A rubber O-ring on the polyelectrolyte solution side seals the system. Chamber I has a capacity of around 250 ml and is stirred by a propeller. The capacity of chamber II is around 20 ml; it is stirred magnetically. The sizes of the chambers were selected such that small changes in polyelectrolyte concentration would result in solvent flux from the reference solution chamber to the

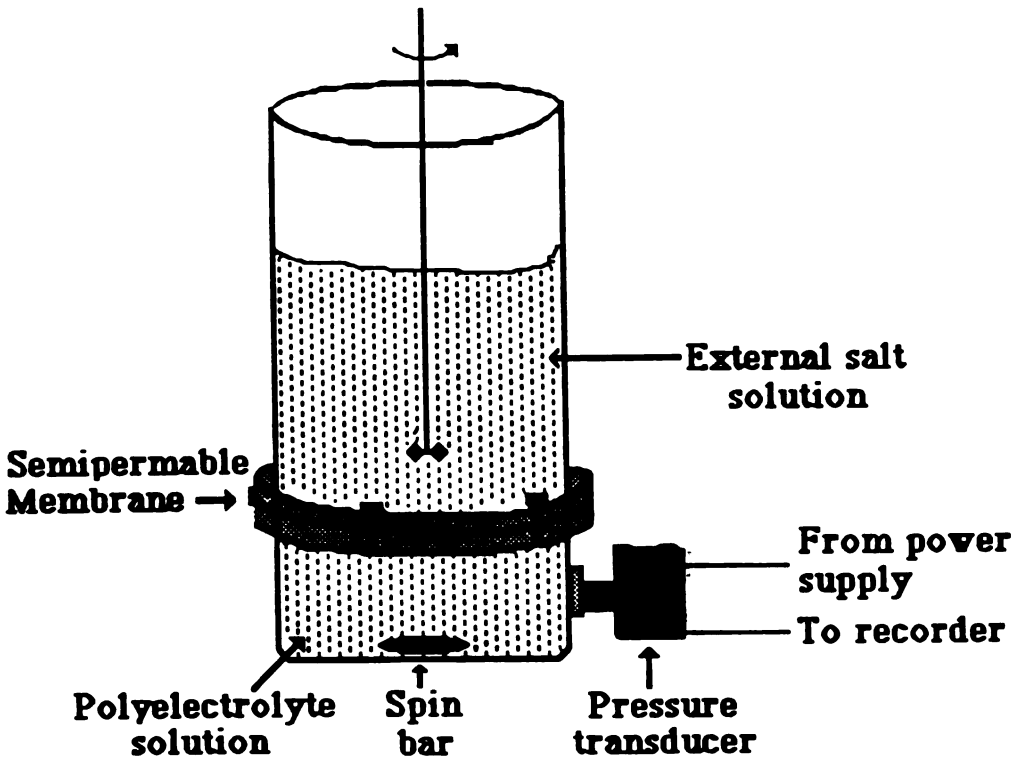

Figure 5.1. Schematic diagram of the osmotic cell used in the equilibrium experiments of colloid osmotic pressure.

polyelectrolyte solution chamber, yet maintain a constant ionic strength in the reference solution. The pressure generated is measured by a membrane pressure transducer (Ametek, Feasterville PA) placed in chamber II.

The principal advantage of this osmometer is its fast response. The pressure is measured by a very small displacement in the sensor membrane inside the pressure transducer and no significant net volume flux is expected, allowing rapid attainment of equilibrium and virtually no change in polyelectrolyte concentration.

5.2 Theoretical Models for Colloid Osmotic Pressure

The Ideal Donnan theory is the simplest theory to predict colloid osmotic pressure generated by polyelectrolyte solutions.

In the following equations, primed quantities refer to the reference solution, while unprimed quantities refer to the polyelectrolyte solution phase. Thus c_i and c_i' are the molar concentrations of the i'th ionic species in those phases, respectively, and a_i and a_i' are the corresponding activities. The subscript i can be Na^+, Cl^-, "s" for the neutral salt NaCl, and "M" for the ionizable amine groups on the polyelectrolyte chains. The term $\bar{v}_i$ stands for the partial molar volume of the i'th species (assumed to be the same in both phases), μ_i^0 is the standard state chemical potential of the i'th species (a function of temperature only). The ionic equilibria require equality of electrochemical potentials, i.e.

$$\mu_i^0 + \bar{v}_i\Delta\pi + RT\ln a_i + z_iF\Psi = \mu_i^0 + RT\ln a_i' \qquad (5.1)$$

the term $\bar{v}_i\Delta\pi$ can be ignored with miniscule loss of accuracy (6). Hence, eqn. 5.1 can be rewritten as

$$\frac{a_i}{a_i'} = e^{-z_iF\Psi/RT} = K^{z_i} \qquad (5.2)$$

where

$$K = e^{-F\Psi/RT} \tag{5.3}$$

the term K is called the *Donnan ratio.* Introducing activity coefficients f_i and f_i', where $a_i = f_i c_i$ and $a_i' = f_i' c_i'$, eqn 5.2 becomes

$$\left(\frac{f_i}{f_i'}\right)\frac{c_i}{c_i'} = K^{z_i} \tag{5.4}$$

Assuming that $f_i \approx f_i'$ gives

$$\frac{c_i}{c_i'} = K^{z_i} \tag{5.5}$$

If the ionic strength is set by NaCl, then $c_{Na+} = Kc'_{Na+}$ and $C_{Cl-} = K^{-1}c'_{Cl-}$, and we obtain

$$(a_{Na+})(a_{Cl-}) = (a'_{Na+})(a'_{Cl-}) \tag{5.6}$$

Considering the ideal case where concentrations and activities are equal, electroneutrality in the two phases leads to the following relations

$$a'_{Na+} = a'_{Cl-} = c_s' \tag{5.7}$$

$$a_{Na+} = c_s \tag{5.8}$$

$$a_{Cl-} = c_s + (1-\alpha)c_M \tag{5.9}$$

where α is the degree of neutralization of the tertiary amine groups (moles NaOH added/moles of initially ionized tertiary amine groups).

Combining eqns. 5.6 to 5.9 gives

$$c_s(c_s + c_M) = (c_s')^2 \tag{5.10}$$

Since c_s' and c_M are specified in the experiment, c_s can be determined.

The colloid osmotic pressure $\Delta\Pi$, is calculated using the van't Hoff eqn.

$$\Delta\Pi = RT(\phi\Sigma c_i - \phi'\Sigma c_i') \quad (5.11)$$

where ϕ and ϕ' are osmotic coefficients.

Combining eqns. 5.10 and 5.11 in the ideal case where the osmotic coefficients equal unity, yields:

$$\Delta\Pi = RT[2c_s-2c_s'+(1-\alpha)c_M] \quad (5.12)$$

Eqn. 5.12 greatly overestimates the observed colloid osmotic pressures (see below). This discrepancy is explained by noticing that the counterions are attracted to the polyelectrolyte by the strong electric fields surrounding the polyions. This attraction decreases the chemical and osmotic activities of the counterions. An estimation based in this notion of the osmotic coefficients of the counterion species in the polyelectrolyte solution is required. In the following we discuss the chosen scheme for modeling osmotic and activity coefficients.

It is assumed that the osmotic activity of the coions is not significantly affected by the largely screened polyion. This assumption leads to the so-called semiempirical "additivity rule" which has been applied to polyelectrolytes in salt solutions (7-11). According to this rule the osmotic pressure of the combined polyelectrolyte/salt solution will be

$$\pi = \pi_p + \pi_s \quad (5.13)$$

where π_p is the osmotic pressure of the polyelectrolyte-associated counterions in a solution with no added salt and π_s is the osmotic pressure of a salt solution in the absence of polyelectrolyte. The Donnan pressure is given by

$$\Delta\pi = \pi_p + \pi_s - \pi_s' \quad (5.14)$$

Furthermore, the activity of the counterions (here, Cl^-) is the sum of the activity of the counterions in the salt-free solution, $(a_{Cl^-})_p$ and the counterion activity in the polymer-free solution, $(a_{Cl^-})_s$ or

$$a_{Cl^-} = (a_{Cl^-})_p + (a_{Cl^-})_s \qquad (5.15)$$

The terms in eqns 5.14 and 5.15 have to be calculated. Assuming the osmotic coefficients for the salt are equal to unity (as deviations due to microion-microion interactions are small compared to deviations associated with polyelectrolyte), then

$$\pi_s = 2RTc_s \qquad (5.16)$$

$$\pi_s' = 2RTc_s' \qquad (5.17)$$

All that remains is to calculate π_p. For this purpose, the "cell model" of polyelectrolyte solutions (8-10) is used. Polyelectrolyte molecules are represented as cylindrical rods aligned in parallel, forming a hexagonal lattice. The charge is evenly distributed along the surface of the rods, which are surrounded by their counterion atmospheres (see figure 5.2). The justification for this representation is that charged polyelectrolytes are sufficiently stretched that they may be considered to be locally rod-like.

The counterion distribution in the absence of salt is calculated using the Poisson-Boltzmann equation (1, 8-16), for the geometry mentioned above, and the osmotic pressure is computed applying the ideal van't Hoff equation at the midpoint between two rod axes (at a distance R from the rod axes in figure 5.2), where the electric field vanishes.

In the absence of added salt, the osmotic coefficient ϕ_p and the activity coefficient f_p of the counter ions are identical. Assuming ideal behavior of the salt ions in both the polyelectrolyte and the reference solution, eqns. 5.6 and 5.15 are combined to obtain

$$c_s[c_s+(1-\alpha)\phi_p c_M] = (c_s')^2 \qquad (5.18)$$

where $(1-\alpha)$ is the fraction of the tertiary amine groups that are ionized. In the case where the polyelectrolyte contains quaternary amines (see chapter 6), the term $(1-\alpha)$ will be replaced by

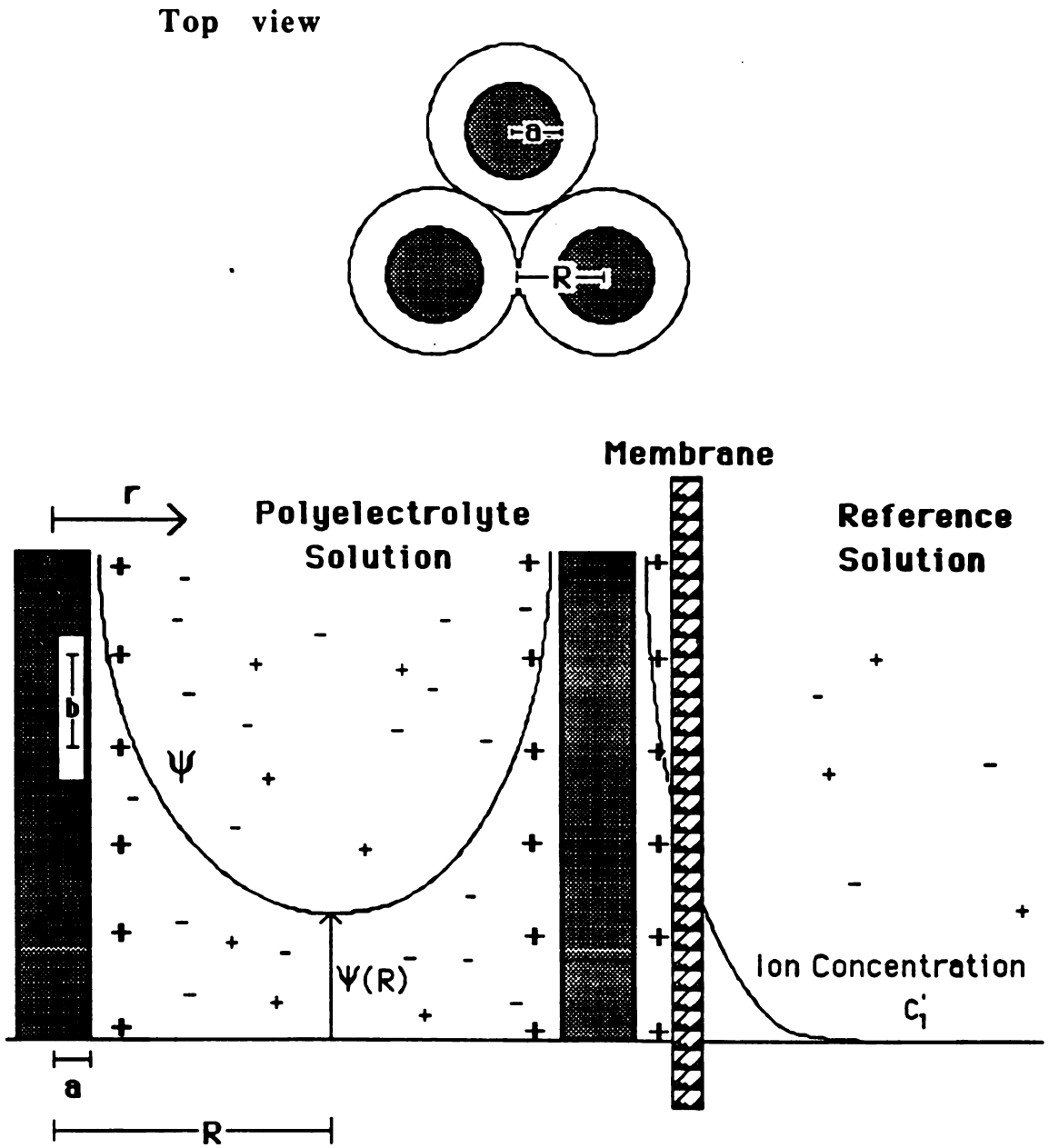

Figure 5.2. Representation of the "cell model".

[q + (1-q)(1-α)], where q is the degree of quaternization. The Donnan osmotic pressure of eqn. 5.14 is then given by

$$\Delta\Pi = RT[(1-\alpha)\phi_p c_M + 2c_s - 2c_s'] \qquad (5.19)$$

According to the "cell model", ϕ_p is a function of the polymer volume fraction V_p and the linear charge density. The latter is defined by

$$\lambda = (1-\alpha)e^2/\varepsilon bkT \qquad (5.20)$$

where e is the protonic charge, ε is the solution dielectric constant (taken to be that of bulk water), b is the average distance between charge groups along the chain backbone (see figure 5.2), and k is the Boltzmann constant. The incorporation of unionizable copolymers into the polyelectrolyte chains, as well as neutralization of the ionized groups, increases b. The change can be calculated as

$$b = b_o/(1-\alpha)X_v \qquad (5.21)$$

where b_o is the distance between the charged groups on the ionizable homopolymer and X_v is the mole fraction of the ionizable units in the copolymer (e.g. quaternary and tertiary amine methacrylates).

Using b_o = 2.56 Å (17) for vinylic copolymers at room temperature,

$$\lambda = 2.83(1-\alpha)X_v \qquad (5.22)$$

The counterion osmotic coefficient ϕ_p is calculated from the following equations (12)

$$\phi_p = (1-\beta^2)/2\lambda, \text{ where } \lambda = (1-\beta^2)/[1+\beta\coth(\beta\gamma)] \qquad \lambda<\gamma/(\gamma+1)$$
$$\phi_p = (1+\beta^2)/2\gamma, \text{ where } \lambda = (1+\beta^2)/[1+\beta\cot(\beta\gamma)] \qquad \lambda>\gamma/(\gamma+1) \qquad (5.23)$$

where

$$\gamma = -(\ln V_p)/2 \qquad (5.24)$$

Assuming that the density of the polyelectrolyte solutions is equal to the density of water (1 g/ml), and that the contribution of MMA to the polymer volume is small (since the molecular weight of an MMA unit is about half that of a DEA unit, and since, in all cases, DEA is the majority comonomer), V_p can be calculated using

$$V_p = C_M/\delta_2 L \qquad (5.25)$$

where δ_2 is the density of the polymer (in g/l) and L is the number of moles of DEA•HCl per gram of polymer determined by elemental analysis. Based on density measurements of the copolymers (chapter 3), V_p was taken as $0.24C_M$ for all the polyelectrolytes

In order to find ϕ_p using equation 5.23, β has to be solved in terms of λ and γ so that ϕ_p can be calculated from β. The FORTRAN programs used to calculate ϕ_p and $\Delta\Pi$ are listed in Appendix 5.A.

5.3 Osmometer Calibration

Transport across a semipermeable membrane can be described by (6,18)

$$J_v = L_p(\Delta P - \sigma\Delta\pi) \qquad (5.3.1)$$

where Jv is the volume flux (flux of solute plus solvent), Lp is the filtration coefficient, ΔP is the hydrostatic pressure difference across the membrane, σ is the reflection coefficient, and $\Delta\pi$ is the osmotic pressure. For the osmometer used in this work, the volume flux is approximately zero; thus

$$\Delta P = \sigma\Delta\pi \qquad (5.3.2)$$

The reverse osmosis membranes used in this work have a $\sigma = 0.99$ for aqueous NaCl solutions (19); so that measured hydrostatic pressures are virtually equal to the osmotic pressures

For NaCl solutions, the osmotic pressure can be calculated using van't Hoff's equation

$$\Delta\pi = \varphi \Sigma C_i RT \qquad (5.3.3)$$

where ΣC_i is the total concentration of all the species in solution (e.g., Na^+, Cl^-) and φ is the osmotic coefficient. Combining eqns. 5.3.2 and 5.3.3, gives

$$\Delta P = \sigma\varphi\Sigma C_i RT \qquad (5.3.4)$$

The value of φ used in the calculation is 1.0 since the NaCl concentration used is very low. A solution of NaCl at a concentration 6.4×10^{-3} M (i.e., above the range studied), has $\varphi = 0.974$ at 25°C (20) which indicates that the approximation used is valid.

5.4. Experimental

5.4.1 Materials

NaCl (Fisher Scientific) used to prepare the calibration solutions for the osmometer was dried at 100°C under vacuum. The NaCl used to set the ionic strength was used as received. Water was double distilled and deionized. NaOH 0.1 N certified solutions and NaOH 50/50% (w/w) were from Fisher Scientific. Reverse osmosis membranes (Desal, Escondido CA) were soaked in water before use. Cellulose acetate membranes MWCO 20,000 (Wescan, Santa Clara CA) were soaked in ethanol (Fisher Scientific) for 10 seconds to eliminate any residual casting solvent, washed with distilled water and left soaking in water until use. The polyelectrolytes used were synthesized as in chapter 2.

5.4.2 Osmometer Calibration

The solution compartment in osmometer cell was loaded with a NaCl solution of known concentration. The reference compartment was loaded with distilled and deionized water. The pressure transducer response (in mV) was recorded after the signal was stable for several hours. The osmotic pressure was calculated using eqn. 5.3.4.

5.4.3 Effect of Polyelectrolyte Concentration and Composition

The colloid osmotic pressures produced by the fully ionized forms of p(DEA•HCl) and the copolymers of DEA•HCl and MMA were measured to concentrations up to 0.2 monomolar (as DEA•HCl). The ionic strength in the reference solution was 0.1 M. The signal from the pressure transducer was recorded after it had been constant for several hours.

5.4.4 Effect of Ionic Strength on the Colloid Osmotic Pressure of p(DEA•HCl)

The effect of the ionic strength in the reference solution was analyzed for a 0.125 monomolar solution of fully ionized p(DEA•Cl).

5.4.5 Effect of Neutralization on the Colloid Osmotic Pressure of p(DEA•HCl)

The colloid osmotic pressures at three different concentrations of p(DEA•HCl) (initially fully ionized), were measured at several degrees of neutralization. The neutralization was realized by adding the proper volume of NaOH 0.1 M certified solution while preparing the polyelectrolyte solutions. For higher degrees of neutralization a 0.4 M NaOH solution was used. The ionic strength in the reference solution was set at 0.1 M by NaCl.

5.5 Results and Discussion

A linear correlation was found between osmotic pressure produced by NaCl solutions, up to 0.3 atm, and osmometer response (figure 5.3). At higher pressures the linearity is lost; this is attributed to bending of the metallic screens that hold the reverse osmosis membrane. Linear regression indicates that 0.1 atm of pressure corresponds to a signal of 31 mV from the pressure transducer; this value is used for all pressure conversions.

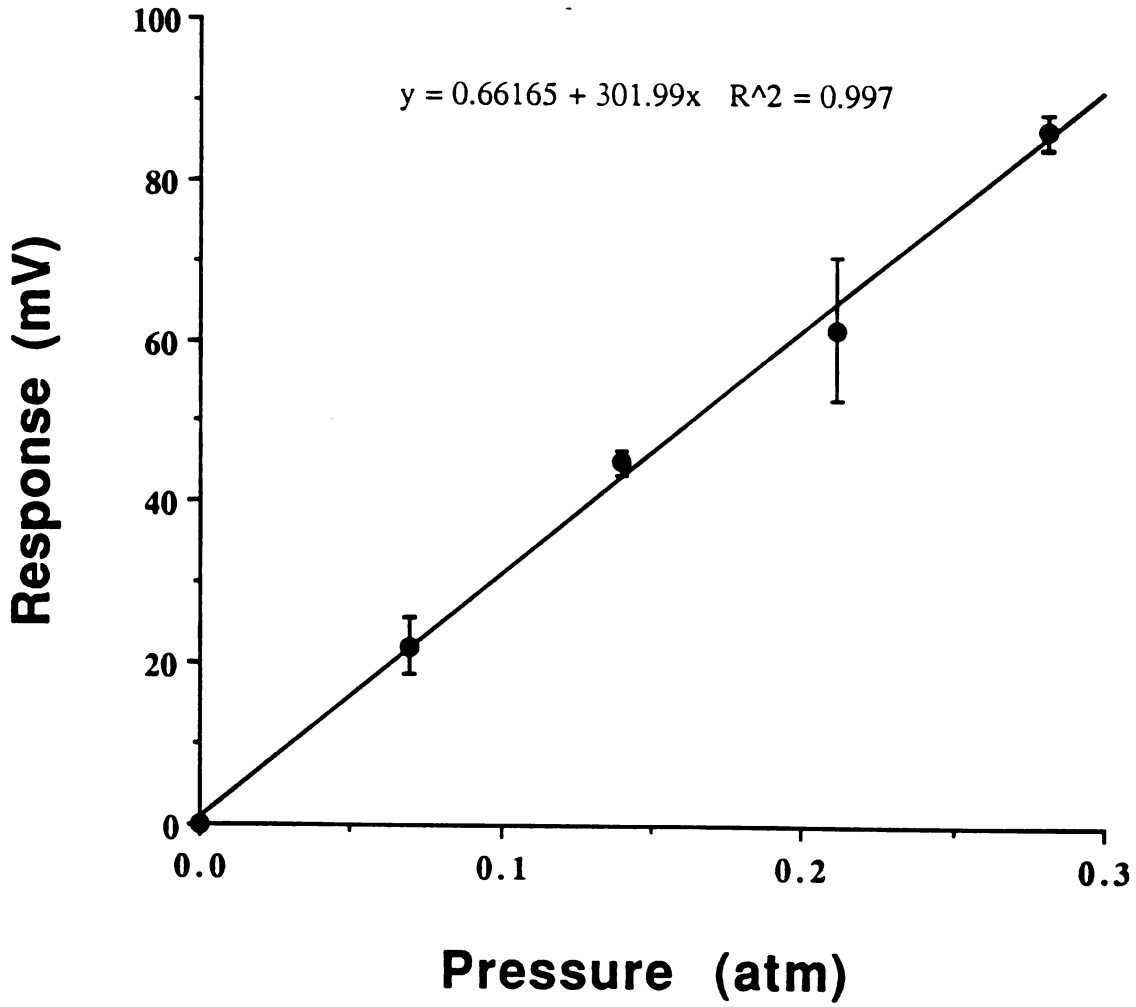

Figure 5.3. Calibration curve for the osmotic cell.

Figure 5.4 shows results for fully ionized copolymers. As the proportion of MMA in the copolymer increases, a higher colloid osmotic pressure is obtained for the same value of charged amine groups (c_M^o). This observation can be explained by the fact that, as the distance between the charged groups increases (due to the inclusion of nonionic comonomers units), the charge density of the copolymer chains decreases. This results in an increase in the osmotic coefficient of the counterions, which gives a higher colloid osmotic pressure for the same concentration of charged groups. The cell model predicts, to a good approximation, the colloid osmotic pressure for fully ionized p(DEA•HCl) up to a 0.2 monomolar concentration. However, the $\Delta\Pi$ prediction for the copolymer containing 75% of DEA is reasonable only up to a concentration of 0.1 monomolar. For the copolymer containing 57% DEA, the model and the experimental results show reasonable agreement only at very low concentrations. At higher concentrations the model underestimates the observed values. In all the cases, the ideal Donnan theory greatly overpredicts $\Delta\Pi$.

The cell model predicts a definite trend of increasing ϕ_p with c_M^o as observed in figure 5.5. The physical explanation is that, as the rods become closer to each other when V_p increases, the attraction of a counterion to a particular rod will be reduced, due to the cancellation of attracting forces pulling in opposite directions between neighboring rods, leading to greater freedom of movement and as a consequence a higher osmotic activity.

Figure 5.6 shows the effect of ionic strength on the colloid osmotic pressure of p(DEA•HCl) at 0.125 monomolar. The screening effect of the added salt to the reference solution decreases the colloid osmotic pressure. The cell model gives a reasonable prediction of the experimental results.

The charged group concentration can be modified by either changing the concentration of fully ionized polyelectrolyte (c_M^o), or by changing the degree of neutralization of a determined

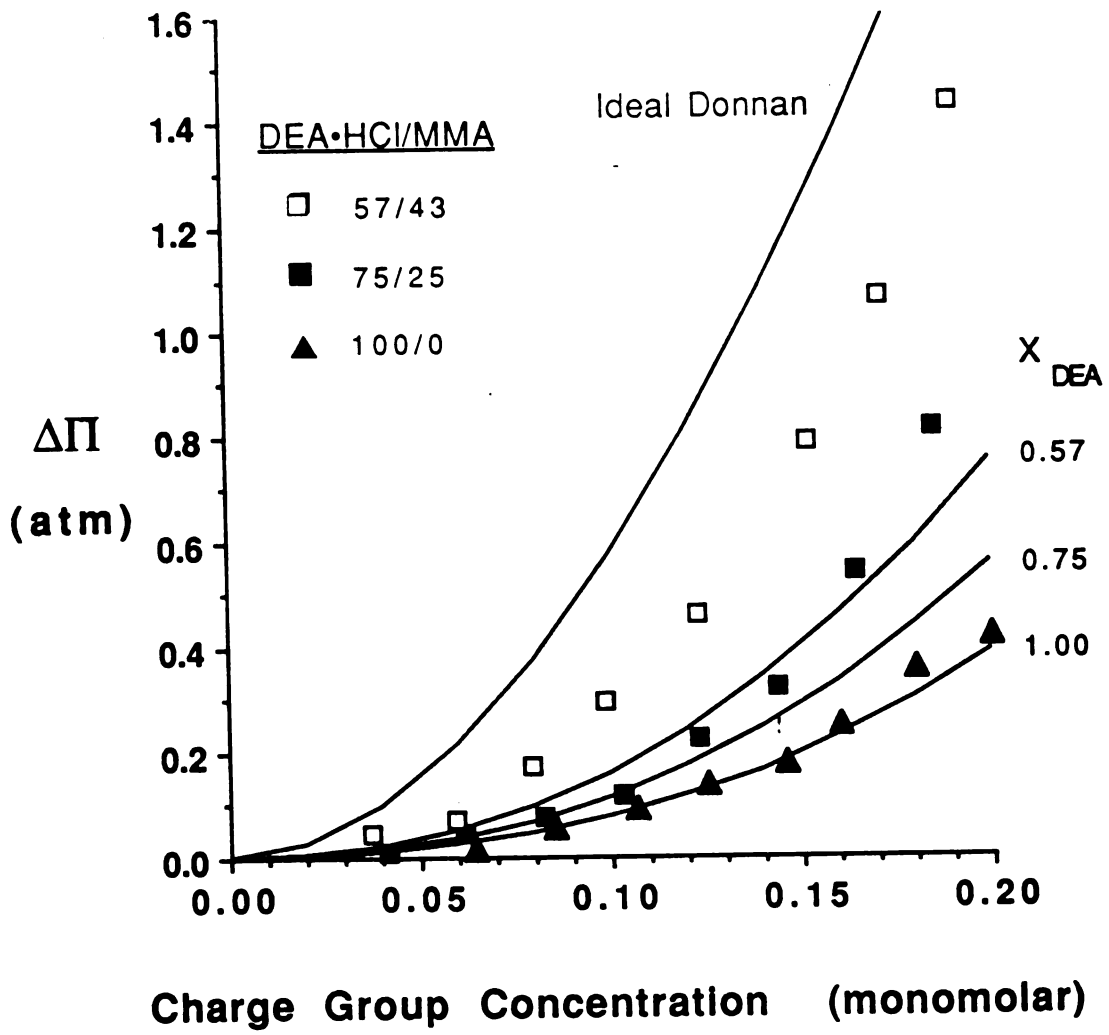

Figure 5.4. Effect of polyelectrolyte concentration and composition on colloid osmotic pressure for fully ionized polyelectrolyte solutions against 0.1 M NaCl reference solutions. (▲) p(DEA•HCl), (■) p(DEA•HCl/MMA) 75/23, (❑) p(DEA•HCl/MMA) 57/43. Curves are predictions based en the cell model. Values of X_{DEA} used on calculations are indicated next to curves.

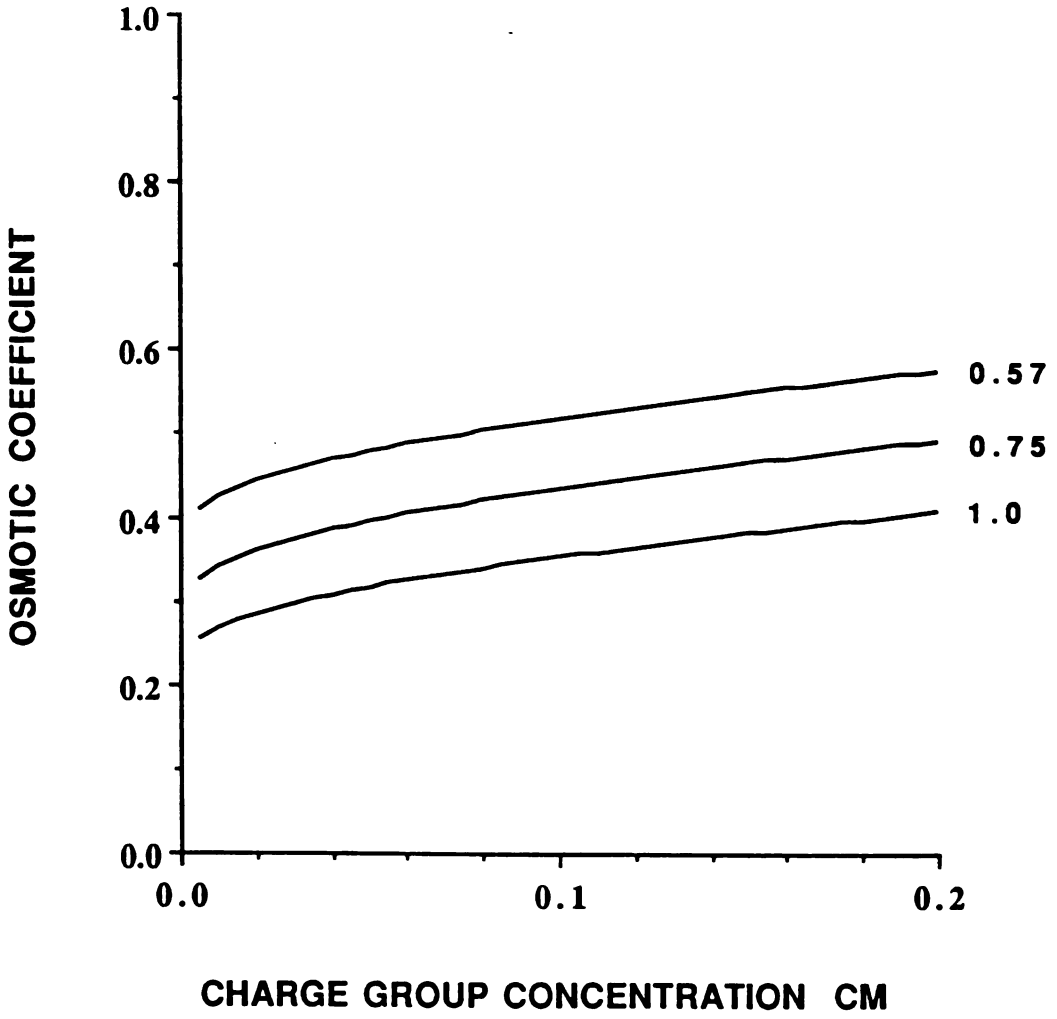

Figure 5.5. Osmotic coefficients vs c_M^o from the cell model.

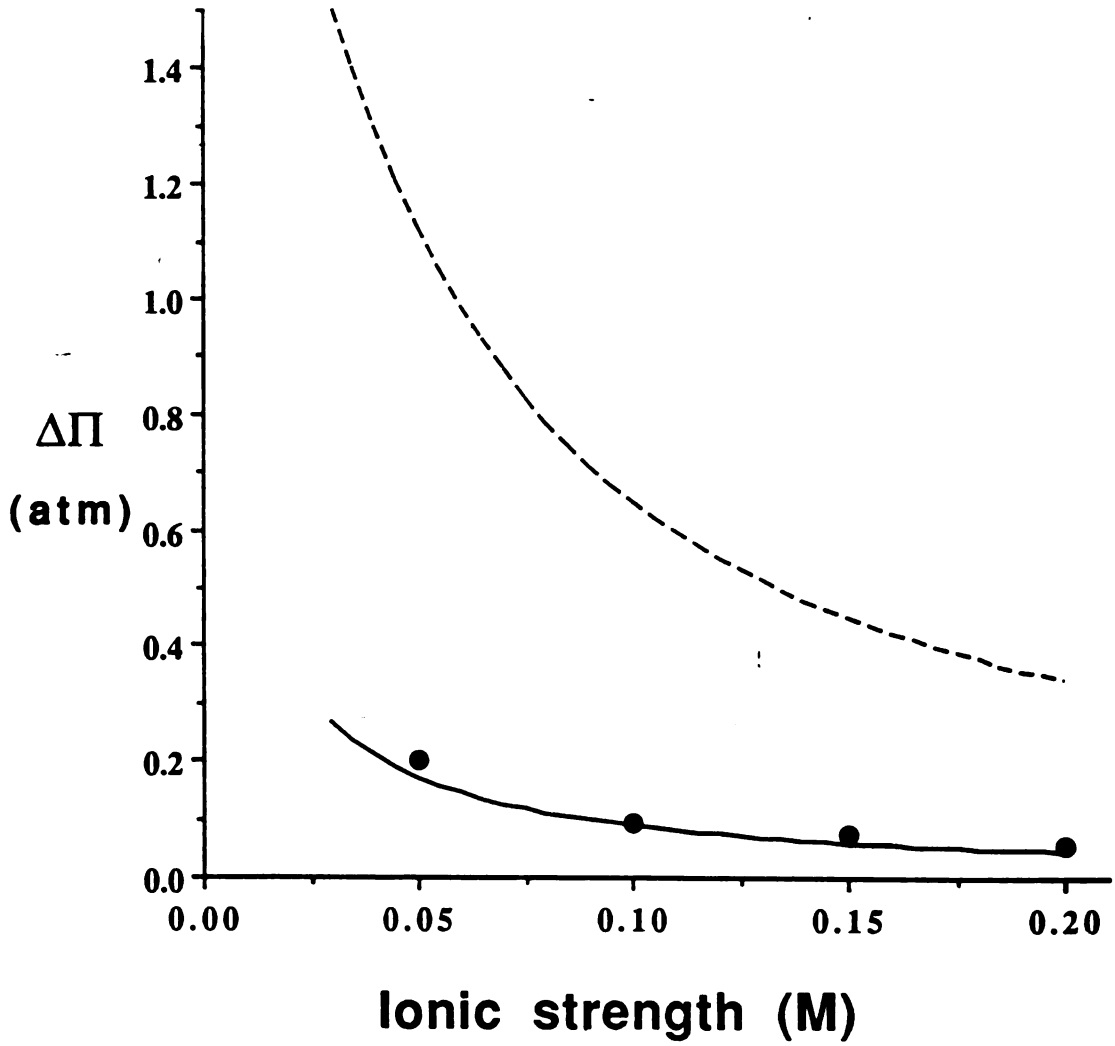

Figure 5.6. Effect of ionic strength on the colloid osmotic pressure of fully ionized p(DEA•HCl). (●) Experimental, (—) cell model, (----) ideal Donnan.

polyelectrolyte solution at fixed c_M^o (or both ways). Figure 5.7 displays values of $\Delta\Pi$ at three concentrations of ionizable groups, and several degrees of neutralization fro p(DEA•HCl). Values of $\Delta\Pi$ are plotted versus C_M, the concentration of ionized amines, which is given by $C_M = C_M^o(1-\alpha)$, where here C_M^o indicates the concentration of potentially ionizable amines.

According to figure 5.7, c_M is not sufficient to prescribe the colloid osmotic pressure, as it would be in the ideal Donnan situation. Specifically, the Donnan pressure obtained for a fully ionized polyelectrolyte ($\alpha = 0$: $c_M = c_M^o$) will be lower than that for a partially neutralized polymer where concentration has been raised in order to yield the same value of C_M as in the former case ($\alpha = 0$). This phenomenon has been termed "osmotic buffering" (10). Osmotic buffering is the result of two opposing factors; as the concentration of counterions decreases due to the decrease in the charged group concentration by neutralization, the osmotic coefficient of the remaining counterions increases due to the increase in the distance between charged groups (b in eqn. 5.20). The osmotic buffering disappears when the polyelectrolyte starts to precipitate. This observation agrees with the proposed mechanism of precipitation for p(DEA•HCl) and their hydrophobic copolymers (chapter 4). When the degree of neutralization reaches the critical precipitation point, the uncharged chains precipitate. The chains kept in solution more further apart, and the counterions are more strongly attracted to the closest chain, which reduces their osmotic coefficient. The effect is a steeper decrease in the colloid osmotic pressure upon neutralization when the precipitate phase appears. The predictions of the cell model were calculated only for the range of neutralization where p(DEA•HCl) is totally soluble since the exact degree of neutralization of the polyelectrolyte chains left in solution when the precipitate appears is unknown at present. Good agreement between theory and experiment is observed in the region of complete polyelectrolyte solubility.

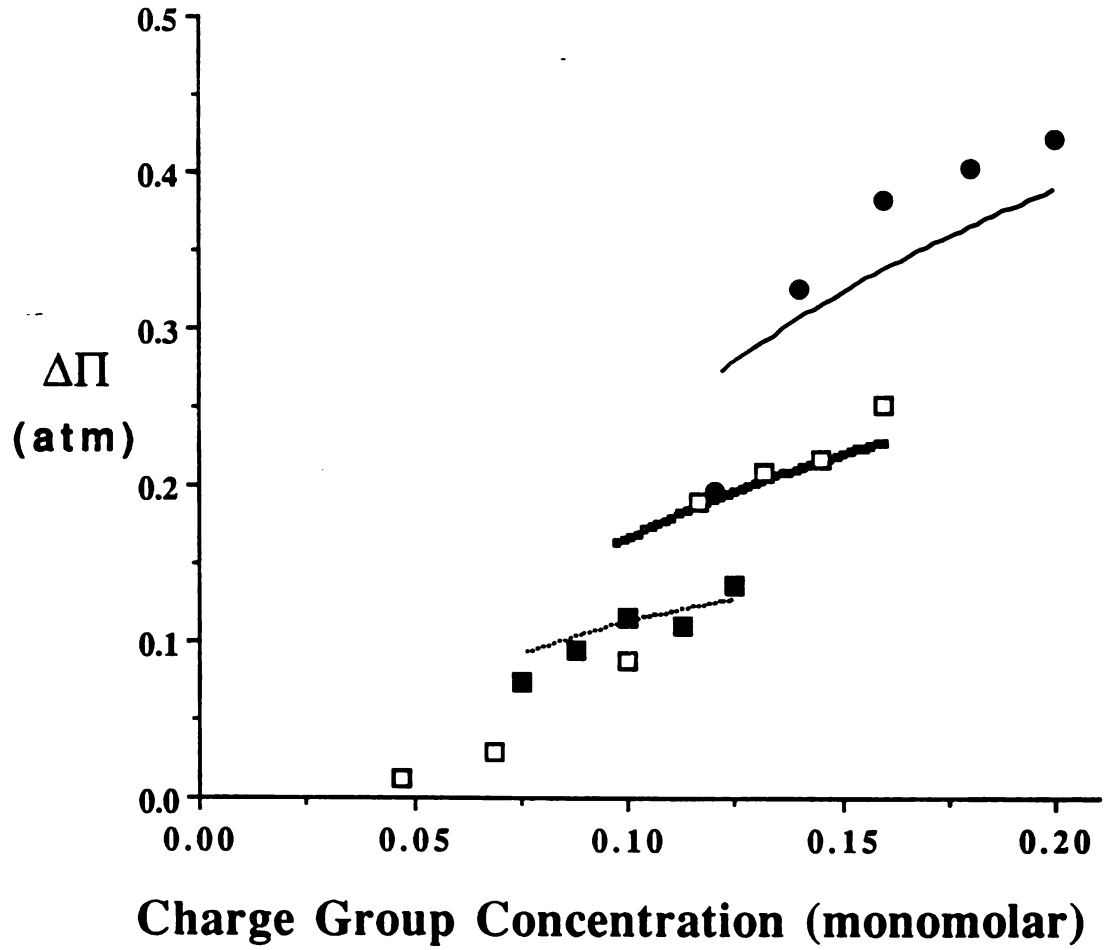

Figure 5.7. Effect of neutralization on the colloid osmotic pressure of p(DEA•HCl). Initial charged group concentration C_M^o (monomolar): (●) 0.2, (❑) 0.16 , (■) 0.125. Predictions of the cell model for different initial concentrations of charged group concentration (monomolar): (—) 0.2, (▬) 0.16 , (·····) 0.125.

5.6 Conclusions

The colloid osmotic pressure produced by p(DEA•HCl) is overestimated by the ideal Donnan model. The Donnan model also fails to predict differences in the colloid osmotic pressure produced by the copolymers of DEA•HCl and MMA at the same charged group concentration. The "cell model", complemented by the "additivity rule", gives a good prediction of the colloid osmotic pressure produced by fully ionized p(DEA•HCl) up to a concentration 0.2 monomolar. However, the theoretical predictions only agree with the experimental values at very low concentration for the colloid osmotic pressures produced by the copolymers. The cell model predicts accurately the effect of ionic strength on the colloid osmotic pressure of fully ionized p(DEA•HCl). The effect of neutralization of the homopolymer is also predicted by the cell model, at least over the range in which all the polyelectrolyte is dissolved. The colloid osmotic pressure produced by p(DEA•HCl) is larger if the charge density is decreased by neutralization of the charged groups than if charge density is decreased by diluting the solution. These observations are substantially predicted by the cell model.

References

1. J. Th. G. Overbeek, *Prog. Biophys. Biophys. Chem.*, **6**, 57 (1956).

2. C. Tanford, Physical Chemistry of Macromolecules, Wiley, New York, 1961.

3. G. Scatchard, *J. Amer. Chem. Soc.*, **68**, 2315 (1946).

4. G. Scatchard, A.C. Batchelder, A. Brown, and M. Zosa, *J. Amer. Chem. Soc.*, **68**, 2610 (1946).

5. M. Shaw, *Biophys. J.*, **16**, 43 (1976).

6. A. Katchalsky, P.F. Curran, Nonequilibrium Thermodynamics in Biophysics, Harvard University Press 1975.

7. Z. Alexandrowicz, *J. Polym Sci.*, **43**, 337 (1960).

8. Z. Alexandrowicz, *J. Polym Sci.*, **56**, 97 (1962).

9. A. Katchalsky, Z. Alexandrowicz, and O. Kedem, in Chemical Physics of Ionic Solutions; C. Barradas, R.G. Conway, Eds.; Wiley: New York, NY, 1966; Chapter 17.

10. A. Katchalsky, *Pure Appl. Chem.*, **26**, 327 (1971).

11. J. Marinsky, in Ion Exchange; J. Marinsky, Ed.; Marcel Dekker: New York, NY, 1966, Vol. 1.

12. S. Lifson, A. Katchalsky, *J. Polym. Sci.*, **13**, 43 (1954).

13. M. Rinaudo, in Polyelectrolytes, E. Selegny, Ed.; D. Reidel: Dordrecht, Holland, 1974, pp. 157-193.

14. K. Sharp and B. Honig, *J. Phys. Chem.*, **94**, 7684 (1990).

15. T.L Hill, *Disc. Faraday Soc.*, **21**, 31 (1956).

16. D. Stigter, *Biopolymers*, **16**, 1435 (1977).

17. G.S. Manning, *J. Chem. Phys.*, **51**, 924 (1969).

18. M.H. Friedman, Principles and Models of Biological Transport, Springer-Verlag, New York, 1986.

19. Desalination Systems, Inc., Technical Bulletin, 1987.

20. R.A. Robinson and R.H. Stokes, Electrolyte Solutions, Butterworths Scientific Publications, London, 1959.

Appendix 5.A. FORTRAN programs for the Calculation of ϕ_p and $\Delta\Pi$ for Polyelectrolytes

```
C    This program calculate the colloid osmotic pressure for fully
C    ionized copolymers of DEA•HCl and MMA containing 100, 75
C    and 57% DEA•HCl up to a concentration 0.2 monomolar with
C    an ionic strength set at 0.1 M. The program calculate the
C    colloid osmotic pressure according to the Ideal Donnan
C    Model and according to the osmotic coefficient obtained
C    from the Lifson-Katchalsky Cell Model. These osmotic
C    coefficients are obtained from a subroutine.

      REAL LAMBDA
      DIMENSION DMAMF(3),DELPI(3),PHIPS(3)
      DATA  DMAMF/1.,0.75,0.57/R,T,CSP/0.082,298.,0.1/
      RT=R*T
      PRINT *,'ENTER LAMBDA EFFECTIVENESS FACTOR'
      READ *,EFFECT
      WRITE(3,1000)0.,0.,0.,0.,0.
      WRITE(4,1000)0.,0.,0.,0.,0.
      DO 1 CM=0.005,0.2,0.005
         GAMMA=-ALOG(0.24*CM)/2.

         DO 2 J=1,3
            LAMBDA=2.83*EFFECT*DMAMF(J)
            PHIPS(J)=PHIP(LAMBDA,GAMMA)
            TERM=CM*PHIP(LAMBDA,GAMMA)/2.
            CS=-TERM+SQRT(TERM*TERM+CSP*CSP)
2        DELPI(J)=RT*2.*(TERM+CS-CSP)
         TERM=CM/2.
         CS=-TERM+SQRT(TERM*TERM+CSP*CSP)
         DELPII=RT*2.*(TERM+CS-CSP)

         WRITE(4,1000)CM,PHIPS
1     WRITE(3,1000)CM,DELPI,DELPII

      STOP

1000  FORMAT(5F8.4)

      END
```

```
C    This program calculates the colloid osmotic pressure
C    according to the Ideal Donnan Model and according to the
C    Cell Model for a given concentration of fully ionized
C    p(DEA•HCl) at different ionic strengths ranging from 0 to 0.2
C  M.

      REAL LAMBDA
      DIMENSION DMAMF(1),DELPI(1),PHIPS(1)
      DATA  DMAMF/1./R,T/0.082,298./
      RT=R*T
      PRINT *,'ENTER AMINE CONCENTRATION'
      READ *,CM
      PRINT *,'ENTER LAMBDA EFFECTIVENESS FACTOR'
      READ *,EFFECT
      WRITE(3,1000)0.,0.,0.,0.,0.
      WRITE(4,1000)0.,0.,0.,0.,0.

      DO 1 CSP=0.005,0.2,0.005
         GAMMA=-ALOG(0.24*CM)/2.
         LAMBDA=2.83*EFFECT*DMAMF(1)
         PHIPS(1)=PHIP(LAMBDA,GAMMA)
         TERM=CM*PHIP(LAMBDA,GAMMA)/2.
         CS=-TERM+SQRT(TERM*TERM+CSP*CSP)
         DELPI(1)=RT*2.*(TERM+CS-CSP)
         TERM=CM/2.
         CS=-TERM+SQRT(TERM*TERM+CSP*CSP)
         DELPII=RT*2.*(TERM+CS-CSP)
         WRITE(4,1000)CSP,PHIPS
1     WRITE(3,1000)CSP,DELPI,DELPII

      STOP

1000  FORMAT(5F8.4)

      END


C    This program calculate the colloid osmotic pressure
C    according to the Cell Model at different degrees of
C    neutralization for three given concentrations of p(DEA•HCl)
C    (0.125,0.16, and 0.2).
```

```
      REAL LAMBDA
      DIMENSION CMR(3),DELPI(3),PHIPS(3)
      DATA  CMR/0.2,0.16,0.125/R,T,CSP/0.082,298.,0.1/
      RT=R*T
      PRINT *,'ENTER LAMBDA EFFECTIVENESS FACTOR'
      READ *,EFFECT
      WRITE(3,1000)0.,0.,0.,0.,0.
      WRITE(4,1000)0.,0.,0.,0.,0.

      DO 1 ALPHA=0.0,0.39,0.01
         DMAMF=(1-ALPHA)

         DO 2 J=1,3
            CM=CMR(J)
            GAMMA=-ALOG(0.24*CM)/2.
            LAMBDA=2.83*EFFECT*DMAMF
            PHIPS(J)=PHIP(LAMBDA,GAMMA)
            TERM=DMAMF*CM*PHIP(LAMBDA,GAMMA)/2.
            CS=-TERM+SQRT(TERM*TERM+CSP*CSP)
2        DELPI(J)=RT*2.*(TERM+CS-CSP)
         TERM=CM/2.
         CS=-TERM+SQRT(TERM*TERM+CSP*CSP)
         DELPII=RT*2.*(TERM+CS-CSP)
         WRITE(4,1000)ALPHA,DMAMF,PHIPS
1     WRITE(3,1000)ALPHA,DELPI,DELPII

      STOP

1000  FORMAT(5F8.4)

      END



C OSMOTIC COEFFICIENT FOR LIFSON-KATCHALSKY CELL MODEL
      C    This is the subroutine that calculates the osmotic coefficients
      C    according to the Cell Model. It requires the values of
      C    LAMBDA and GAMMA (see text chapter 5) and returns φp.

      FUNCTION PHIP(LAMBDA,GAMMA)
      REAL LAMBDA
      IF(LAMBDA-GAMMA/(1.+GAMMA))20,10,30
```

```
      C  "CRITICAL" VALUE
10    PHIP=1./(2.*LAMBDA)
      RETURN

      C  "REAL" BRANCH
20    B=0.5
21    BG=B*GAMMA
      F=1.-B*B-LAMBDA*(1.+B*COTH(BG))
      DF=-2.*B-LAMBDA*(COTH(BG)-BG*CSCH2(BG))
      DB=-F/DF
      B=B+DB
      IF(ABS(DB).GT.1.E-6)GO TO 21
      PHIP=(1.-B*B)/(2.*LAMBDA)
      RETURN

      C "IMAGINARY" BRANCH
30    B=3.14159/(2.*GAMMA)
31    BG=B*GAMMA
      F=1.+B*B-LAMBDA*(1.+B*COT(BG))
      DF=2.*B-LAMBDA*(COT(BG)-BG*CSC2(BG))
      DB=-F/DF
      B=B+DB
      IF(ABS(DB).GT.1.E-6)GO TO 31
      PHIP=(1.+B*B)/(2.*LAMBDA)
      RETURN
      END

      C  AUXILIARY TRIGONOMETRIC AND HYPERBOLIC FUNCTIONS

      FUNCTION COTH(X)
      COTH=1./TANH(X)
      RETURN

      FUNCTION COT(X)
      COT=1./TAN(X)
      RETURN
      END

      FUNCTION CSCH2(X)
      CSCH=1./SINH(X)
      CSCH2=CSCH*CSCH
      RETURN
      END
```

```
FUNCTION CSC2(X)
CSC=1./SIN(X)
CSC2=CSC*CSC
RETURN

END
```

Chapter 6

Soluble Hydrophobic Polyelectrolytes

6.1 Introduction

The mechanochemical insulin pump described in chapter 1 requires the rapid development of colloid osmotic pressure after the increase of blood glucose concentration is detected. The formation of a precipitate phase for the unionized form of the DEA family of polyelectrolytes indicates possibly slow dissolution kinetics (see chapter 7). A non-precipitating system with the same buffering properties of the DEA copolymers would be the ideal osmotic agent for this particular application, since one would not expect dissolution kinetics to play a role.

It has been found that introducing permanent charges by partially quaternizing the amine groups of hydrophobic polyelectrolytes can inhibit the formation of the precipitate phase; nevertheless, the polyelectrolytes produced maintain some of the buffering properties of the non-quaternized form (1,2). The buffering produced by partially quaternized polyelectrolytes has been attributed to the formation of a soluble globular structure on neutralization. The unionized hydrophobic segments of the polyelectrolyte form the core of the globular structure while the permanent charges are located at the surface of the globule in contact with the aqueous solution phase.

Soluble polyelectrolytes have many industrial applications (3). As indicated in chapter 2, soluble hydrophobic polyelectrolytes are especially interesting because of their viscosity enhancing properties even in solutions containing high concentrations of salt.

In this chapter the potentiometric and colloid osmotic pressure behavior of partially quaternized forms of p(DEA•HCl) are studied. Considered first are copolymers of DEA•HCl and methacryloxyethyl trimethyl ammonium chloride (MTAC). The latter monomer is the

quaternized form of N,N-dimethylaminoethyl methacrylate (Figure 6.1). The predictions of the cell model are compared to the results of the colloid osmotic pressure experiments performed with p(DEA•HCl/MTAC). The second series of experiments involves the synthesis and titration of partially quaternized forms of the copolymer p(DEA/MMA) 38/62.

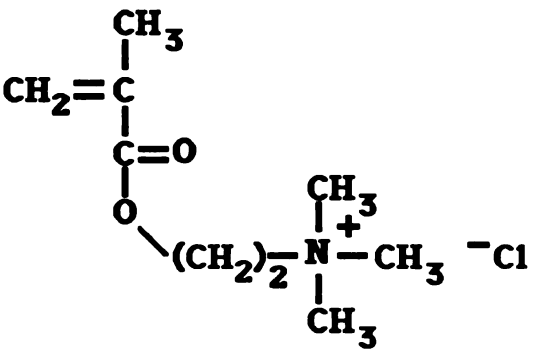

Figure 6.1. Structure of methacryloxyethyl trimethyl ammonium chloride (MTAC).

6.2 Experimental

6.2.1 Materials

DEA and MMA (Polysciences Inc.) were purified as described in chapter 2. Methacryloxyethyl trimethyl ammonium chloride 70% (m/v) aqueous solution (Polysciences Inc.), sodium chloride (Fisher Scientific), acetone (Fisher Scientific), diethyl ether (Fisher Scientific), potassium persulfate (Polysciences Inc.), methanol (Fisher Scientific), NaOH 0.1 M certified solution (Fisher Scientific), NaOH 50% (w/w) (Fisher Scientific), sodium methoxide (Aldrich), dimethyl sulfate (Aldrich), benzene (Fisher Scientific) were used as received. Water was double distilled and deionized.

6.2.2 Synthesis of p(DEA•HCl/MTAC) Copolymer

The formation of DEA•HCl is described in chapter 2. DEA•HCl was copolymerized with MTAC by radical copolymerization in aqueous solution (400 g monomers/l) at 40°C using potassium

persulfate as the initiator (0.55 g/l). The copolymerization reaction was stopped after 1 hour (to keep the conversion below 10%) by rapidly cooling the reaction mixture. The polymerization mixture was precipitated into acetone. The polymer was purified by redissolving the precipitate in a minimum volume of 0.1 M HCl . The solution produced was diluted with methanol and precipitated in acetone. The polyelectrolyte was separated by filtration, dried at room temperature under vacuum for at least 24 hrs, and finally dried at 60°C under vacuum for 1 hr. Dried samples were submitted for C and N elemental analysis.

6.2.3 Titration Curves for p(DEA•HCl/MTAC) Copolymers

The titration curves for the copolymers of p(DEA•HCl/MTAC) copolymers were obtained by titrating 0.01 monomolar (as amine groups) solutions of the fully ionized polyelectrolytes with 0.1 M NaOH solution using an automatic titrator (Radiometer, Copenhagen Denmark). The ionic strength of the polyelectrolyte solution was set at 0.1 M using NaCl.

6.2.4 Colloid Osmotic Pressure Studies for p(DEA•HCl/MTAC) Copolymers

The colloid osmotic pressure properties of the copolymer p((DEA•HCl/MTAC) 88/12 were studied. The effect of concentration was studied by measuring the colloid osmotic pressure produced by different charged group concentrations (up to 0.2 monomolar) of fully ionized polyelectrolyte. The reference solution was a 0.1 M NaCl solution at pH 4 or below.

The effect of neutralization on the colloid osmotic pressure of p(DEA•HCl/MTAC) 88/12 was studied by measuring the colloid osmotic pressure produced by solutions containing 0.175 M amine groups concentration, at different degrees of neutralization. Neutralization followed from by adding the appropriate volume of a 0.1 M NaOH solution during preparation of the solutions. For high degrees of neutralization, a 0.4 M NaOH solution was used. The

reference solution for each experiment was 0.1 M NaCl at a pH similar to the pH of the solution to be studied.

6.2.5 Synthesis of Partially Methylated p(DEA•HCl)/MMA copolymers.

The copolymer p(DEA•HCl/MMA) 62/38 was synthesized and characterized as described in chapters 2 and 3.

The partial methylation of this copolymer was performed using the method of Vallin *et al.* (2). The polyelectrolyte was partially deprotonated by addition of sodium methoxide (a very strong base), to solutions of the protonated polyamine in methanol (1 g polyelectrolyte per 40 ml methanol), with further addition of benzene to obtain a 40:60 (v/v) methanol/benzene mixture. Dimethyl sulfate (the methylating agent) was then added, and the mixtures were stirred at room temperature for a definited reaction time. After acidification with 6 M HCl, the mixtures were dialyzed (MWCO 12 000-14 000) against methanol. The solvent of the dialyzed solutions was evaporated. The partially methylated products were further dried under vacuum. The experimental parameters are in table 6.1.

6.2.6 Titration Curves for partially methylated p(DEA•HCl/MMA) 38/62

The titration curves for the partially methylated p(DEA•HCl/MMA) 38/62 polyelectrolyte were obtained as in 6.2.3.

6.3 Results and Discussion

The proportion of the comonomers in the p(DEA•HCl/MTAC) copolymers was determined as follows. The number of moles of total nitrogen per gram of polymer was determined by elemental analysis. The number of moles of titrable nitrogen (tertiary amines) per gram of polymer was obtained from the titration curves of the polyelectrolytes. The end point of the titration was equated with the

Table 6.1. Experimental conditions and results of the partial methylation of p(DEA•HCl/MMA) 38/62.

Run No.	$\frac{[CH_3ONa]}{[Nitrogen]}$	$\frac{[(CH_3)_2SO_4]}{[Nitrogen]}$	Reaction time (hrs)	Degree of quaternization
1	0.59	1.21	7.4	18.25%
2	0.46	1.20	7.0	13.65%
3	0.36	1.20	7.2	4.21%

maximum slope (dpH/dvolume) of the titration curves. Figure 6.2 shows the titration curve and its derivative for 20 ml of a p(DEA•HCl/MTAC) 88/12 0.01 monomolar (approximately) solution (0.1 M NaCl). A distinct end point is observed. The ratio of the number of moles of titrable amine groups per gram to the number of moles of total nitrogen per gram gives the proportion of the DEA monomer in the polyelectrolyte. The results of three copolymer syntheses and analyses are shown in table 6.2, which indicates that the proportion of the monomers incorporated into the copolymers is very similar to the proportions in the feed. This implies a random copolymerization.

Table 6.2. Results of the copolymerization of DEA•HCl and MTAC.

Proportion in feed DEA•HCl/MTAC	Proportion in polymer DEA•HCl/MTAC
95/5	94.7/5.3
92.5/7.5	94/6
85/15	88/12

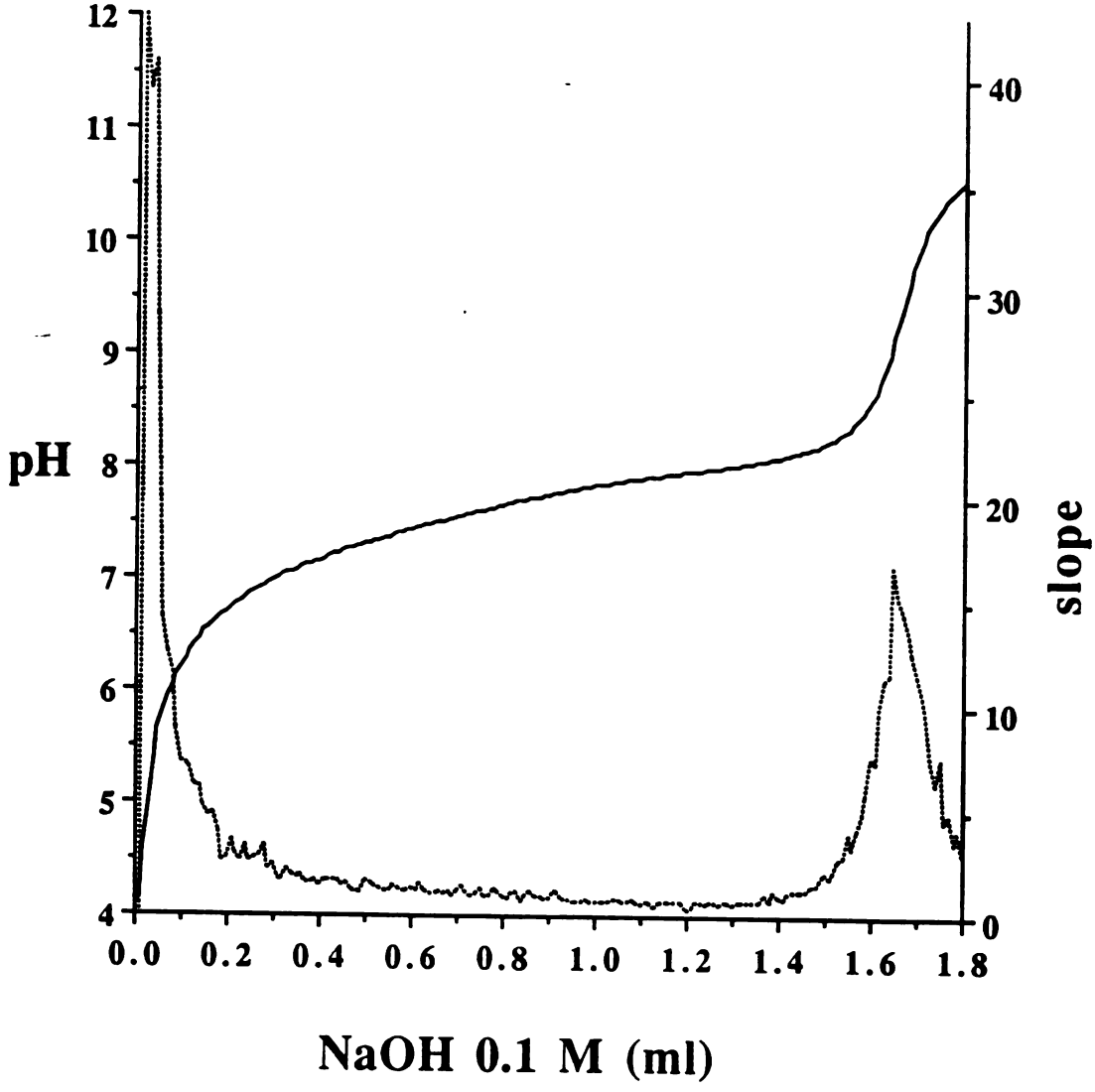

Figure 6.2. Titration curve and its derivative for p(DEA•HCl/MTAC) 88/12. (—) pH, (----) slope.

Figure 6.3 presents the titration curves (pH against α) for two copolymers of DEA•HCl/MTAC, 94.7/5.3 and 88/12. The titration curves do not display the excellent buffering properties that are shown by the precipitating polyelectrolytes (compare figures 4.2-4.5). It is also observed that the "buffering" pH is higher than that presented by p(DEA•HCl). The copolymer 94.7/5.3 forms a transparent, swollen precipitate at the end of the titration The precipitate was also observed in the titration of the 94/6 copolymer. This indicates that greater than 6% quaternized comonomer is required to maintain the polyelectrolyte in solution at any pH.

According to the Cell Model of polyelectrolyte solutions, fully ionized p(DEA•HCl) and fully ionized p(DEA•HCl/MTAC) copolymers have the same linear charge density (same number of carbon atoms between each ionized monomer in the polymer chain). Assuming the same gravimetric density for the two polyelectrolytes (highly probable since the proportion of MTAC in the copolymers is very small), p(DEA•HCl) and p(DEA/MTAC) copolymers should produce the same amount of colloid osmotic pressure at a given charge group concentration. This prediction is corroborated in figure 6.4 where the colloid osmotic pressure for p(DEA•HCl/MTAC) 88/12 is plotted against charge group concentration. The cell model adequately predicts of the experimental colloid osmotic pressure up to 0.2 M charge group concentration. The same results were obtained for p(DEA•HCl) in chapter 5.

Figure 6.5 shows the colloid osmotic pressure produced by a 0.175 M p(DEA•HCl/MTAC) 88/12 solution at different degrees of neutralization (charge density is reduced by neutralizing the polyelectrolyte with NaOH solutions). An "osmotic buffering" is observed during the entire range of neutralization. This differs from the behavior of p(DEA•HCl) in chapter 5, where the "osmotic buffering" disappears as the polyelectrolyte forms a precipitated phase. The cell model reasonably predicts the experimental results. The proportion of methylation of p(DEA•HCl/MMA) 38/62 was determined in the same way that the proportions of comonomers in

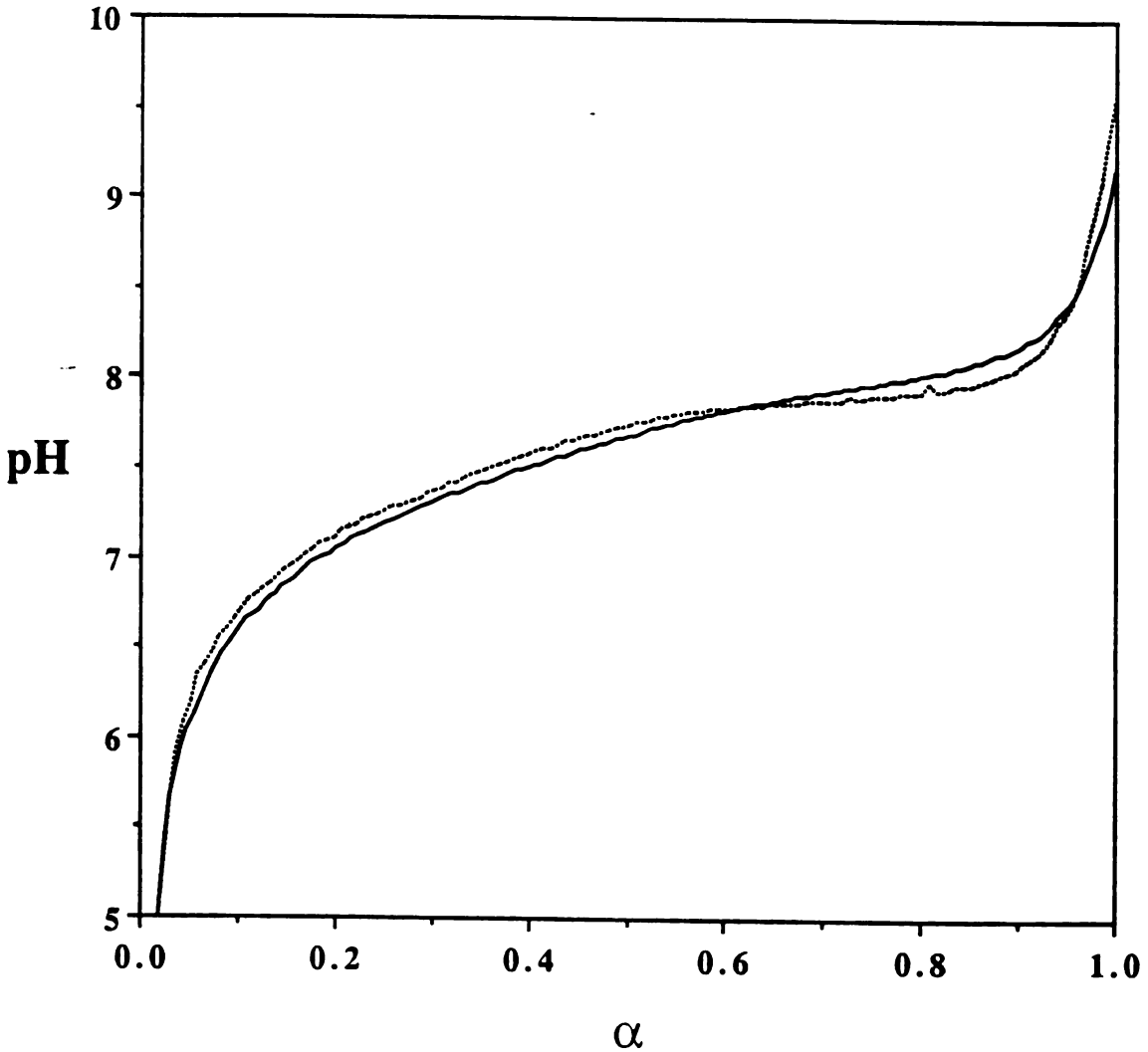

Figure 6.3. Titration curves for p(DEA•HCl/MTAC) copolymers in 0.1 M NaCl solutions. (—) p(DEA•HCl/MTAC) 88/12, (----) p(DEA•HCl/MTAC) 95/5.

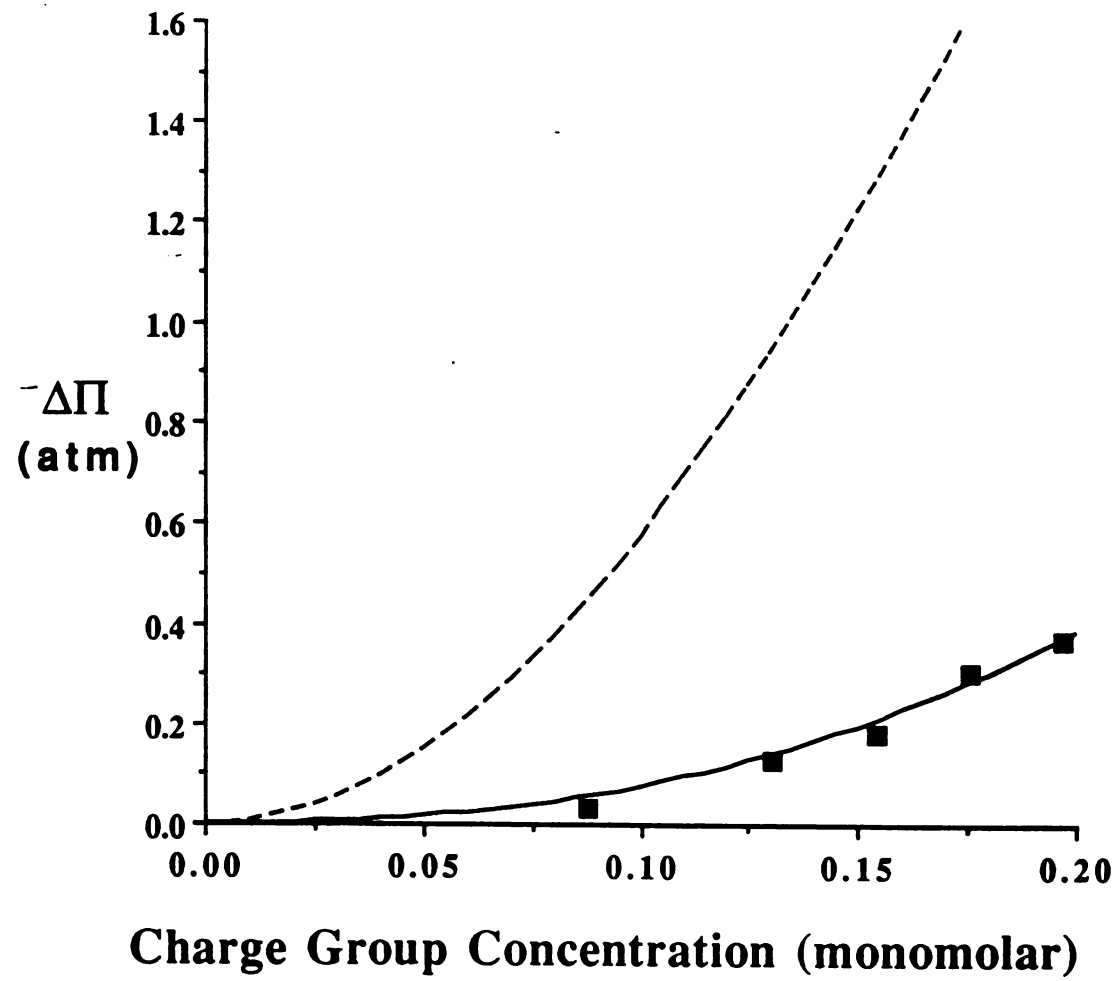

Figure 6.4. Effect of concentration on the colloid osmotic pressure of p(DEA•HCl/MTAC) 88/12. Polyelectrolyte is fully ionized. Ionic strength is set at 0.1 M with NaCl. (■) experimental results, (—) cell model prediction, (----) ideal Donnan prediction.

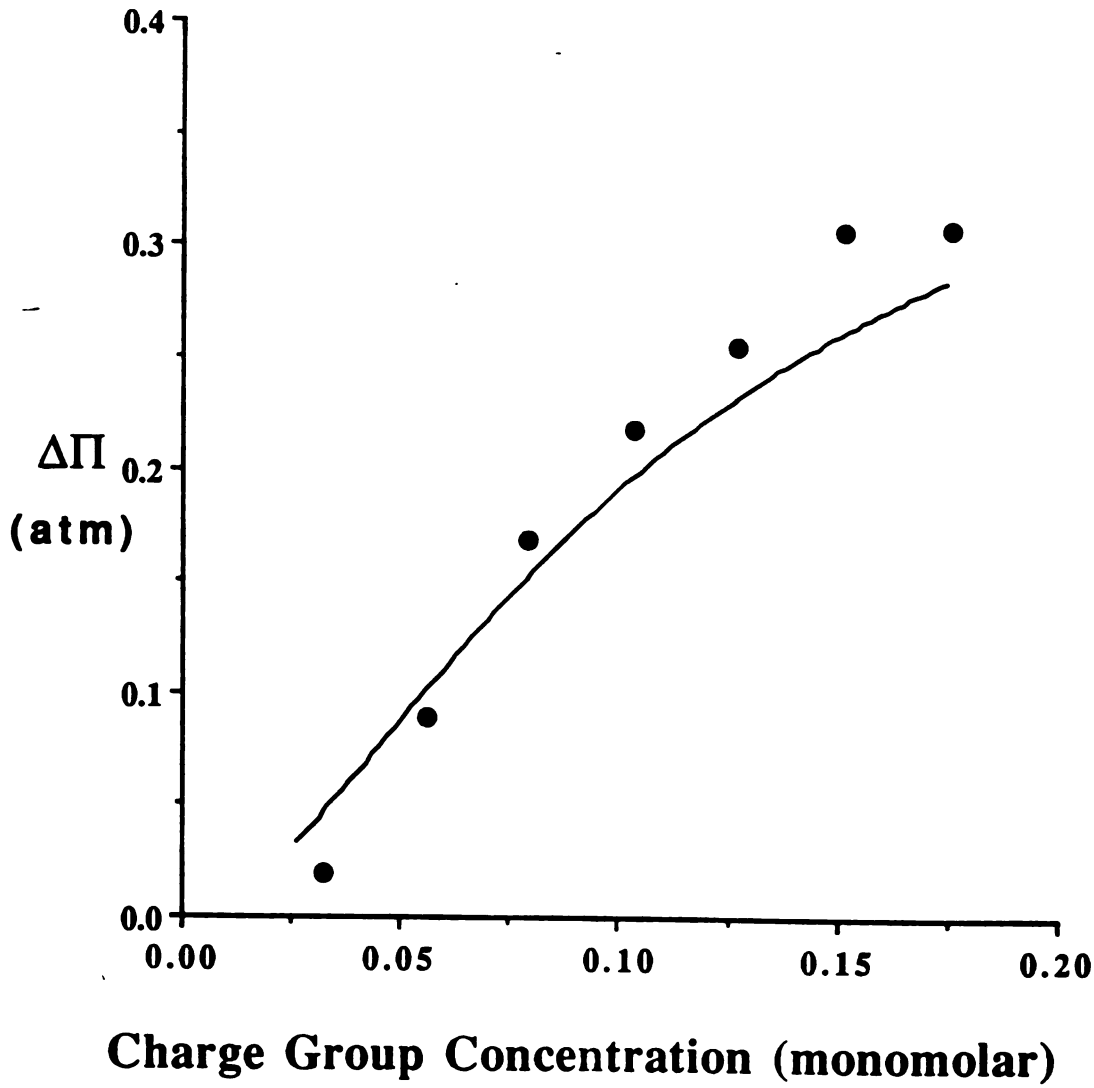

Figure 6.5. Effect of neutralization on the colloid osmotic pressure of p(DEA•HCl/MTAC) 88/12. (●) experimental results, (—) cell model prediction.

the copolymers of DEA•HCl and MTAC were found. The results are listed in table 6.1. The titration curves for the partially methylated polyelectrolytes are compared to the corresponding curve for the parent copolymer in figure 6.6. It is observed that the "buffering pH" increases as the degree of methylation increases. It is also observed that the buffering capacity decreases as the degree of methylation increases. The polyelectrolyte with only 4% methylation shows a precipitate phase at a degree of neutralization of 0.9. The polyelectrolytes containing 13 and 18% methylation do not form precipitates. These results agree with those obtained for the copolymers of DEA•HCl and MTAC. Similar observations were made by Vallin et *al.* (2) for another class of hydrophobic, partially N-alkylated poly(tertiary amines).

Hueget and Vert have proposed this kind of polyelectrolyte for water solubilization and pH-sensitive release of hydrophobic drugs in aqueous solution (4). The hydrophobic drugs are trapped in the core of the water soluble polymer globules at high pH. When the pH of the medium drops to the point at which the globular structure is lost, the hydrophobic drugs are released into the medium. The system studied in the present work has the advantage that the pH of drug release can be specified by using the appropriate copolymer. In this way, hydrophobic drugs could be released to a target body compartment having a pH lower than physiological pH (e.g., lysozomes or tumor cells).

6.4 Conclusions

The formation of a precipitated phase by hydrophobic polyelectrolytes can be inhibited by interposing permanent charges along the polymer. The minimum fraction of permanent charges required to inhibit the precipitation is between 6 and 12%. The "buffering" pH increases as the proportion of quaternary amines increases. The partially methylated polyelectrolytes produced do not possess the high buffering capacity presented by the precipitating polymers.

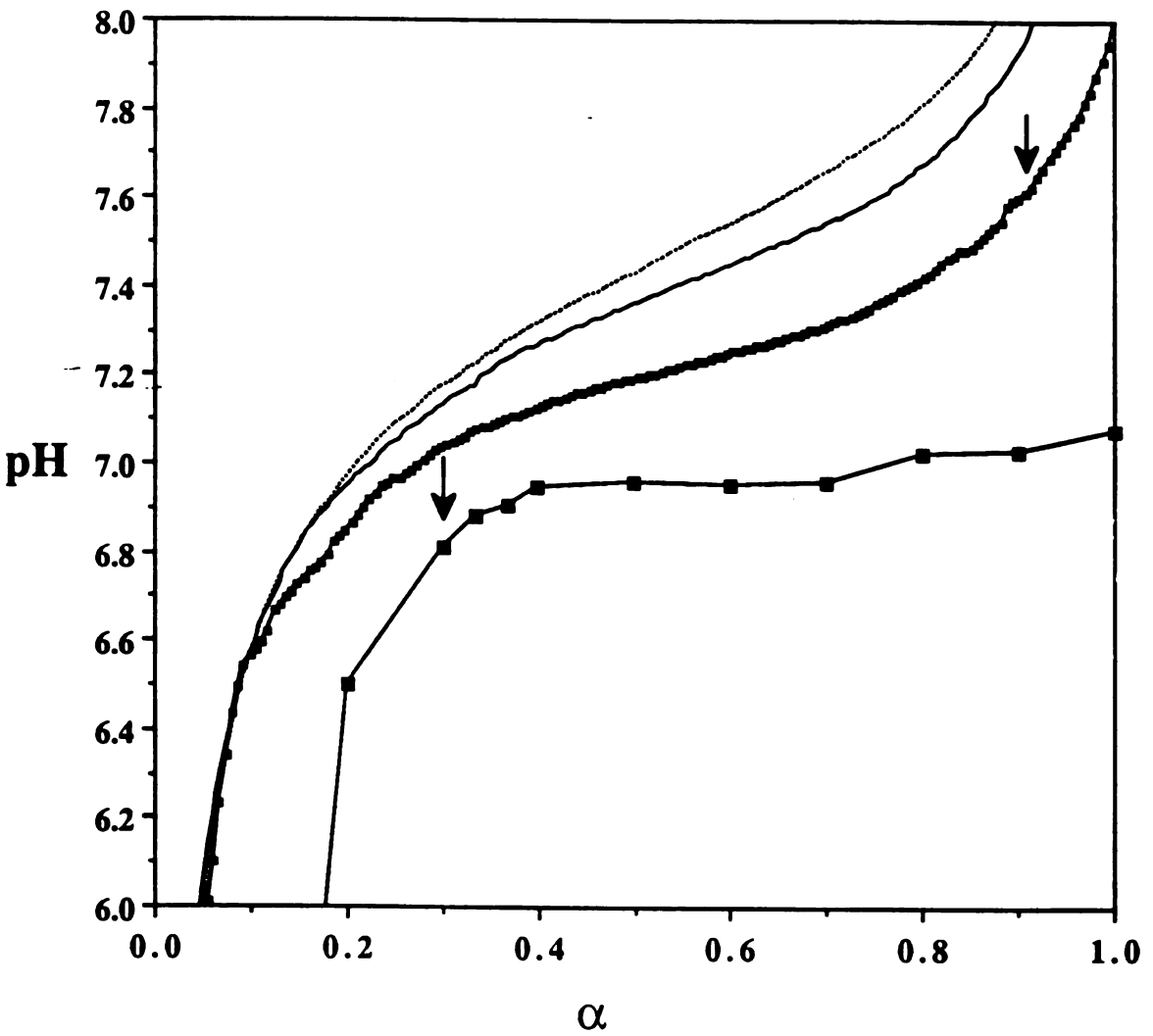

Figure 6.6. Titration curves of partially methylated samples of p(DEA•HCl/MMA) 38/62 in 0.1 M NaCl solutions. Arrows indicate the point at which precipitate is initially observed. Fraction of quaternized amine groups; (■) 0%, (▬) 4%, (—)13%, (·····)18%.

The colloid osmotic pressures produced by the fully ionized copolymer p(DEA•HCl/MTAC) 88/12 are similar to those produced by fully ionized p(DEA•HCl). An "osmotic buffering" is observed in the whole range of neutralization for p(DEA•HCl/MTAC) 88/12. The Cell Model gives a good prediction of the effect of concentration and neutralization on the colloid osmotic pressure of the polyelectrolyte.

References

1. Y.E. Kirsh, N.R. Pavlova, and V.A. Kabanov, *Eur. Polym. J.*, **11**, 47 (1975).

2. D. Vallin, J. Hueget, and M. Vert, *Polymer Journal*, **12** (2), 113 (1980).

3. M.F. Hoover, *J. Macromol. Sci.-Chem.*, **A4**, 1327 (1970).

4. J. Hueget and M. Vert, *J. Controlled Release*, **1** (3), 217 (1985).

Chapter 7

Kinetics of Colloid Osmotic Pressure Development and Release

7.1 Introduction

The use of polyelectrolytes as the osmotic agent for the proposed mechanochemical pump requires fast kinetics of colloid osmotic pressure development, after ionization of the polymer by the acid produced by enzymatic oxidation of glucose. Once insulin has been released and the glucose levels are back to the basal concentration, the polyelectrolyte should be neutralized by the medium, so that the colloid osmotic pressure may return to its basal state. The kinetics of colloid osmotic pressure produced by the polyelectrolyte studied in this work are then of great importance. The present chapter deals with the kinetics of colloid osmotic pressure development and release for the precipitating and non-precipitating polyelectrolytes.

Several osmotic pumps utilize the difference in osmotic pressure between the device and the environment as the driving force for drug release (1-4). These systems generally use a saturated low molecular weight salt solution as the osmotic agent. The salt is contained behind a semipermeable membrane, usually made of cellulose acetate, which permits the flux of water but retains the salt. The flux of water into the osmotic agent compartment causes drug to be expelled from its reservoir. Drug release from an osmotic pump is zero-order with rate equalling the rate of water imbibition, as long as a saturated salt solution is maintained in the device by excess solid salt. The rate of water imbibition is directly proportional to the osmotic pressure difference ($\Delta\Pi$) across the membrane (4). The proportionality constant may be called the membrane osmotic permeability. Usually the permeability is independent of the osmotic agent, but dependent on the geometry and structure of the

membrane (5). In many cases, the water flow, and hence the delivery rate, is independent of changes in physiologic variables such as pH, enzymatic activity, surface tension, viscosity, and salt concentration in the external solution (2). Usually, the osmotic pressure inside the device is sufficiently high to dominate any fluctuations in osmotic pressure in the physiological reservoir in which the pump is placed.

With polyelectrolytes, the relation between osmotic pressure and osmotic flow appears to be more complex. A decrease in membrane osmotic permeability with increasing osmotic pressure has been observed in several polyelectrolyte systems, and has been attributed to an unstirred layer on the solution side of the membrane (6,7). This layer represents a thin film of fluid with a lower solute concentration than the bulk solution, due to convection of solute away from the membrane. The presence of the boundary layer leads to a lower effective osmotic pressure and flow compared to that expected from the concentration in the bulk solution. The existence of an unstirred layer can be avoided to some extent with efficient stirring. Williams *et al.* studied the effect of osmotic pressure on water flow for uncharged polymers (8) and polyelectrolytes (9) in a well-stirred cell and observed decreases in the permeability with increasing osmotic pressure even for nearly perfectly well-stirred system. Moreover, they did not find any significant difference between well-stirred experiments and unstirred ones. The authors concluded that the assumed unstirred layer does not exist, but that the limiting event is volume exchange diffusion of osmotic agent and solvent adjacent to the membrane. The proportionality constant between water flow and osmotic pressure is then determined primarily by the diffusive mobility of the osmotically active solute. Diffusive mobility can be determined independently by measuring the hydrodynamic friction coefficient of the molecule.

Another observation made by Williams et al. is that charged polyelectrolyte solutions produce osmotic flows similar to those generated by uncharged polymer solutions at the same osmotic

pressures. Thus, the charged nature of the polyelectrolyte does not affect the osmotic flow mechanism, although the charge does affect the osmotic driving force.

Due to the complicated interplay of factors involved in the kinetics of colloid osmotic pressure development, it was decided to study the kinetics for the precipitating and non-precipitating polyelectrolytes discussed in chapter 2 and 6. To do so, it was necessary to redesign the osmometer cell to mimic more closely the actual mechanochemical insulin pump. The redesigned cell is diagrammed in figure 7.1. The reference solvent compartment and the polyelectrolyte solution compartment have volumes of 52 ml and 3.8 ml respectively. The reference compartment is stirred by a spin bar while the polyelectrolyte compartment is unstirred. There are two filling valves in each compartment. The cell is placed in the horizontal position. A pH electrode (Orion 91-03, semimicroelectrode) is introduced into the reference compartment through a hole drilled in the cell casing.

Choice of the polymer system was driven by the nature of the precipitate formed by different compositions. Neutralization of the homopolymer p(DEA•HCl) produces a gummy precipitate which will not disperse in water. The copolymers of DEA and MMA form powder-like precipitates which are dispersible in water with proper stirring. Since a gummy precipitate with a very small surface area was expected to present very slow and impractical dissolution (and hence colloid osmotic pressure) kinetics, we decided to use the copolymer p(DEA•HCl/MMA) 56/44 in the kinetics experiments. We also studied kinetics with the soluble p(DEA•HCl/MTAC) system.

7.2. Kinetics of Colloid Osmotic Pressure Development

7.2.1 Materials

NaOH 0.1 N certified solution, HCl 0.1 M certified solutions, and NaOH 50% (w/w) were from Fisher Scientific. NaCl (Fisher Scientific)

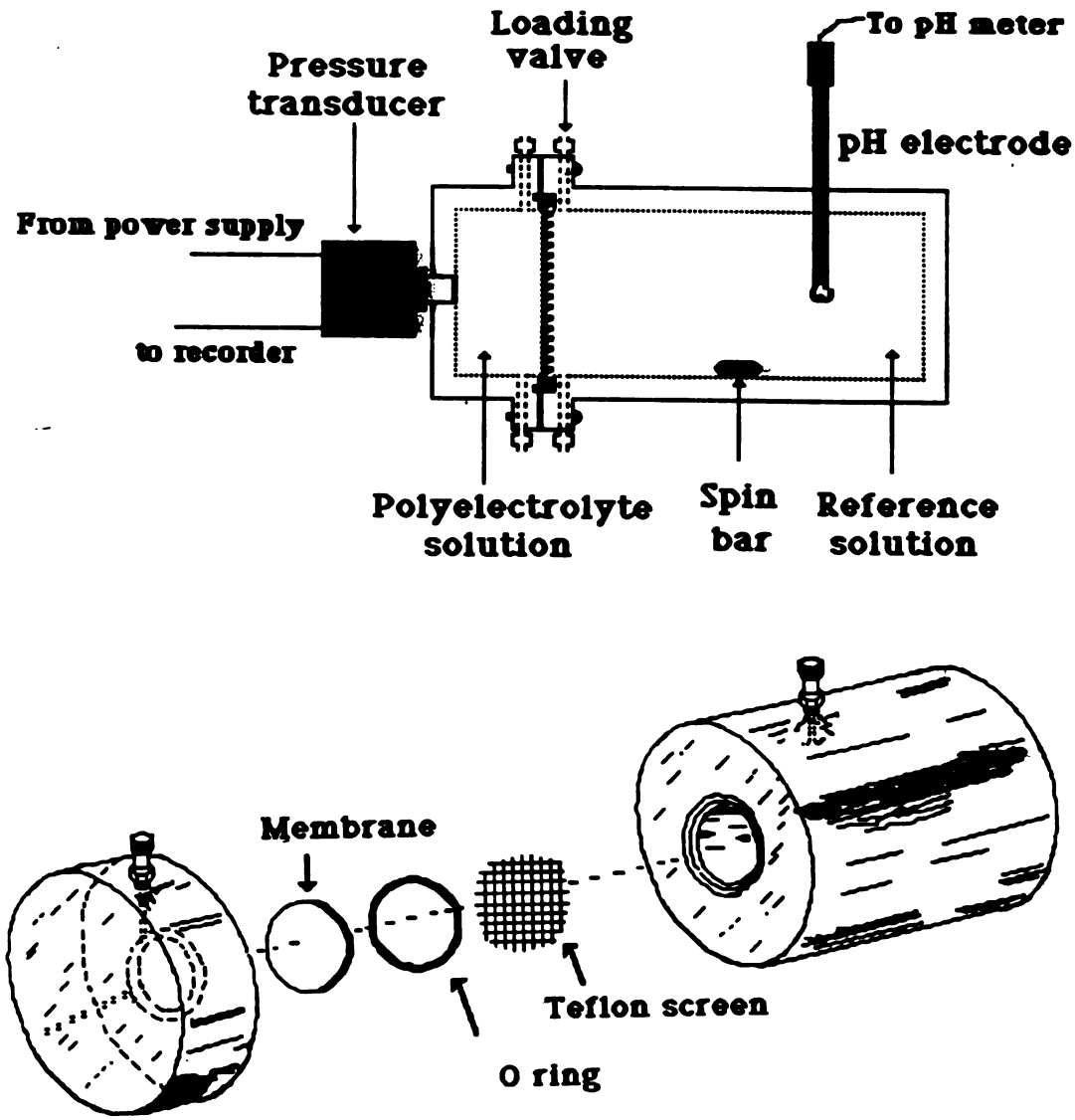

Figure 7.1. Schematic diagram of the osmotic cell used to measure the kinetics of colloid osmotic pressure.

was used as received. Water was distilled and deionized. Semipermeable membranes were prepared as in chapter 5. Polyelectrolytes were synthesized and purified as in chapters 2 and 6.

7.2.2 Procedure

Changes in colloid osmotic pressure after addition of base or acid to the reference chamber in the osmotic cell were studied for p(DEA•HCl/MMA) 56/44 and for p(DEA•HCl/MTAC) 88/12. Simultaneously, the pH in the reference compartment was measured using a pH electrode. The following protocol was performed for each polyelectrolyte: A solution of the hydrochloride form of the polyelectrolyte was completely neutralized by the NaOH solution. Neutralization was accelerated by stirring. The desired polymer concentration was obtained by diluting the resulting dispersion (for the MMA copolymer) or solution (for the MTAC copolymer) with distilled water. The dispersion or solution was loaded into the smaller compartment of the osmotic cell (3.8 ml). The reference solution compartment was loaded with a 0.1 M NaCl solution (52 ml) of a pH similar to the pH of the polyelectrolyte suspension or solution. The system was allowed to equilibrate until a constant reading from the pressure transducer was obtained. A volume of HCl 0.1 M corresponding to half the number of monomoles of DEA units in the polyelectrolyte chamber was then injected into the reference chamber. The resulting pressure signal from the pressure transducer and the pH measured by a pH meter (Corning 145) were recorded in a data logger (Omega, Stamford CT) at a sampling rate of 650 ms. After a pre-determined time, a volume of NaOH 0.1 M equal to the volume of HCl previously injected was added to the reference solution compartment. Alternating additions of HCl and NaOH were repeated.

7.2.4 Results

Figure 7.2 shows typical results from a kinetics of colloid osmotic pressure experiment for a 0.12 monomolar dispersion of p(DEA/MMA) 54/44. Figure 7.2 also shows the amount of HCl transported to the polyelectrolyte compartment. The amount of acid transported was calculated from pH measurements in the following way: when acid is injected into the reference solution compartment, the amount of acid transported is determined by calculating the difference between the amount of acid loaded and the amount of acid remaining in the compartment, as determined from the pH measurements. When NaOH is loaded in the compartment, the amount of acid remaining in the polyelectrolyte compartment is assumed to be equal to the concentration of NaOH in the reference compartment, as determined from the pH measurements (this assumption is based on the fact that equivalent amounts of acid and base are successively added).

In figure 7.2 it is noticed that the colloid osmotic pressure development is very slow, requiring about 12 hrs to reach 0.04 atm. The pressure release process seems to be even slower. The result is an increase in pressure (accumulation) with repeating acidification and neutralization cycles. The precipitate sediments in the bottom of the compartment. Before the addition of acid, some precipitate seems to be disperse in the supernatant solution in the polyelectrolyte chamber. The supernatant solution clarifies after the addition of acid. After a neutralization cycle (i.e. after addition of NaOH), precipitate sticks to the membrane.

The results of a typical experiment using a p(DEA/MTAC) 88/12 0.2 monomolar solution are shown in figure 7.3. It is observed that the pressure before adding the first volume of HCl 0.1 M is not zero. This is due to the quaternary amine groups in the polyelectrolyte which cannot be neutralized; their associated counterions are osmotically active at any pH. The kinetics of colloid osmotic pressure development for the soluble polyelectrolyte are much faster than the kinetics for the precipitating system. A pressure change of around 0.1 atm is achieved in approximately an

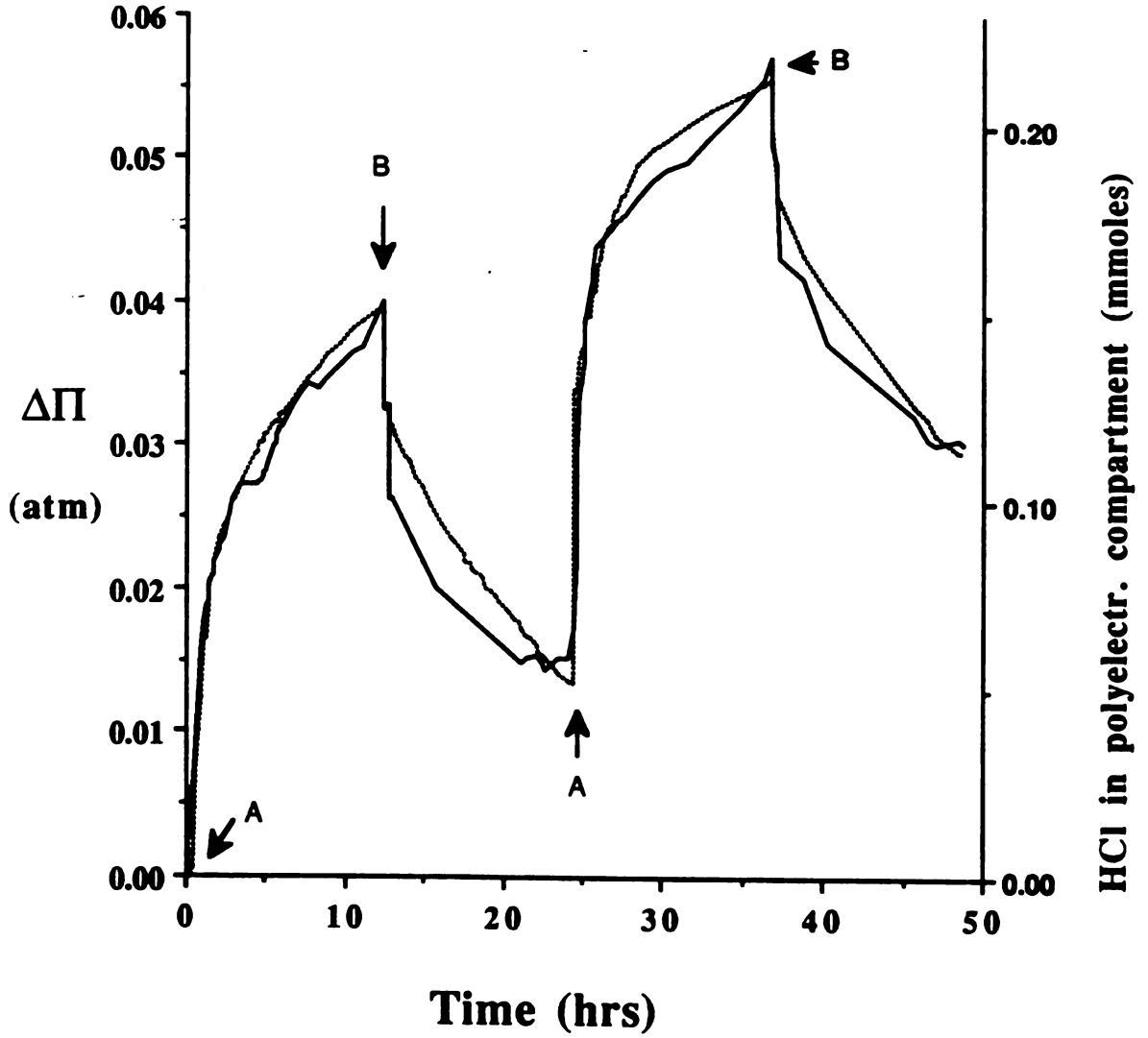

Figure 7.2. Kinetics of colloid osmotic pressure development for p(DEA/MMA) 56/44. (——) Colloid osmotic pressure, (·····) mmoles of HCl in polyelectrolyte chamber. A = HCl, B = NaOH.

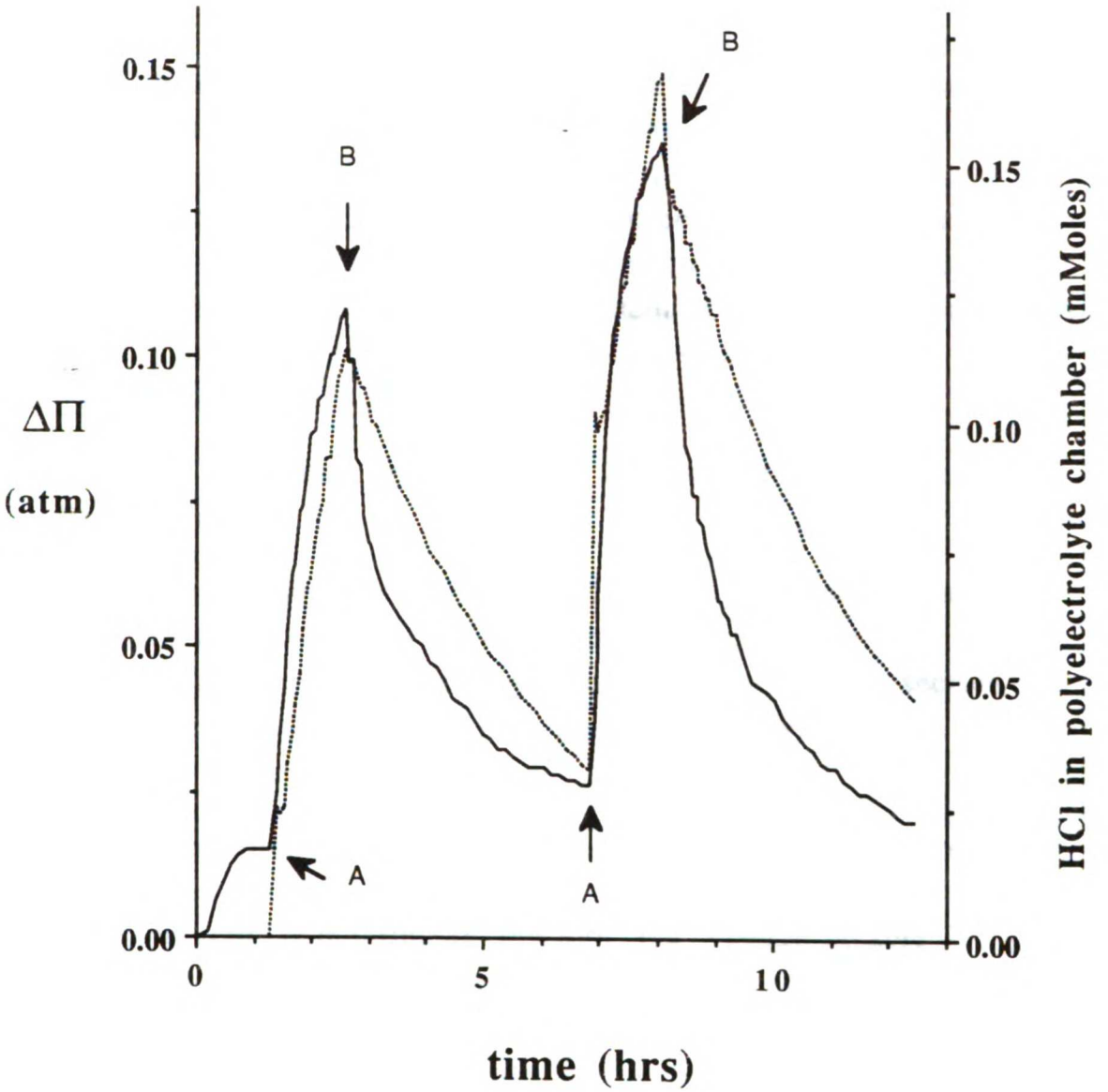

Figure 7.3. Kinetics of colloid osmotic pressure development for p(DEA/MTAC) 88/12. (——) Colloid osmotic pressure, (·····) mmoles of HCl in polyelectrolyte chamber. A = HCl, B = NaOH.

hour. It also observed that the drop in colloid osmotic pressure upon neutralization is slower than the colloid osmotic pressure production upon acidification; nevertheless, the neutralization kinetics are still much faster than those for the precipitating polyelectrolytes. Figure 7.3 also shows the amount of acid in the polyelectrolyte compartment (calculated as above). The processes of acid transport to the polyelectrolyte compartment and neutralization are faster in this system than in the precipitating system. Observe that changes in $\Delta\Pi$ actually lead changes in acid concentration in colloid compartment.

7.3 Factors Affecting the Kinetics of Colloid Osmotic Pressure.

As observed in figures 7.2 and 7.3, there is a substantial difference in the kinetics of colloid osmotic pressure for the precipitating and non-precipitating polyelectrolytes. This section presents a series of experiments to elucidate the factors that underlay this difference.

The generation of colloid osmotic pressure by the hydrophobic polyelectrolytes requires several steps: 1) transport of acid from the reference solvent compartment through the semipermeable membrane, 2) protonation of the amine groups (and dissolution of the precipitate in the case of the precipitated polymer), and 3) generation of colloid osmotic pressure.

Since the polyelectrolyte solution is unstirred, the precipitating polymer sediments at the bottom of the compartment. The area of contact for ionization must be greatly decreased. To investigate the effects of contact area, an experiment was performed to determine how the lack of stirring affects the ionization and dissolution of the hydrophobic polyelectrolyte.

The very slow kinetics of neutralization were also studied. The presence of precipitate adhered to the membrane after a neutralization cycle suggested that the membrane might be blocked.

To obtain evidence to support this hypothesis, transport of NaOH and of a neutral molecule, salicylamide, in the presence of the membrane-associated precipitate was studied.

The kinetics of neutralization also seem to be slower than the kinetics of acidification for the non-precipitating polyelectrolyte. Several experiments were performed to elucidate the reason(s) for this observation. The possible blocking of the membrane by the polyelectrolyte was studied by measuring the transport of salicylamide against the polyelectrolyte (fully ionized and undergoing neutralization). Experiments were also performed to study the transport of HCl and NaOH through the semipermeable membrane.

7.3.1 Materials

HCl (0.01 and 0.1 N) certified solution, concentrated HCl, NaOH 50% (w/w), and NaOH 0.1 M were from Fisher Scientific. NaCl (Fisher Scientific) was used as received. Water was distilled and deionized. Polyelectrolytes were synthesized and purified as in chapters 2 and 6. Membranes were prepared as in chapter 5. Salicylamide (Sigma) was used as received.

7.3.2 Dissolution Kinetics of the Precipitating Polyelectrolyte.

A solution of the p(DEA•HCl/MMA) 56/44 was completely neutralized by NaOH solution. Neutralization was accelerated by stirring. The desired concentration (0.1 monomolar) was obtained by diluting the resulting dispersion. In one experiment, 15 ml of the dispersion were stirred in a beaker. A volume of 0.4 M HCl, containing that number of acid equivalents required to ionize all the amine groups, was added to the dispersion. Rapid stirring was maintained. Complete dissolution of the precipitate was observed in a few seconds.

In a second set of experiments, the dispersion was allowed to sediment for a least 12 hours. A volume of 0.4 M HCl was added to

the supernatant (being careful not to disturb the precipitate). In the first and second experiments the amount of acid added corresponded to 86% and 120% the equivalents of amine groups in the precipitate, respectively. Samples of the supernatant were taken at several times to determine the amount of polyelectrolyte dissolved. After several hours the mixture was stirred. Total dissolution was observed in the case where excess of acid was added. Samples were extracted and filtered. The samples were diluted with five volumes of 0.1 M NaCl in 0.01 M HCl to bring them all to the same ionic strength and degree of ionization in all the samples. The viscosities of the resulting solutions were determined using an Ostwald viscometer. A standard curve was used to determine the polyelectrolyte concentration of the solutions.

7.3.3 Membrane Permeability

7.3.3.A HCl and NaOH Transport Through a Semipermeable Membrane

The rate of HCl and NaOH transport through the semipermeable membrane used in the previous experiments was measured using a side-by-side glass diffusion cell (Crown Glass Co., Inc. Somerville NJ) with 3.4 ml reservoir capacity on both sides of the membrane. The water soaked membrane was sandwiched between the two half cells. One of the cell halves (the donor) was filled with a NaCl 0.1 M solution containing HCl or NaOH at a concentration similar to the concentration used in the colloid osmotic pressure kinetics experiments (2.7×10^{-3} M). The second half cell (the receptor) was filled with a NaCl 0.1 M solution at pH 7. The pH in the receptor chamber was measured with a pH microelectrode (Model PHR-146, Lazar, Sunnyvale CA) and the signal was recorded in the data logger at a sampling period of 640 ms. Temperature was set at 25°C by a water circulator. The two half cells were stirred with stirring bars. The setup is shown in figure 7.4. The amount of HCl or NaOH that diffused from the donor cell to the receptor cell was calculated from the pH measurements.

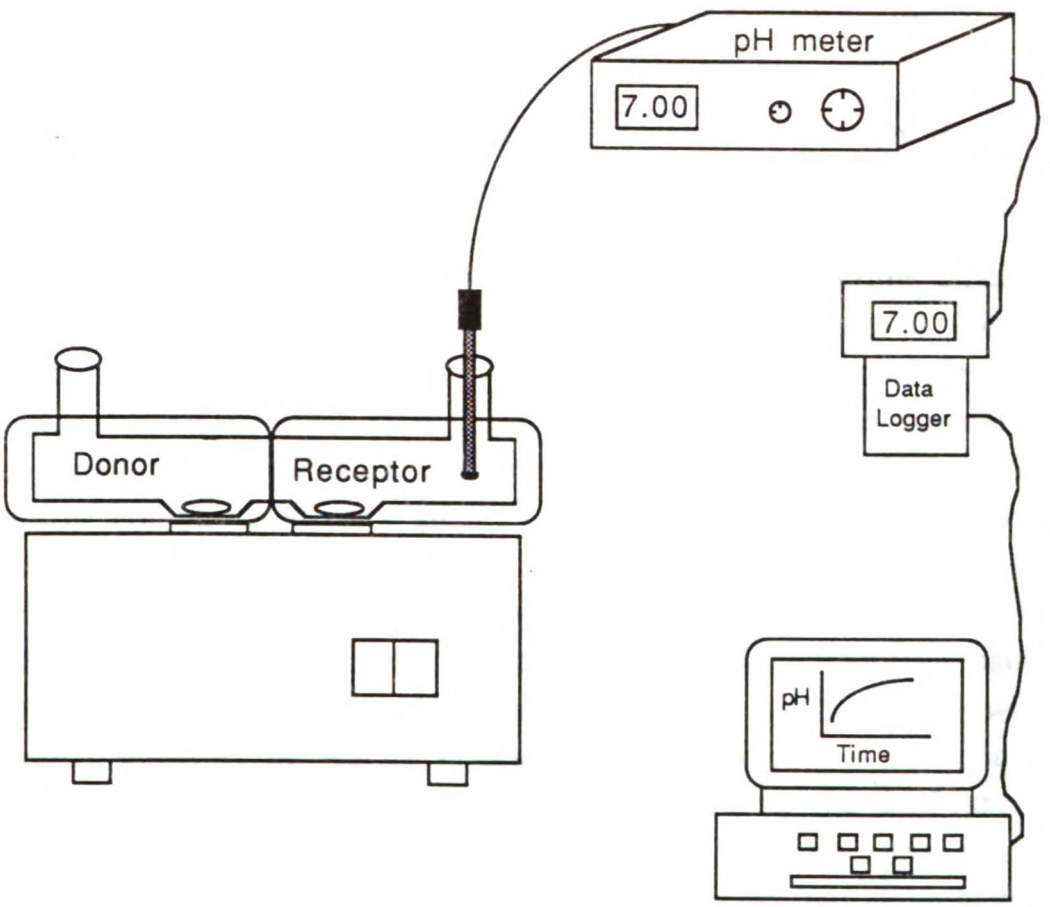

Figure 7.4. System used for the HCl and NaOH transport experiments.

In a second set of experiments, both chambers of the osmotic cell were loaded with a 0.1 M NaCl solution. A volume of 1 ml of 0.1 M HCl was added to the reference chamber. About one hour later, 1 ml of 0.1 M NaOH was added to the reference chamber. The pH was recorded during the course of the experiment.

7.3.3.B Transport of NaOH Against a Precipitating Polyelectrolyte Solution.

The effect of a precipitating polyelectrolyte on the transport of NaOH was studied in the following way. The polyelectrolyte chamber in the osmotic cell was loaded with a 0.2 monomolar solution of fully ionized p(DEA•HCl/MMA) 56/44. The reference solution chamber was loaded with distilled water. At time zero, a measured volume of 0.1 M NaOH was injected into the reference solution chamber and 0.1 ml samples were taken at different elapsed times. The volume of each sample was replaced with distilled water. The reference solution compartment was stirred with a stirring bar while the polyelectrolyte compartment was unstirred. The NaOH concentration in the sample was determined by potentiometric acid/base titration in an automatic titrator (Radiometer, Copenhagen Denmark) using HCl 0.01 M as the titrating agent. The experiment was repeated with different amounts of NaOH injected into the reference solution compartment. The number of base equivalents in the highest concentration solution of NaOH studied was approximately equal to the number of moles of ionized amine groups in the polyelectrolyte chamber.

7.3.3.C Back-transport of HCl

The smaller chamber in the osmotic cell was loaded with fully ionized, 0.1 monomolar p(DEA•HCl/MTAC) 88/12. The reference chamber was loaded with 0.1 M NaCl, and the pH change in that chamber was recorded. As a control experiment, the small chamber was loaded with 0.1 M HCl solution. The amount of HCl back-

transported into the reference chamber was calculated from the pH measurements.

7.3.3.D Transport of Salicylamide Through a the Semipermeable Membrane

The transport of salicylamide through the semipermeable membrane was measured as follows: The membrane was sandwiched between the two halves of a side-by-side diffusion cell. One half cell was filled with a 0.1 M NaCl solution at pH 3.1 (receptor) The other half cell was filled with a salicylamide solution in 0.1 M NaCl (donor). Samples were taken at several times from the receptor side. The volume extracted was replaced with fresh solution. The absorbance of the samples was measured at 300 nm using a UV spectrophotometer. The concentration of the samples was calculated using a standard curve.

In a second set of experiments, the donor chamber was loaded with fully ionized p(DEA•HCl/MMA) 56/44 or p(DEA•HCl/MTAC) 88/12. The donor chamber was loaded with salicylamide (0.12 mg/ml) in 0.1 M NaOH. The amount of salicylamide transported was determined as above. In another experiment the donor compartment was loaded with salicylamide (0.12 mg/ml) in 0.1 M NaCl.

7.3.3.E. Dynamic Response of the pH-Electrode

The dynamic response of the pH-electrode used in the experiments (Orion 91-03) was measured in the following way. The osmometer cell, without the membrane, was filled with a 0.1 M NaCl solution (pH 6.5). An amount of 0.1 M HCl was injected into the cell. The pH changes were recorded in the data logger. The concentration of HCl was calculated from the pH measurements.

7.3.4 Results and Discussion

As mentioned before, two main differences were observed in the kinetics of colloid osmotic pressure for precipitating and non-precipitating polyelectrolytes. First, the kinetics of pressure

development and neutralization are much faster in the non-precipitating system than in the precipitating system. Second, in the non precipitating system $\Delta\Pi$ leads the acid/base transport, whereas in the precipitating system the acid/base transport matches the kinetic of colloid osmotic pressure. In this section the results of the experiments performed to examine these differences are discussed. Since we do not expect dissolution kinetics to play a role in the non-precipitating polyelectrolyte, this system can be considered simpler and, for this reason, is discussed first.

7.3.4.A Non-precipitating Polyelectrolytes

For non-precipitating polyelectrolytes, colloid osmotic pressure development is apparently more rapid than the rate of pressure release (see figure 7.3). To understand this observation, the transport rates of HCl and NaOH across the membrane were studied in a side-by-side cell. Figure 7.5 shows that the transport of HCl is no faster than the transport of NaOH. Thus, the difference in the rates of increase and decrease of osmotic pressure can not be attributed to a difference in the transport rates of acid and base.

In the experiments whose results are shown in figures 7.2 and 7.3, the amount of NaOH added to the reference compartment is equal to the amount of acid initially added to that compartment to ionize the polyelectrolyte. Since a certain amount of acid remains in the reference compartment when NaOH is added (about 67% for the non-precipitating polyelectrolyte experiment), an equivalent fraction of the NaOH dose is immediately neutralized by the HCl in the compartment. The result is a smaller gradient of NaOH than for HCl, and this leads to slower apparent kinetics of neutralization compared to acidification. This supposition is supported by figure 7.6 which shows the results of an experiment where both compartments were loaded with a NaCl solution and alternating doses of HCl and NaOH (same amounts) were added to the larger compartment. The transport of HCl into the small compartment is apparently faster than the neutralization process. Since there is no sink for the acid (no amine groups), only a small amount of acid crosses into the small

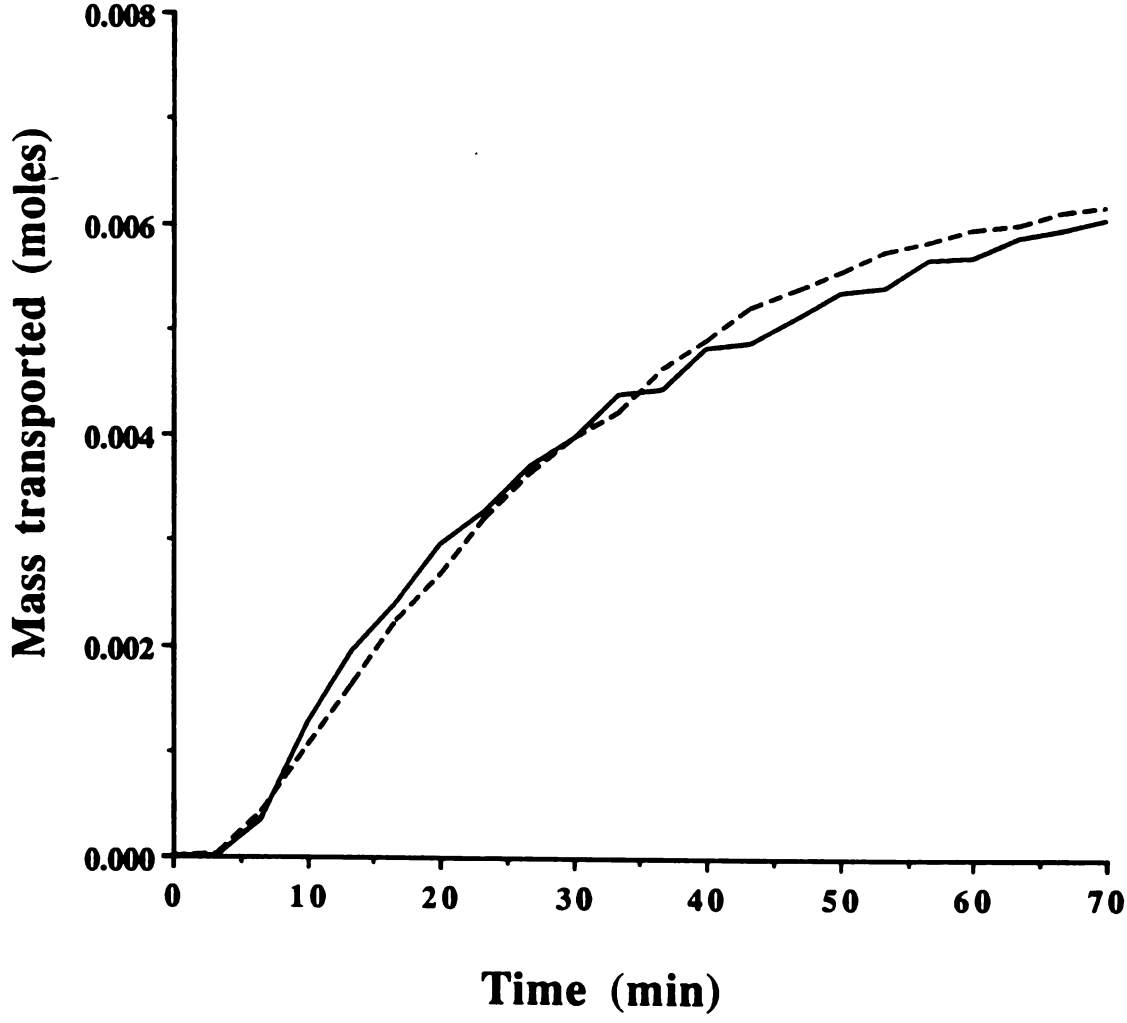

Figure 7.5. HCl and NaOH transport through a semipermeable membrane. (----) NaOH, (——) HCl.

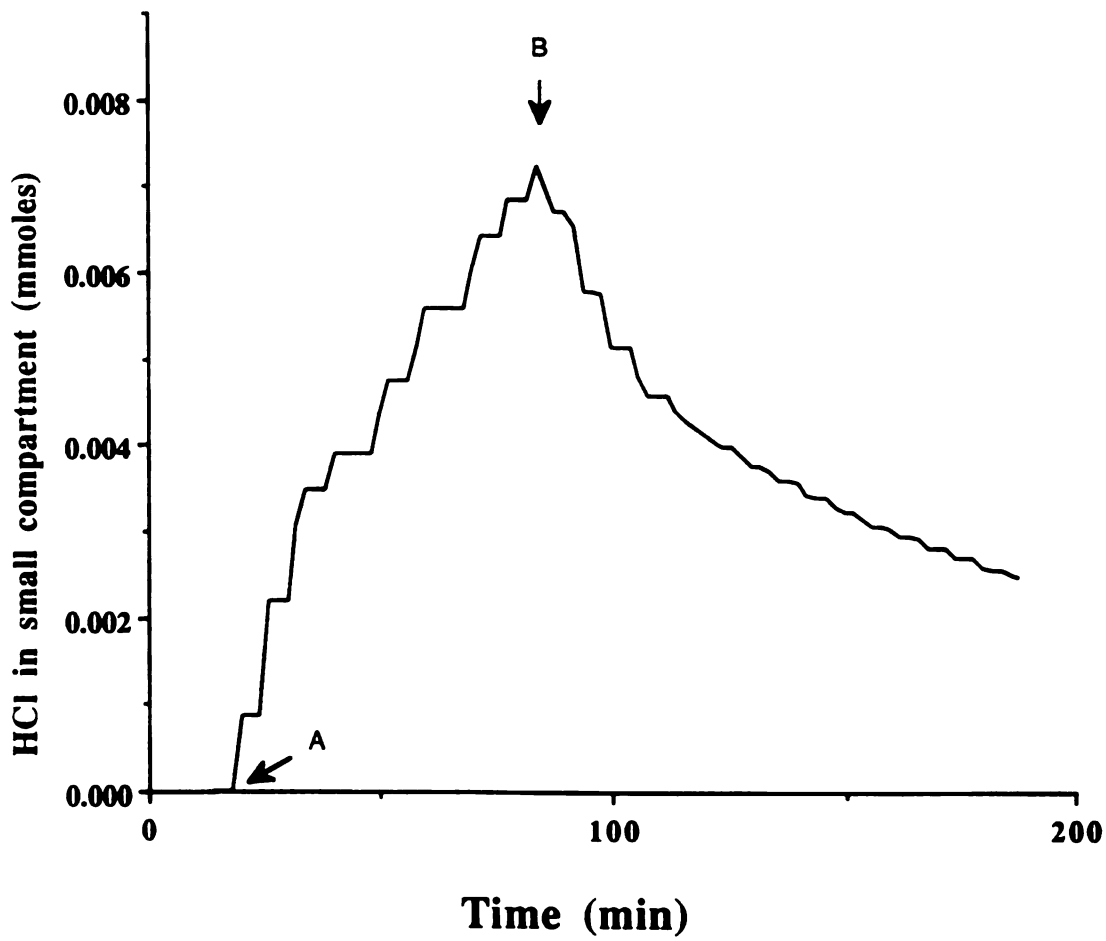

Figure 7.6. HCl and NaOH transport in the osmotic cell. A = HCl, B = NaOH.

compartment, and most of the base added is neutralized in the reference compartment, resulting in a significant difference in gradient between acid and base. This result indicates that, effectively, the difference in gradients between acid and base causes the apparent difference in rates of transport. In this experiment, the neutralization process can occur by either the base diffusing to the smaller compartment or the acid back-diffusing to the larger compartment. However, when the smaller compartment is loaded with polyelectrolyte, the process of neutralization occurs only when the base diffuses into the polyelectrolyte compartment since acid does not back-diffuse once it has ionized the amine groups, (see figure 7.7).

In the osmotic experiment, the results of which are presented in figure 7.8, the amount of acid remaining in the reference compartment was calculated before adding the base. The dose of base added equalled the amount of acid remaining in the reference compartment plus the initial amount of acid. In this way the initial concentration of base is equal to the initial concentration of acid. In this case, very similar rates of colloid osmotic pressure and neutralization are observed. This result demonstrates that similar rates of pressure buildup and pressure release are produced by the non-precipitating polyelectrolyte, provided that the same gradient of both acid and base is imposed.

Figures 7.3 and 7.8 show very rapid changes in colloid osmotic pressure immediately after the addition of acid or base to the reference chamber. These figures also show a delay of about ten minutes in the transport of acid into and out of the polyelectrolyte chamber compared to the change in colloid osmotic pressure. A potential artifact due to delay in the pH-sensing by the pH electrode was ruled out by direct measurement of electrode response time. Figure 7.9 shows that the electrode requires only about one minute to reach equilibrium, which is considerably less than the delay observed in Figs. 7.3 and 7.8.

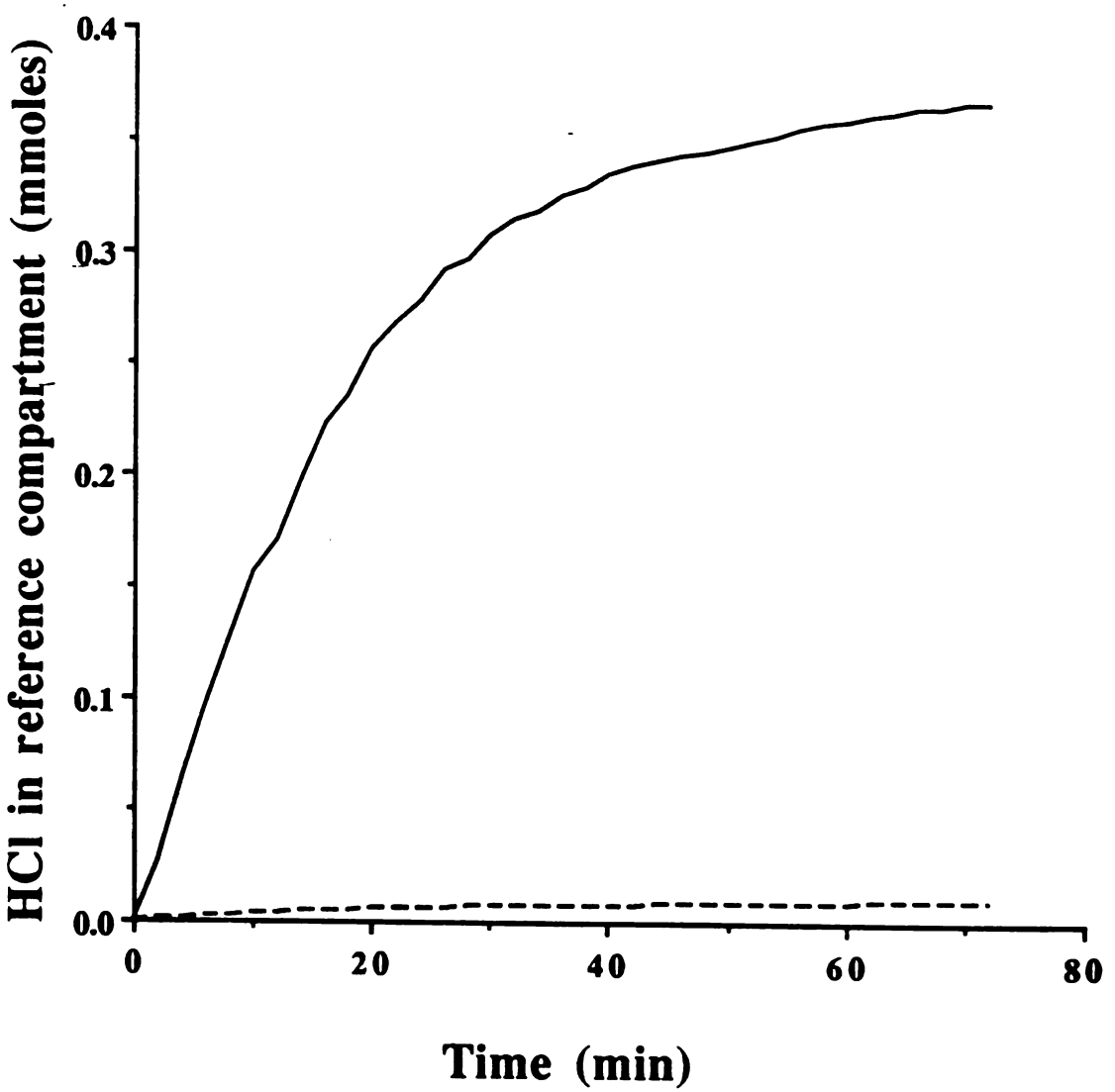

Figure 7.7. Back-transport of HCl. Loaded in the small compartment: (——) 0.1 M HCl, (----) 0.11 monomolar p(DEA•HCl/MTAC) 88/12.

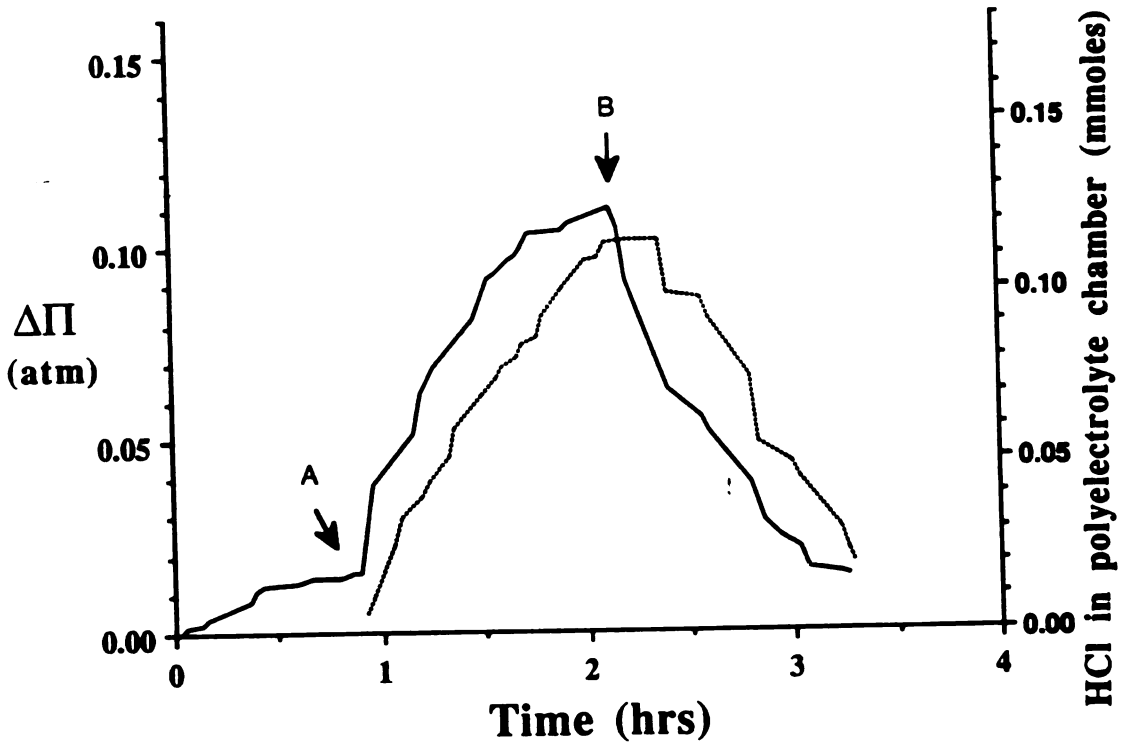

Figure 7.8. Kinetics of colloid osmotic pressure development for p(DEA/MTAC) 88/12. Same initial gradient for HCl and NaOH. (——) Colloid osmotic pressure, (----) HCl in polyelectrolyte chamber. A = HCl, B = NaOH.

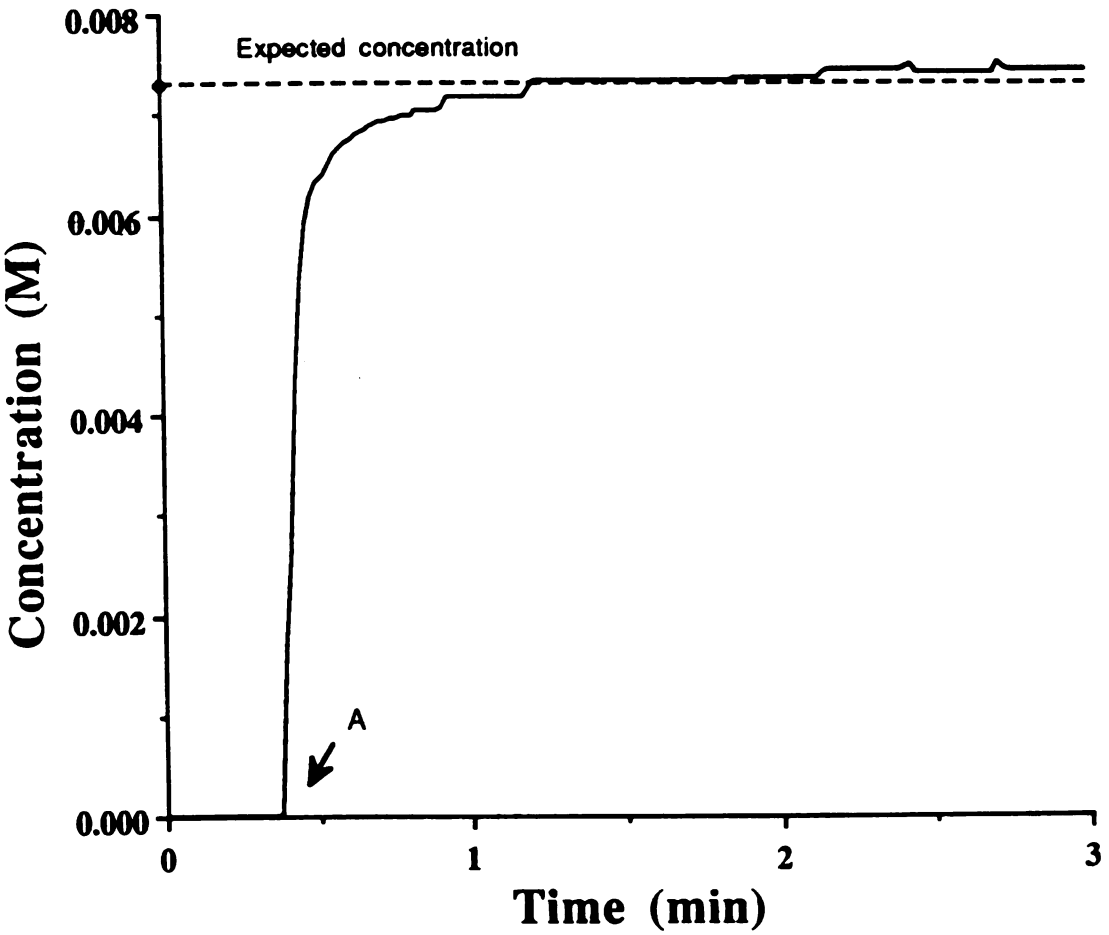

Figure 7.9. Dynamic response of pH-electrode. A = HCl added.

We believe the observed delays in acid transport relative to osmotic pressure buildup can be attributed to a boundary layer effect, as illustrated in figure 7.10. Systems where the osmotic pressure is governed by a boundary layer of solution adjacent to the semipermeable membrane have been previously described in the ultrafiltration and cell membrane transport literature (14,15). Since the polyelectrolyte chamber is unstirred, the addition of acid to the reference chamber will initially ionize a layer of polyelectrolyte solution near the surface of the membrane. The initial ionization of this thin layer will not consume a significant amount of acid, and the change in acid concentration in the reference compartment may not be detectable; however, ionization of this layer will produce a significant increase on colloid osmotic pressure. Subsequent transport of acid further ionizes the polyelectrolyte proximal to the membrane, as well as other polyelectrolyte molecules which are farther from the membrane. The former polyelectrolyte will be effective in increasing osmotic pressure, while the latter will not. On the other hand, the ionization of the distal polyelectrolyte layers will be more detectable with respect to acid transport. The same situation occurs during the neutralization process. Here, the neutralization occurs first near the membrane surface, leading to the fast initial drop in colloid osmotic pressure.

7.3.4.B Precipitating Polyelectrolyte

The kinetics of colloid osmotic pressure development and decay for precipitating polyelectrolytes are much slower than those for the non-precipitating counterparts, and must likely involve different processes, therefore.

We first consider the kinetics of colloid osmotic pressure development. The observed sluggish kinetics of colloid osmotic pressure development are due either to the small surface area presented by the polyelectrolyte to the acid, or to a long diffusion time of acid to the polyelectrolyte. Stirring of a dispersion of p(DEA/MMA) 56/44 with enough acid to ionize all the amine groups

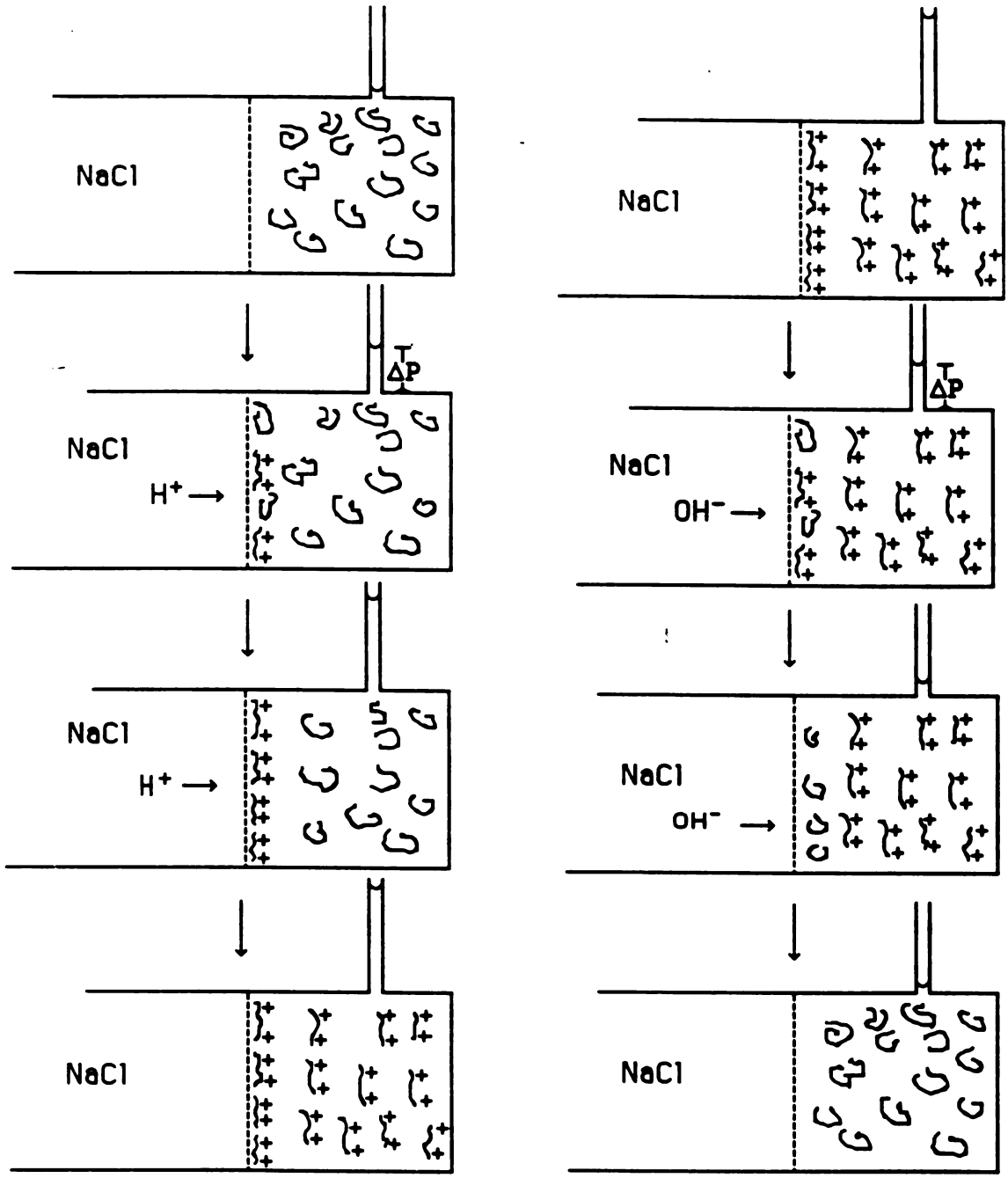

Figure 7.10. Boundary layer effect on the transport of acid/base and on the development/release of colloid osmotic pressure.

produces very rapid dissolution (caused by ionization) of the precipitate. The absence of stirring greatly retards the dissolution of polyelectrolyte, as observed in figure 7.11. These results show that the slow kinetics of dissolution are due to the reduced contact area between the unionized precipitated polyelectrolyte and the acid, as well as transport delays when the polyelectrolyte is precipitated.

The slow kinetics of neutralization can be attributed to clogging of the membrane pores or to an increase in the transport distance of the NaOH due to the precipitation of the polymer at the membrane surface. This conclusion is supported by the following experimental results. The transport of the neutral salicylamide in a basic solution against the precipitating polyelectrolyte was studied in a side-by-side diffusion cell. A few minutes after the experiment was started, a slab of precipitate was observed growing from the membrane. The growth of the slab stops after about two hours. The transport of salicylamide in this system is shown in figure 7.12: transport is blocked after about one hour. Conversely, transport of salicylamide proceeds unhindered when no polyelectrolyte is available to block the transport. Figure 7.12 also shows that, even though the transport of salicylamide against the non-precipitating polyelectrolyte is decreased, it is not shut off (this decrease is probably due to an increase in unstirred layer thickness due to viscosity enhancement by the polyelectrolyte). Very similar transport rates are observed when salicylamide is diffused from a NaOH solution or from a NaCl solution. Therefore, there is no membrane clogging with the non-precipitating system, as is to be expected.

The transport of NaOH in the osmometer against fully ionized p(DEA•HCl/MMA) 56/44 was studied. The results are shown in figure 7.13. The transport of NaOH is shut down long before the polyelectrolyte is fully neutralized. As the initial amount of NaOH loaded into the reference chamber is increased, the time of shut down of NaOH transport decreases. This result, along with the observations discussed above indicate that, effectively, as the polyelectrolyte is neutralized near the membrane surface, it

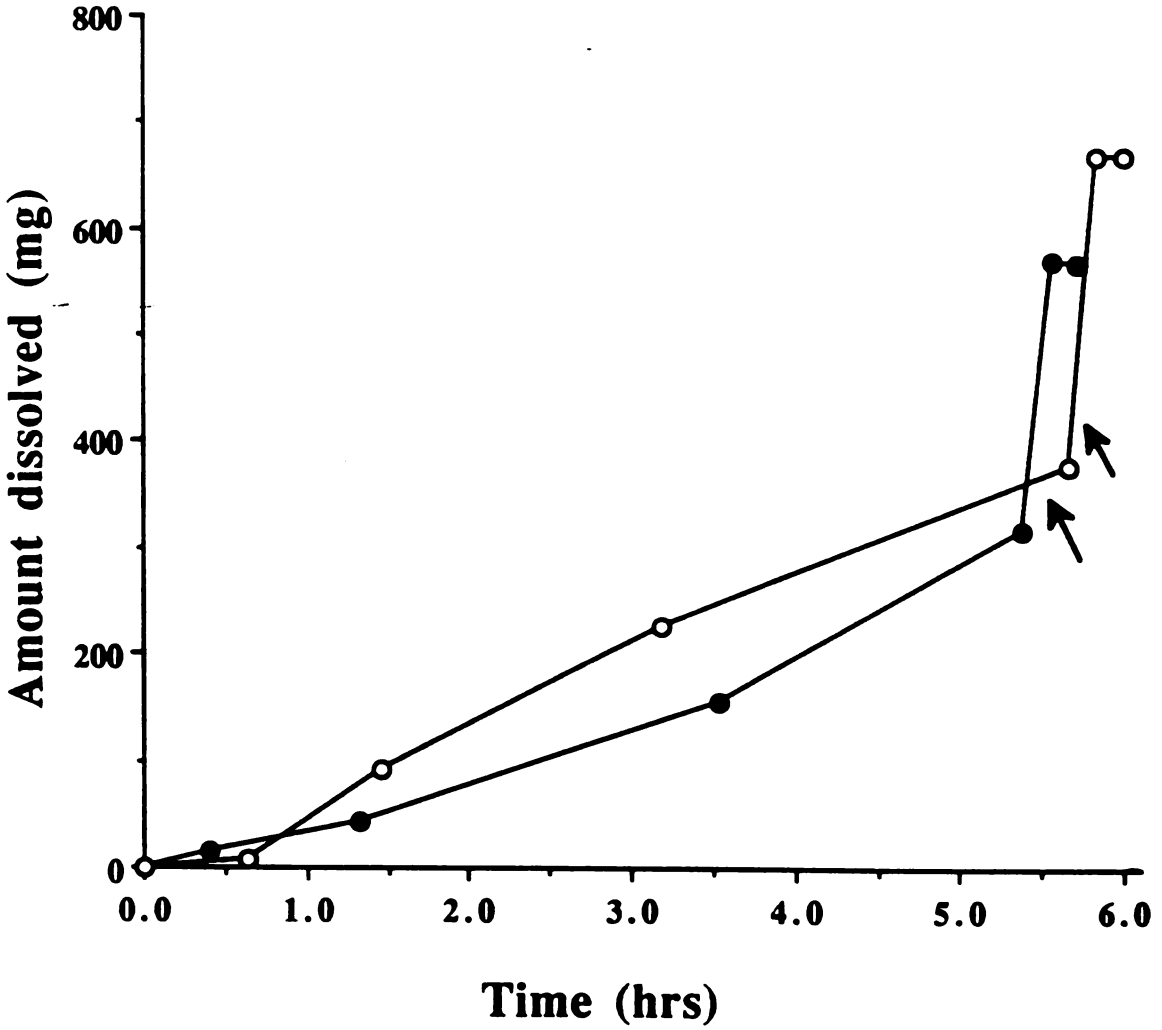

Figure 7.11. Dissolution of p(DEA/MMA) 56/44. Moles HCl/moles amine; (○) 1.20, (●) 0.88. Arrows indicate start of stirring.

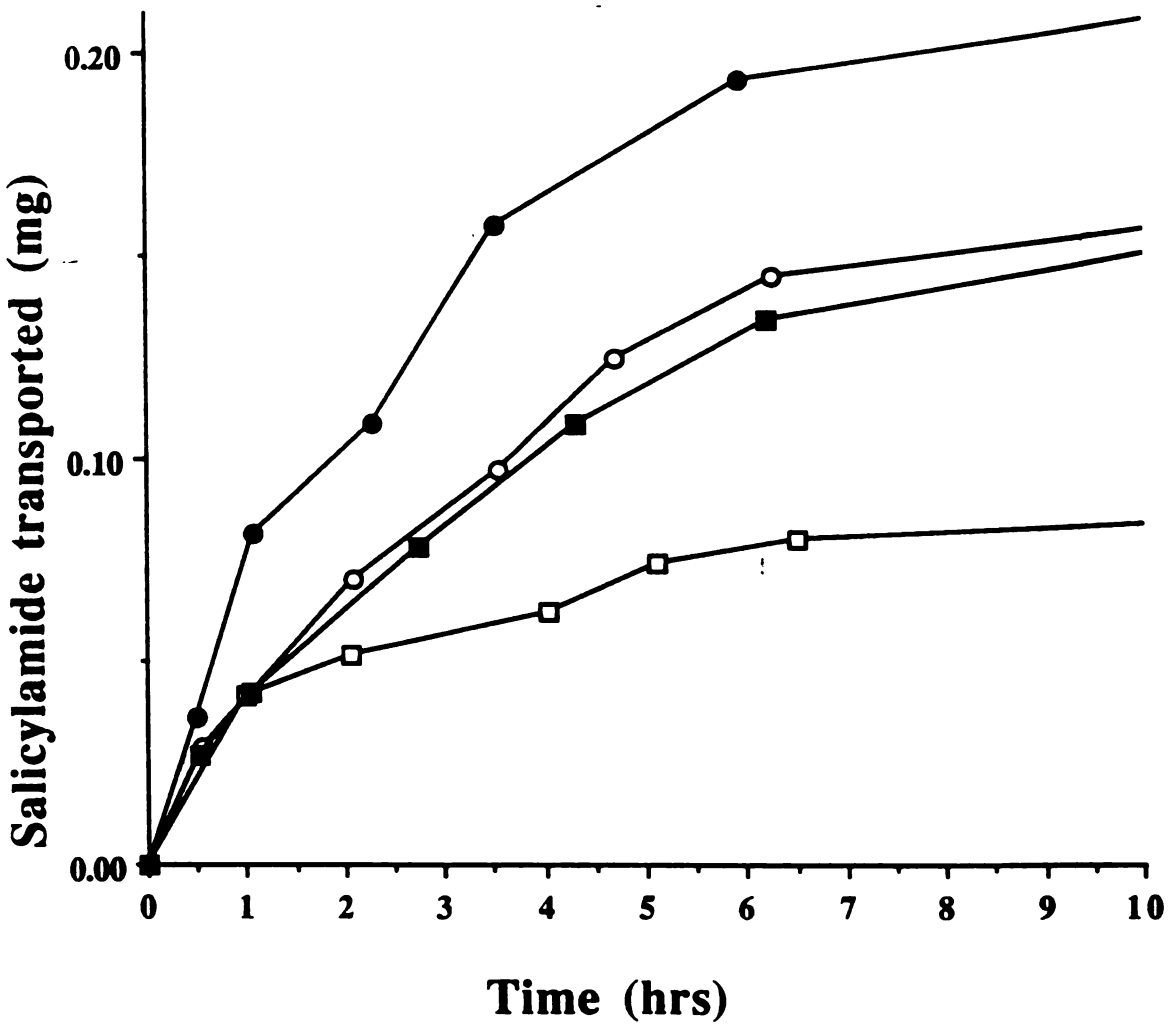

Figure 7.12. Transport of salicylamide through a semipermeable membrane. (●) in 0.1 M NaCl against 0.1 M NaCl, (○) in 0.1 M NaOH against p(DEA•HCl/MTAC) 88/12 %mole, (■) in 0.1 M NaCl against p(DEA•HCl/MTAC) 88/12 %mole, (❑) in 0.1 M NaOH against p(DEA•HCl/MMA) 56/44 %mole.

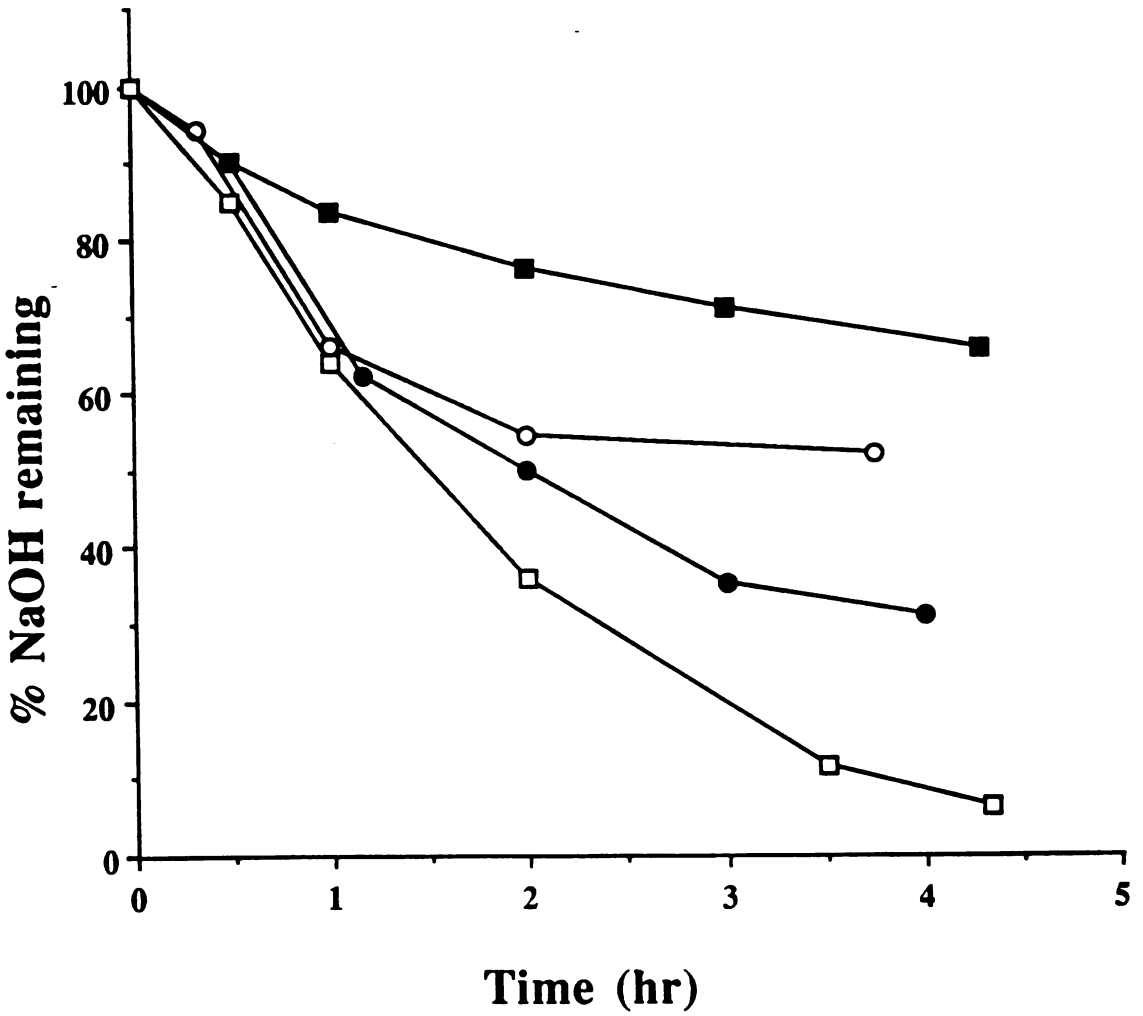

Figure 7.13. Transport of NaOH against a precipitating polyelectrolyte solution. Initial NaOH concentration in the reference chamber; (■) 4.9 mM, (○) 3.8 mM, (●) 2.6 mM, (❑) 0.94 mM.

precipitates, retards the further transport of NaOH, and greatly decreases the colloid osmotic pressure drop process.

A closer look at the kinetics of colloid osmotic pressure development in figure 7.2 shows a relatively fast development of colloid osmotic pressure immediately after addition of HCl and a rapid drop of the colloid osmotic pressure immediately after adding NaOH. This observation is consistent with the mechanism postulated above. After addition of HCl to the reference chamber, the acid ionizes the polyelectrolyte stuck on the membranes or dispersed in the solution (high surface area); after this initial burst in colloid osmotic pressure the surface area greatly decreases, slowing down the kinetics. During the neutralization process a different situation occurs: initially, the membrane is unclogged and the neutralization process is fast. However, the membrane is clogged by precipitate formed on the former during NaOH transport, shutting down the neutralization process soon after the latter has commenced.

7.4 Conclusions

The precipitating polyelectrolytes present very slow kinetics of colloid osmotic pressure development. The rate limiting step appears to be the dissolution of the precipitate. The precipitate sticks to the membrane and sediments in the bottom of the cell. The adherence to the membrane affects the neutralization kinetics greatly. The kinetics presented for the precipitating polyelectrolytes are probably impractical for the mechanochemical insulin pump. A much faster response is observed for the non-precipitating polyelectrolytes.

References

1. F. Theeuwes, *J. Pharm Sci.*, **64**(12), 1987 (1975).

2. G. Kallstrand, B. Ekman, *J. Pharm. Sci.*, **72**(7) 772 (1983).

3. F. Theeuwes, in Controlled Release Technologies: Methods, Theory, and Applications, A.F. Kydonieus, Ed.,CRC: Boca Raton Fl., Vol. II, Chapter 10, 1980.

4. R.W. Baker, in Controlled Release of Biologically Active Agents, John Wiley & Sons, New York NY, Chapter 4, 1987.

5. A. Katchalsky and P.F. Curran, Non Equilibrium Thermodynamics in Biophysics, Harvard University Press, Cambridge, Mass., 1976.

6. T.J. Pedley and J. Fischbarg, *J. Theor. Biol.*, **70**, 427 (1978).

7. H.A. Massaldi and C.H. Borzi, *J. Membrane Sci.*, **12**, 87 (1982).

8. R.P.W. Williams and W.D. Comper, *J. Phys. Chem.*, **91**, 3443 (1987).

9. R.P.W. Williams and W.D. Comper, *Biophys. Chem.*, **36**, 223 (1990).

10. O. Kedem and A. Katchalsky, *Biochim. Biophys. Acta*, **27**, 229 (1958).

11. R.H. Stokes, *J. Am. Chem. Soc.*, **72**, 2243 (1950).

12. C.V. Nocholas, M.A. Desai, and P.M. Vadgama, *J. Chem. Soc. Faraday Trans.*, **87**(2) 293 (1991).

13. F.W. Billmeyer Jr., Textbook of Polymer Science, John Wiley & Sons, Chapter 3, 1984.

14. T.J. Pedley, *Quarterly Review of Biophysics*, **16** (2), 115 (1983).

15. K.L. Lee, R.W. Baker, and H.K. Lonsdale, *J. Membrane Sci.*, **8**, 141 (1981).

Chapter 8

Conclusions and Suggestions for Future Work

8.1 Conclusions

The titration curve of the hydrophobic polyelectrolyte p(N,N-diethylaminoethyl methacrylate•HCl) [p(DEA•HCl)] differs from the titration curves presented by more hydrophilic polyelectrolytes. During titration of p(DEA•HCl) with a NaOH solution, a precipitate phase appears at a certain degree of neutralization. After the precipitate phase appears, the polyelectrolyte system behaves as an excellent buffer. The "buffering pH" occurs at a pH of 7.6 when the ionic strength is set at 0.1 M with NaCl. The buffering pH is affected by the ionic strength of the solution and by the anion of the sodium salt used to set the ionic strength. The ionic strength also affects the point were the precipitate phase initially appears.

The buffering pH can be shifted to higher or lower pH values by incorporating hydrophilic or hydrophobic neutral comonomers into the chains, respectively.

We have proposed the following pseudochemical scheme for the titration process of this class of hydrophobic polyelectrolytes:

$$p(DEA)_{ppt} \rightleftharpoons p(DEA)_{sln} + nHCl \rightleftharpoons p(DEA{\bullet}HCl)_{sln}$$

An increase (decrease) in the hydrophobicity of the chains shifts the equilibrium to the left (right); i.e., the precipitated (solution) form of the polymer. An accompanying increase (decrease) in the concentration of free acid leads to a decrease (increase) in the pH of the supernatant solution. This means that the "buffering pH" will be shifted down (up). These expectations are confirmed experimentally.

A second prediction of the scheme displayed above is that the addition of salt to the polyelectrolyte solution will stabilize the

soluble, ionized form of the polymer, shifting the reaction to the right. This will result in a decrease in the concentration of free HCl in the solution and a shift in the buffering pH to higher values. Again, this prediction is confirmed by the experimental results.

The colloid osmotic behavior of p(DEA•HCl) and the copolymers of DEA•HCl and MMA was also studied. It was found that incorporation of the unionizable comonomer (MMA) increases the osmotic coefficient of the counterions; in other words, at constant concentration of fixed charges and reference solution composition, higher colloid osmotic pressures are obtained as the proportion of MMA increases. The cell model for polyelectrolyte solutions (1-3) predicts adequately the colloid osmotic pressure produced by fully ionized p(DEA•HCl) up to 0.2 monomolar concentration; however, this model only fits experimental results for the copolymers at very low concentrations. The theory also accounts reasonably for the effect of ionic strength and degree of neutralization on the colloid osmotic pressure of p(DEA•HCl).

Polyelectrolytes containing permanent charges were produced by copolymerizing DEA•HCl and the quaternized monomer methacryloxyethyl trimethyl ammonium chloride (MTAC). The precipitation process was inhibited when a small fraction of permanent charges was introduced. These copolymers present lower buffer capacities than the homopolymer. The cell model predicts well the colloid osmotic pressure produced by the fully ionized copolymers up to a 0.2 monomolar concentration of ionized groups on the polymer. It also predicts well the effect of neutralization on the colloid osmotic pressure.

A copolymer of DEA•HCl and MMA was partially methylated at several degrees of quaternization. These copolymers present decreased buffer capacities, and the titration curves are shifted to higher pH values as the degree of the methylation increases.

It was observed that the colloid osmotic pressure can be switched on and off by adding acid and base to the reference solution

in a osmotic cell containing the studied polyelectrolytes. Unfortunately the kinetics of colloid osmotic development are very slow for the unquaternized polymer. Clogging of the membrane by the precipitate is observed. The kinetics are improved significantly when a quaternized, non-precipitating form is used.

The results suggest that the non-precipitating polyelectrolytes can be used as osmotic agents for a proposed mechanochemical insulin pump. However, excellent buffer capacities are required for the osmotic agent of the insulin pump. Unfortunately, some of the buffering properties of the precipitating system are lost during the methylation of the polyelectrolytes. Some solutions to this problem are proposed in the next section.

8.2 Suggestions for Future Work

The titration experiments in this study were performed in dilute polyelectrolyte solutions (0.01 monomolar) where the ionic strength was set by a sodium salt. However, the colloid osmotic experiments were performed at relatively high concentrations (up to 0.2 monomolar). A complete characterization would require the measurement of titration curves of the polyelectrolytes at higher concentrations. Due to the difficulty in defining ionic strength for a concentrated polyelectrolyte solution, these experiments should be performed in an osmotic cell where the ionic strength can be set in the reference solution by a low molecular weight salt.

The development of a theoretical model to predict the titration and colloid osmotic behavior of the precipitating and non-precipitating polyelectrolytes would aid in designing a proper osmotic agent for the mechanochemical insulin pump and also would facilitate understanding of the various factors that affect the titration behavior of hydrophobic polyelectrolytes. Such a model should include the Flory-Huggins theory of phase separations (4) and a term to account for the electrostatic free energy (5-7).

The specific effects of the counterions on the titration curves of

the polyelectrolytes are not yet well explained. Although it appears that the effect of size of the counterions on the screening of charges can explain some of the observations, there remain some unanswered questions. For example, the point at which the precipitate appears is shifted to lower values of α as the ionic strength increases. The opposite is predicted by the scheme proposed for the titration of hydrophobic polyelectrolytes, since the increase in the salt concentration stabilizes the ionized form of the polyelectrolyte; hence, the precipitate should appear at higher values of α as ionic strength increases. It is also unknown why iodide reduces the buffering strength of p(DEA•HCl).

As described above, the main disadvantage of the precipitating polyelectrolytes as osmotic agents for the proposed mechanochemical insulin pump is the slow kinetics of colloid osmotic pressure development after addition of acid. This phenomenon has been attributed to the small surface area presented by the precipitated polyelectrolyte to the acid. The surface area can be increased by minimizing the volume to diameter ratio of the polyelectrolyte compartment. A very thin polyelectrolyte chamber filled with a polyelectrolyte suspension will improve the kinetics of colloid osmotic pressure by increasing the surface area, and by decreasing the amount of acid needed to reach the concentration of ionized groups that produces the required colloid osmotic pressure.

To avoid the problem of the precipitated polymer sticking to the surface of the semipermeable membrane and blocking the transport of molecules, a more hydrophilic membrane should be used. A possibility is the use of asymmetric membranes where the selective "skin" is supported by a porous hydrophilic material. The "skin" can be made of a hydrophilic material such as polysulfone.

The use of a partially quaternized polybase as the osmotic agent for the mechanochemical insulin pump requires the search for the proper polyelectrolyte. First, the titration curve of the required polyelectrolyte should show buffering close to, but below, 7.4 at the physiological ionic strength of around 0.15 M. Secondly, the fraction

of quaternized charges on the polyelectrolyte should be chosen so as to maximize the polyelectrolyte's buffer strength, subject to the constraint that the polymer remains soluble at all degrees of neutralization. A small amount of swollen precipitate at high degrees of neutralization could be acceptable provided that the kinetics of colloid osmotic pressure development are fast and that no sticking to the membrane occurs. To obtain such a polyelectrolyte requires the synthesis of a proper parent (unquaternized) polyelectrolyte. This parent compound should have a minimal of unionizable monomer units, so that the fraction of permanent charges needed to produce a polymer soluble at any pH is as small as possible: it is then necessary to select the proper unionizable comonomer to be used in the polyelectrolyte. It was observed in these studies that a high proportion of MMA is required to obtain a copolymer with a buffering pH below 7.4 (at I = 0.1 M). A more hydrophobic comonomer is then required. Butyl methacrylate is probably not a good choice since it appears to produce block copolymers with DEA.

The hydrophobicity of the polyelectrolyte can also be increased by increasing the size of the groups bound to the nitrogen atom in the monomer (i.e., changing a ethyl group to a propyl group), or by increasing the number of carbons in the bridge between the methacrylate group and the amine atom. In this way the number of permanent charges needed to keep the polyelectrolyte in solution can be minimized. However, the ionization constant (pKa) of the amine functionality may be altered by such modifications.

Mechanochemical forces can be produced in a pH sensitive fashion using some other polyelectrolyte systems. One possibility is to use polyelectrolyte complexes between a strong polybase (charged at any pH) and a weak polyacid (8-10). At high pH the weak acid exists in the ionized form and, a polyelectrolyte complex is formed with the strong base. If the molar concentrations of the oppositely charged polyelectrolytes are the same and the conversion to the polyelectrolyte complex is complete, all the charges will be neutralized and the colloid osmotic pressure will be zero. If the pH of

the medium drops, the weak acid becomes unionized, and the polyelectrolyte complex is broken; the charged strong polyelectrolyte will then produce colloid osmotic pressure (see figure 8.1).

Depending in the characteristics of the individual polyelectrolyte components (i.e., charge density) and the conditions of the medium (i.e., ionic strength, temperature, pH), polyelectrolyte complexes exist in solution or separate from the solvent as precipitates or complex coacervates (8,11).

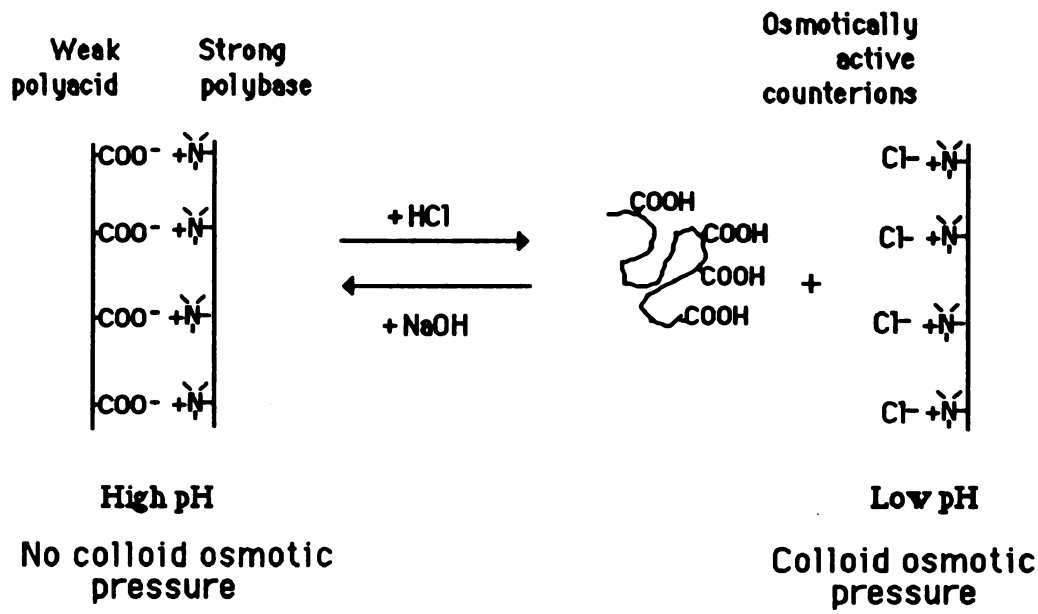

Figure 8.1. pH dependent development of colloid osmotic pressure by polyelectrolyte complexes.

The task, then, is to find a weak polyacid/strong polybase combination whose acid-base equilibrium will produce colloid osmotic pressure at the proper pH (i.e below pH 7.4). The polyelectrolyte complex formed has to be water soluble or form a complex coacervate to insure fast kinetics of colloid osmotic pressure development.

References

1. Z. Alexandrowicz, *J. Polym Sci.*, **56**, 97 (1962).

2. A. Katchalsky, Z. Alexandrowicz, and O. Kedem, in Chemical Physics of Ionic Solutions; C. Barradas, R.G. Conway, Eds.; Wiley: New York, NY, 1966; Chapter 17.

3. A. Katchalsky, *Pure Appl. Chem.*, **6**, 327 (1971).

4. P.J. Flory, Principles of Polymer Chemistry, Cornell University Press 1953.

5. A. Katchalsky and S. Lifson, *J. Polym. Sci.*, **11** (5), 409 (1953).

6. K.A. Sharp and B. Honig, *J. Phys. Chem.*, **94**, 7684 (1990).

7. D. Stigter and K.A. Dill, *J. Phys. Chem.*, **93**, 6737 (1989).

8. E. Tsuchida and K. Abe, *Advances in Polymer Science*, **45**, 1 (1982).

9. V.A. Kabanov and A.B. Zezin, *Soviet Scientific Reviews. Section B, Chemistry Reviews*, **4**, 207 (1982).

10. V.A. Kabanov, *ACS Proceedings. Division of Polymeric Materials: Science and Engineering*, **66**, 9 (1992).

11. I. Michaeli, J.Th.G. Overbeek, and M.J. Voorn, *Journal of Polymer Science*, **23**, 443 (1957).

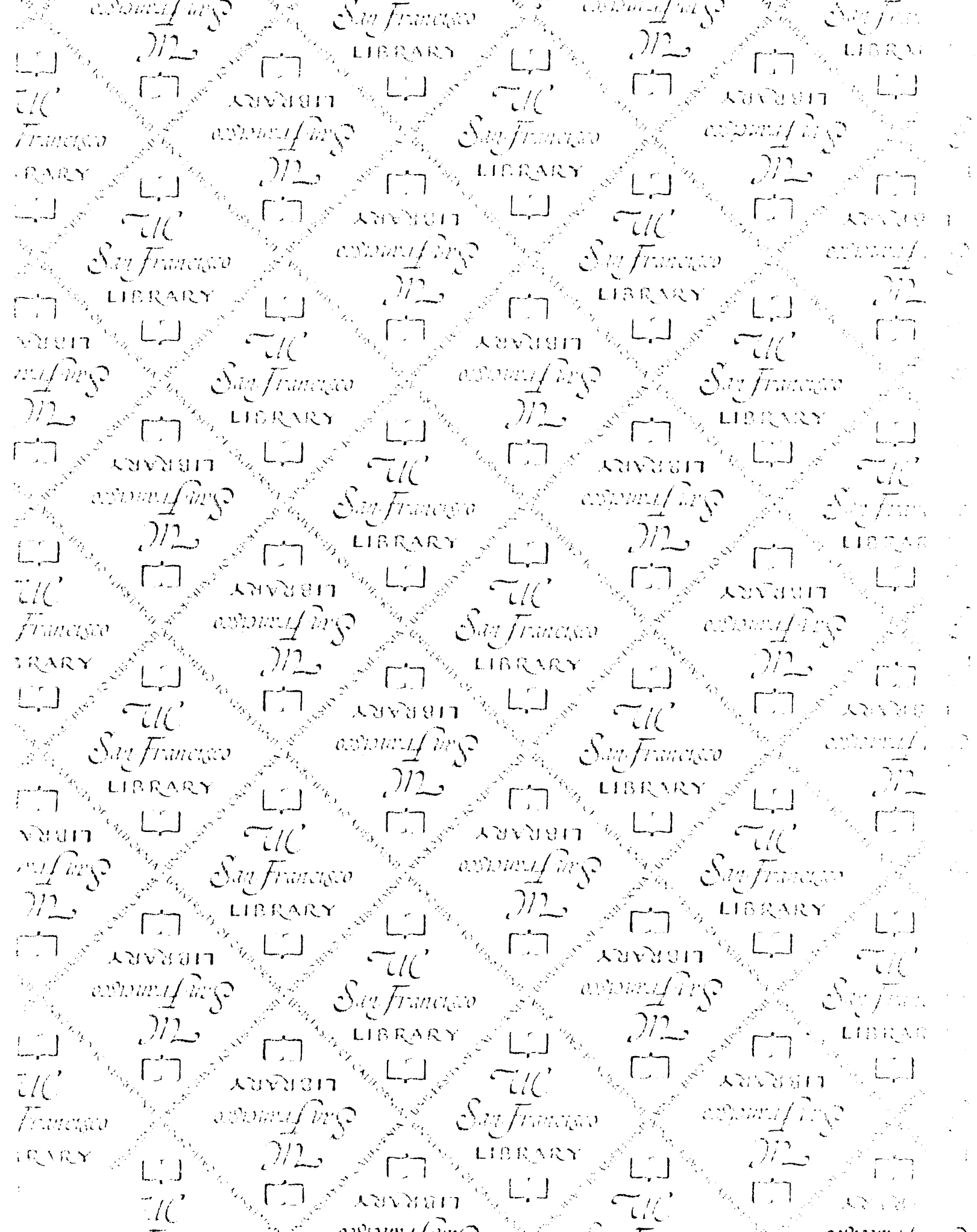
San Francisco
LIBRARY